Genehmigt vom Department Biologie
der Fakultät für Mathematik, Informatik und Naturwissenschaften
an der Universität Hamburg
auf Antrag von Herr Professor Dr. R. MARTIN
Weiterer Gutachter der Dissertation:
Professor Dr. T. BURMESTER
Tag der Disputation: 09. Juli 2010

Hamburg, den 22. Juni 2010

Professor Dr. Axel Temming
Leiter des Departments Biologie

ROLE OF AUTOIMMUNE INFLAMMATION AND IMPAIRED NEUROREGENERATION IN THE PATHOGENESIS OF EXPERIMENTAL AUTOIMMUNE ENCEPHALOMYELITIS

Dissertation

zur Erlangung der Würde des Doktors der Naturwissenschaften

des Departements Biologie, der Fakultät für Mathematik, Informatik und Naturwissenschaften,

der Universität Hamburg

vorgelegt von

Karin Steinbach

aus Ulm/ Donau

Hamburg 2011

Universitätsklinikum Hamburg-Eppendorf

ZMNH Center for Molecular Neurobiology Hamburg

Kent Duncan, PhD.

Falkenried 94, 20251 Hamburg
Telefon: (040) 7410-56274
Telefax: (040) 7410-53436
kent.duncan@zmnh.uni-hamburg.de

Universitätsklinikum Hamburg-Eppendorf Martinistraße 52 20246 Hamburg
Zentrum für Molekulare Neurobiologie (ZMNH)
Institut für Neuroimmunologie und Klinische Multiple Sklerose Forschung (inims)

Universität Hamburg
Department Biologie
Departmentleitung
Prof. Dr. Jörg Ganzhorn
Martin-Luther-King-Platz 2
20146 Hamburg

26.05.2010

Bestätigung der Korrektheit der englischen Sprache

Sehr geehrter Herr Prof. Ganzhorn,

hiermit bestätige ich, dass die Dissertation von Frau Karin Steinbach in korrekter englischer Sprache abgefasst ist.

Mit freundlichen Grüßen,

Kent Duncan, PhD

CONTENT

1 INTRODUCTION

The diaries of King George III's illegitimate grandson, Augustus d'Este, reveal that he suffered for over 26 years from recurrent episodes of visual impairments, motor symptoms and weaknesses of the lower extremities, suggesting he suffered from the disease we now call multiple sclerosis (MS). However, at the beginning of the nineteenth century, the so-called „nervous disorders" were only beginning to be recognized by physicians and scientists[1]. New neuropathological methods and systematic investigations of autopsy tissue allowed identification of disseminated sclerotic lesions in brain and spinal cord of people suffering from episodic neurological disease in the following decades, but the definite description and naming of the underlying disease is attributed to Jean-Martin Charcot[2]. His description in 1868 of „*sclérose en plaques*" contains many hallmarks of MS-pathology which are still in focus of research today: the localisation of lesions around cerebral blood vessels, suggesting inflammation, as well as evidence for de- and remyelination, axonal loss and atrophy. Since then, research has been focused on the identification of the natural cause of MS. During the twentieth century, experimentally induced MS-like diseases have been described in animals, and a combination of research in animals and humans has identified many factors involved in the pathogenesis of MS, leading to our current concept of MS as a $CD4^+$ T-helper (Th) cell mediated demyelinating autoimmune disease of the central nervous system (CNS). With the discovery of the autoimmune nature of the disease, research and therapy have mainly focused on the immunological aspects of MS. This has led to the identification of many immune cell types and signalling pathways involved in the development and/ or progression of the disease. Recently, early neurodegeneration in the course of the disease has been rediscovered[3], which now extends the foci of MS research to neuronal damage and lack of neuronal repair, leading to new therapeutic approaches.

1.1 Clinical presentation of multiple sclerosis

MS is a neurological disease which primarily affects young adults between 20 and 40 years of age and ranks second to trauma as cause for permanent disablilty in this age group[4]. 122,000 patients have been diagnosed with MS in Germany by the end of 2000[5], and 2.5 million people are estimated to suffer from MS worldwide according to the Multiple Sclerosis International Federation. The worldwide distribution of MS shows a latitude gradient, with the prevalence increasing with the distance from the equator. Migration studies suggest that the geographical risk of developing MS is linked to an environmental factor, which exerts its

effect during late childhood[6-8]. A concordance rate of 30% in monozygotic twins compared to 5% for dizygotic and the low incidence of MS among adopted children of patients with MS suggests that genetic factors are also relevant for disease susceptibility[9].

MS is a heterogeneous disease in terms of clinical course, response to treatment and the observed morphological alterations in the CNS[10-12]. Clinical signs and symptoms are diverse and depend on the regions in the CNS that are affected. They include motor, sensory, autonomic and cognitive disabilities[4]. Pathological findings in MS include blood-brain-barrier (BBB) breakdown at distinct sites throughout the CNS, lymphomononuclear inflammatory foci, demyelination, reactive gliosis and axonal loss. Based on their composition MS lesions can be classified into different patterns characterised by either T cell and macrophage infiltration (pattern I), antibody and complement deposition (pattern II), distal oligodendrogliopathy and apoptosis (pattern III) or primary oligodendrocyte death (pattern IV)[12]. It is still under debate whether different lesion patterns indicate disease heterogeneity between patients or reflect more different stages of lesions within an individual patient.

In the majority (~85%) of MS patients the disease is initially characterized by bouts of neurological deficits (relapses) and subsequent remission during which the disease is clinically silent (relapsing-remitting MS; RR-MS). RR-MS typically starts between 20 and 40 years of age and is 1.5 to two times more frequent in women than in men. 85-90% of these patients suffering from RR-MS convert within a period of approximately 30 years to a secondary progressive disease stage (SP-MS), which is characterised by absent or only few relapses but a steady progression of irreversible neurological disability.

Ten to 15% of affected patients show a primary progressive (PP) disease course, characterised by gradually progressive clinical deficits from the time of onset. PP-MS affects women and men with the same frequency and usually starts between 30 and 40 years of age. PP-MS patients often present with paraparesis, which worsens gradually and may be accompanied by fatigue, neurocognitive problems and autonomous dysfunction.

Currently approved MS therapeutics act mainly by immunsuppressive or immunomodulatory mechanisms. For general disease management of RR-MS, the first-line treatments glatiramer acetate (GA) and three slightly different versions of recombinant interferon (IFN)-β proteins are used. GA and IFN-β moderately reduce relapse rate, decrease CNS inflammation as measured by magnetic resonance imaging (MRI), and possibly slow progression of permanent neurological disability[13-16]. IFN-β exerts multiple anti-inflammatory effects, but the main

mechanisms of immunmodulation that underlie its effects in MS remain poorly understood. GA is a mixture of random polypeptides composed of the four amino acids alanine, lysine, glutamic acid and tyrosine at a fixed molar ratio and peptide lengths up to 90 amino acids. GA was designed to mimic myelin-basic protein (MBP), one of the major autoantigens in MS. GA reduces antigen presentation and stimulates secretion of anti-inflammatory cytokines from T cells[17]. Patients with highly active RR-MS, who have failed at least one of these treatments, can be escalated to more aggressive therapies such as natalizumab, a humanized monoclonal antibody targeting α4 integrins or mitoxantrone, an anthracycline-derived chemotherapeutic agent. Natalizumab inhibits binding of leukocytes to vascular endothelium, a critical step for immune cell entry into the CNS[18]. Mitoxantrone acts via elimination of a broad range of immune cells[19]. In addition to these four immunomodulatory treatments, several other small molecule drugs and monoclonal antibodies are in phase III clinical testing or filed for approval.

There is currently no treatment for PP-MS and progressive disease stages of SP-MS, where cumulative neuronal and axonal loss is the predominant feature of the disease. Therefore, in addition to the multiple immunomodulatory and –suppressive treatments, neuroprotective therapies are urgently needed. Several different approaches are currently being investigated including ion channel blockers[20-25], inhibitors of excitotoxicity[22,26-29] and growth factors like erythropoietin[30,31]. Recently, a slow release inhibitor of voltage-dependent potassium channels, 4-aminopyridine (fampridine), has successfully been tested in a phase-III clinical trial[32]. Fampridine leads to symptomatic benefits such as increased muscle strength in approximately 30% of MS patients, probably by increasing conduction in demyelinated axons[33].

1.2 Multiple sclerosis as prototypical autoimmune disease

Although the etiology of MS is currently still incompletely understood, a combination of genetic and environmental factors is considered responsible for the development of a deregulated $CD4^+$ T cell-mediated autoimmune response, which leads to chronic CNS inflammation, demyelination and axonal loss. Genetic linkage and association studies implicate alterations of the immune system as the most important etiologic factors of MS, as they mainly identified genes with suggested immune functions as risk factors. Of these, the strongest association has been mapped to the major histocompatibility complex (MHC) class II region[9,34-36], in particular the *DR15/ DQ6* haplotype[37,38]. MHC molecules are expressed on

the surface of cells in all jawed vertebrates and present peptides from self and foreign proteins. These peptide-MHC complexes can be recognized by specific T cell receptors (TCR) expressed on either $CD4^+$ T helper cells or $CD8^+$ cytotoxic T cells. MHC class I (MHCI) molecules, which are present on all nucleated cells, are loaded in the endoplasmic reticulum (ER) with peptides originating from proteasomal degradation of endogenous proteins synthesized in the cell. Upon transport to the cell surface, peptide-MHCI complexes can be recognized by $CD8^+$ cytotoxic T cells. MHC class II (MHCII) molecules are expressed on professional antigen-presenting cells (APC) like dendritic cells, macrophages and B cells. MHCII molecules are loaded with peptides originating from lysosomal degradation of exogenous proteins ingested by the cell, and present these peptides to $CD4^+$ T helper (Th) cells. By a process called cross-presentation, professional APCs can also present peptides derived from exogenous proteins on their MHCI molecules to $CD8^+$ T cells. When a $CD4^+$ T cell recognizes its cognate antigen in the context of MHCII, it clonally expands and co-ordinates the immune response against the recognized pathogen. When a $CD8^+$ T cell recognizes its cognate antigen in the context of MHCI on a professional APC, it clonally expands and can then travel throughout the body in search of an antigen-positive somatic cell, which is then subject to cytolysis by the specific $CD8^+$ T cell. The genetic association of the MHCII region with the risk for developing MS therefore implies that $CD4^+$ T cells contribute to disease pathogenesis. Recent data also implies a contribution of MHC class I genes to this genetic risk [39-42], which might suggest a pathogenic role for $CD8^+$ T cells as well[43]. In addition to the MHC region, genes encoding for cytokine receptors involved in lymphocyte growth and survival, e.g. Interleukin (IL)-7 receptor (*IL7R*) and IL-2 receptor alpha (*IL2RA*), have also been associated with the disease[44-47]. The success of recent therapy trials with monoclonal antibodies specifically targeting immune cells underlines the importance of the immune system in MS. Examples are the prevention of CNS infiltration by natalizumab (anti-$\alpha 4\beta 1$ integrin)[48], T cell and monocyte depletion by alemtuzumab (anti-CD52)[49] as well as B cell depletion with rituximab (anti-CD20)[50].

1.2.1 The role of $CD4^+$ T cells

The hypothesis that MS is mediated by autoreactive T cells is supported by several lines of evidence[51]. In humans, myelin-specific T cells can be isolated from peripheral blood and cerebrospinal fluid (CSF) of MS patients[52-58], and a phase II clinical trial with altered peptide ligands (APL) has shown that relapses are preceded by expansion and activation of MBP-specific $CD4^+$ T cells in the peripheral immune compartment[59]. In animals, a disease that

recapitulates key histopathological features of MS, experimental autoimmune encephalomyelitis (EAE), can be experimentally induced by immunization with myelin proteins and peptides emulsified in complete Freunds Adjuvant (CFA)[60,61]. This immunization leads to peripheral expansion and CNS-infiltration of myelin-specific $CD4^+$ T cells[62,63]. The ability to transfer this disease from immunized animals to naive recipient animals by adoptive transfer of these $CD4^+$ T cells[64,65], has identified myelin-specific $CD4^+$ T cells as the triggers of autoimmune demyelination in the CNS in this disease model. Transgenic mouse models provide further evidence for the causality of $CD4^+$ T cells for MS. Transgenic mice expressing MHCII-restricted myelin-specific mouse TCRs can spontaneously develop optic neuritis and paralytic EAE[66-70]. Moreover, several humanized transgenic mice expressing both MS-associated HLA-DR molecules and myelin-specific TCRs derived from $CD4^+$ T cell clones of MS patients also show spontaneous disease[71-73], demonstrating the encephalitogenic potential of human $CD4^+$ T cells.

As mentioned above, $CD4^+$ T cells are the central co-ordinators of an adaptive immune response. They drive immune responses against a wide variety of pathogens but can also suppress immune responses to control autoimmunity. They stimulate antibody production by B cells, enhance and maintain $CD8^+$ cytotoxic T lymphocyte (CTL) responses and regulate the function of phagocytes at the site of infection. After the invading pathogen is cleared, most antigen-specific $CD4^+$ T cells die, but some cells save the acquired status of immunity by differentiating into memory cells.

Naive $CD4^+$ T cells that have not previously encountered an antigen are activated by professional APCs presenting the cognate antigen in lymph nodes. Depending on the cytokine milieu present during $CD4^+$ T cell activation, T helper (Th) cells acquire diverse effector Th phenotypes, like Th1, Th2 and Th17. Depending on the Th phenotype acquired by $CD4^+$ T cells, different effector functions of the immune system are activated. Th1 cells promote a cell-mediated immune response to intracellular pathogens by production of IFN-γ and activation of macrophages, while Th2 cells organize humoral immunity against extracellular pathogens by secretion of IL-4, -5 and -13 and the activation of B cells[74]. The production of IL-17 by e.g. Th17 cells plays an important role in the recruitment of neutrophils[75] and their homeostasis[76]. Th17 cells are mainly involved in the defense against extracellular bacteria and fungi[77].

$CD4^+$ T cells differentiate into Th1 cells in the presence of IL-12[78], while IL-4 drives Th2 differentiation[79]. Th17 cells originate in the presence of TGF-β, IL-6 and IL-23[80,81]. If anti-

inflammatory cytokines like TGF- β or IL-10 are present, naive $CD4^+$ T cells can differentiate into induced regulatory T cells (iTreg), which are able to suppress responses of $CD4^+$ effector T cells together with thymus-derived naturally occuring regulatory T cells (nTreg)[74,82].

Until a couple of years ago, Th1 cells were thought to be the only $CD4^+$ T cell subset involved in the pathogenesis of MS and EAE[51]. However, interference with Th1-differentiation or anti-IFN-γ treatment aggravates EAE[83-89]. In contrast, inhibition of Th17 differentiation by blocking IL-23[90,91] is clearly beneficial in this model. Both Th1 and Th17 cells have been shown to elicit adoptive transfer EAE, albeit with different pathological outcomes[92]. Therefore Th17 cells are now considered an additional responsible $CD4^+$ T cell subset for the development of EAE[93]. In MS, the contribution of Th subsets to the development and progression of the disease is much less clear. Strong and long-lasting evidences argue for an important role of Th1 cells for the pathogenesis of MS[51]. The importance of Th1 cells for MS is particularly demonstrated by elevated levels of Th1 polarizing cytokines like IL-12 and IL-18 in serum, CSF and CNS lesions in MS patients[94-99] and the production of IFN-γ and TNF-α by myelin-specific T cells[51,58,100-103]. Furthermore, MS is exacerbated by administration of IFN-γ[104]. Only very recently human Th17 cells have been implicated in the pathogenesis of MS and IL-17 production by CNS-infiltrating T cells has been associated with active disease[105,106], suggesting that maybe Th17 cells are involved in the pathogenesis of MS in addition to Th1 cells.

1.2.2 Experimental autoimmune encephalomyelitis (EAE)

Most of our current understanding about the inflammatory processes in the development of autoimmune CNS inflammation in MS stems from research in its most accepted animal model, which is EAE. In vaccination studies performed by Louis Pasteur in 1885, the inoculation of rabies virus preparations that had been generated in rabbit spinal cord lead to vaccination-induced encephalitis as an adverse effect. In 1933, Thomas Rivers showed that brain homogenates can trigger encephalitis and that the above cases of encephalitis after rabies vaccination were most likely due to contaminations of the vaccine by brain constituents[107]. He repeatedly injected rabbit brain homogenate into rhesus monkey and oberserved in two out of eight treated animals the development of paralytic disease, which was later termed EAE.

This model has evolved considerably in the intervening years. Current immunization regimens include whole spinal cord, myelin proteins and even defined peptides, usually

emulsified in complete Freunds adjuvant (CFA), which is composed of paraffin oil, mannite mono-oleate as surfactant and heat-inactivated mycobacterium[108]. Subcutaneous injection of several CNS antigens has been shown to induce EAE in certain strains of mice and rats, as well as guinea pigs, rhesus monkey and common marmosets[61]. In inbred rodents, susceptibility to EAE critically depends on the genetic background and on the autoantigen applied. Even though many myelin and non-myelin proteins have been studied as autoantigens in EAE, only a few models are commonly used in research. These are immunization of Lewis rats with myelin basic protein (MBP), immunization of C57BL/6 mice with myelin oligodendrocyte glycoprotein (MOG) or immunization of SJL/J mice with proteo-lipid protein (PLP). Whereas Lewis rats and C57BL/6 mice experience a mononophasic or chronic disease course, SJL/J mice show a relapsing-remitting EAE. Since many transgenic mouse strains are bred onto C57BL/6 genetic background, MOG-induced EAE in these mice is by far the most popular of those. In these models, clinical symptoms usually start 10-12 days after immunization, leading to ascending paralysis. EAE-severity is ususally determined on a 5-point scale, which accounts for motor function (see also 4.2.2). In addition to the active induction by immunization, EAE can also be transferred from immunized animals to naive recipient animals. For this, $CD4^+$ T cells are isolated from draining lymph nodes of immunized animals, restimulated *in vitro* with autoantigen, and then injected into recipient animals. Usually, passively induced EAE shows an accelerated and aggravated disease course compared to actively induced EAE[63].

Additionally to these ‚conventional' EAE models, transgenic animals expressing myelin-specific TCRs or B cell receptors have also been developed[66-71,109,110]. In these models, a significant proportion of animals develops spontaneous EAE and can therefore serve as valuable tools for the investigation of early events during disease pathogenesis.

Pathologically, EAE reflects some features of MS such as $CD4^+$ T cell infiltration into the CNS, demyelination and axonal loss[111], but research in these ‚conventional' EAE models has clear limitations. In particular mouse models of MS show only a minor involvement of B cells and antibodies in disease pathology. This characteristic feature of MS lesions can only be well reflected in primate EAE models[112].

One major bias of EAE in general is the mode of induction. Since we do not know the natural cause of MS, the active induction of myelin-specific $CD4^+$ T cells in the animal might by-pass important processes for the development of the disease in humans. Additionally, the use of mycobacteria as adjuvant leads always to a Th1/17 polarized $CD4^+$ T cell response[113], which

allows little variability in disease initiating pathways. Furthermore, the different time courses of human disease and animal model are another obstacle in the translation of results from EAE to MS. While disease induction in the animal takes days to weeks, MS patients suffer from a disease course over years and decades. Therefore, long-term outcomes or late adverse effects of treatments are rarely observed in EAE, but occur in humans.

Most importantly, there have been significant problems in the translation of efficacious treatments from EAE to MS. Most therapeutic approaches based on concepts derived from EAE studies were either less effective in patients, worsened disease or caused unexpected, severe adverse events[114]. In order to improve the predictive value of EAE experiments, partially humanized EAE models have been developed. Transgenic expression of human TCRs and MHC molecules is now used to investigate the pathogenicity of certain TCRs and the genetic control of disease susceptibility[71-73,115]. These transgenic models often develop spontaneous disease in a significant proportion of animals, similar to transgenic animals expressing mouse TCRs.

In summary, EAE is an excellent tool for studying basic mechanisms of brain inflammation and immune-mediated tissue injury, and for obtaining proof of principle, whether a certain therapeutic strategy has the potential to block these pathways. The relevance of results from EAE models for MS has then to be determined by research with human material or in respective clinical studies. Clearly, dissimilarities in the immune system of model animals and humans have to be considered when results from EAE are translated to MS. One possibility to incorporate human molecules and genetic risk factors of MS are partially humanized transgenic animals, but the development of more animal models is urgently needed to reflect the complexity of MS in experimental systems.

1.3 Development of autoimmune CNS inflammation in multiple sclerosis

1.3.1 Autoimmune T cell response in the CNS

In order to initiate inflammation in the CNS, naive myelin-specific $CD4^+$ T cells have to be activated in peripheral lymphatic tissues, migrate to the CNS and then be reactivated by local APC displaying their cognate antigen[116]. The CNS, however, constitutes an environment, where the initiation of destructive immune responses is impeded by a number of different mechanisms. The CNS is mainly protected by its endothelial barriers, the blood-brain-barrier

and the blood-CSF-barrier, which tightly regulate the access of soluble mediators and cells[117]. As unactivated T cells are unable to migrate into the intact CNS[118,119], prior peripheral activation and conversion to memory T cells is a prerequsite for the initiation of CNS inflammation.

The generation of self-specific memory T cells in the periphery is still incompletely understood. First, a susceptible individual has to express MHC molecules, which are able to present peptides from myelin-proteins, a factor, which is probably reflected in the genetic association of certain MHC alleles with the risk to develop MS and the correlation of the MHC haplotype of different mouse strains with their susceptibility to EAE[51]. The presented peptide has then to be recognized by an appropiate myelin-reactive T cell. In the thymus, where T cells mature, T cells recognizing self peptides are normally negatively selected and deleted from the repertoire. It is evident, that this process of so-called central tolerance is incomplete, as myelin-specific T cells can not only be detected in MS patients, but also occur in comparable amounts in healthy individuals[52,53,56,57,120], suggesting that autoreactive T cells are part of the normal repertoire. These probably mostly low-avidity T cells do not engage their self-antigen in the periphery in non-pathological conditions and circulate in a state of 'ignorance'[121,122]. But if APCs sensing an infection or tissue damage upregulate MHC complexes and costimulatory molecules, the avidity of the interaction between the self-reactive T cell and the APC might be increased, so that the T cell now is activated and might convert to a memory T cell. Indeed, a higher frequency of *in vivo* activated high-avidity myelin specific $CD4^+$ T cells can be detected in the peripheral blood of MS patients compared to healthy controls[103].

Apart from myelin proteins expressed in the thymus that promote central tolerance[123-127], most myelin proteins implicated as autoantigens in MS are exclusively expressed by oligodendrocytes in the CNS. Exceptions are MBP, which is also expressed in lymphatic tissue[128-130], although at low levels, and MOG, which is not restricted to the CNS but also occurs in peripheral nervous system (PNS) myelin[131]. It is unclear, how T cells that are specific for CNS-restricted myelin proteins are activated in the periphery. In mouse models where the transgenic expression of MBP- and PLP-specific TCRs results in the development of spontaneous EAE, the T cell response seems to start in cervical lymph nodes[132,133]. Since cervical lymph nodes play a major role in the lymphatic drainage of the CNS[134], self-antigens might drain from the injured CNS and thus be available there for presentation by APCs. Another hypothesis is based on the discovery of T cell degeneracy. The observed cross-

reactivity of myelin-specific T cell clones with pathogen-derived peptides can be based on either sequence homology or structural similarities (molecular mimicry)[135-140]. A peripheral myelin-specific T cell that expresses a cross-reactive TCR could therefore be activated in the context of an infection by recognizing its cross-reactive foreign antigen, resulting in the conversion to a memory T cell which gains access to the CNS and can there be reactivated by the corresponding self antigen. So far, cross-reactivity for peptides from several viruses, like Epstein-Barr-virus (EBV)[140] and human herpes virus 6 (HHV6)[141], has been identified, but no infectious trigger for MS has been conclusively established yet[142].

Memory T cells probably first cross the blood-CSF-barrier at the choroid plexus, which constitutively expresses the required selectins, adhesion molecules and chemokine receptor ligands[117,143,144]. After their infiltration into the subarachnoid space (SAS), memory T cells are reactivated by autoantigens presented on local MHCII-expressing APC, probably brain-resident macrophages or dendritic cells[145,146]. The resulting local inflammatory response and the occuring damage probably leads to local and distal activation of microglia and the production of pro-inflammatory cytokines, which induce the upregulation of adhesion molecules and chemokines at other sites of brain endothelium, facilitating leukocyte entry and initiation of CNS inflammation at multiple locations[144].

1.3.2 Innate immune contributions to the development of multiple sclerosis

Although self-reactive $CD4^+$ T cell subtypes seem to be instrumental to the initiation of MS, additional immune cell subsets may also play essential roles in initiation or progression and modification of the disease. For example, disease-promoting roles for B cells and $CD8^+$ T cells have recently been suggested[50,147-149], and also cells from the innate immune system can influence disease pathogenesis. The role of innate lymphocytes, like natural killer (NK) cells or NKT cells is controversially discussed. These cells can either contribute to the inflammatory damage in the CNS or also regulate the autoimmune T cell response[150,151]. However, it has been clearly shown that innate immune cells with antigen-presenting function like microglia, macrophages and dendritic cells have fundamental influences on disease onset, relapses and disease progression[152-156].

The avidity between a self-reactive T cell and the APC can be increased if MHC complexes and costimulatory molecules are upregulated, e.g. in case of an infection. Infections are generally first recognized by cells of the innate immune system, which then deliver signals to

APCs or T cells to initiate an adaptive immune response. Innate immune cells sense infectious triggers by recognizing conserved surface structures by germline-encoded pattern recognition receptors (PRR). Among those, Toll-like receptors (TLR), which are the best understood family of PRRs, have been shown to play an essential role in the development of EAE[157]. Stimulation of a TLR on innate immune cells leads to changes in the activated cells including upregulation of surface molecules like MHC or costimulatory molecules and the production of chemokines and cytokines, which influence the modality of the resulting immune response respectively[158,159]. In addition to the role of TLRs, epidemiological evidence argues for the involvement of signals from the microbial environment in the development of MS. Systemic infection increases the risk to experience a MS relapse in the next two months by a factor of 1.3 – 3.4[160-162]. Relevance for the microbial environment can also be found in animal models. In one strain of MBP-specific TCR transgenic mice the incidence of spontaneous EAE that develops increases as the level of microbial exposure increases[163], and in another model of PLP-specific TCR transgenic B10.S mice, the administration of microbial products leads to breakdown of tolerance and the development of autoimmune disease in these normally resistent animals[69]. The importance of innate immune signals for the development of an autoimmune T cell response in the CNS is further supported by the fact that induction of EAE requires immunization with CFA supplemented with *Mycobacterium tuberculosis*.

1.3.3 Neutrophil granulocytes in multiple sclerosis

Neutrophil granulocytes (neutrophils) are vital effector cells of the innate immune system, involved in the first line defence against pathogens. Neutrophils are terminally differentiated ready-to-act effector cells and have a short half-life. They can be immediately released from a pool of mature cells retained in the bone marrow, therefore neutrophils are easily expandable in numbers, quickly recruited to inflamed tissue and act without delay[164]. Neutrophils exhibit potent phagocytic properties and have a unique arsenal of microbicidal mediators that are rapidly released upon contact with pathogens. Microorganisms are either phagocytosed by neutrophils, destroyed via oxygen-dependent and independent mechanisms or sequestered in extracellular traps[165,166].

Besides their effector functions, neutrophils are also involved in the onset and orchestration of adaptive immune responses. They secrete multiple cytokines and chemokines, which recruit monocytes and dendritic cells to the site of infection and influence their maturation[167-169]. Neutrophils can further directly influence T cell responses, as they migrate into T cell areas in

the spleen upon TLR-stimulation[169], are able to secrete T cell attracting chemokines[165,170] and can secrete T cell modulating cytokines such as IL-12, IFN-γ, TNF-α, IL-6, TGF-β or even IL-10[171-176], which are known to influence the differentiation of encephalitogenic Th1 and Th17 cells. Vice versa, IL23-driven differentiation of IL-17 producing T cells, e.g. Th17 cells, mediates neutrophil recruitment and homeostasis[75,76]. IL-17 mediates neutrophil recruitment directly and indirectly by inducing the expression of neutrophil-attracting proteins like G-CSF, GM-CSF and CXCL8[177,178]. High numbers of IL-17-producing T cells in inflamed tissues generally correlate with a prominent neutrophil infiltration[179,180].

In the context of MS, neutrophils have so far been implicated only in specific forms of the disease, like neuromyelitis optica (NMO), opticospinal MS and aggressive MS-like diseases: Chemokines that attract neutrophils have been detected in CSF, brain endothelial cells and microglia of MS patients[181-183] and CNS-infiltrating neutrophils have been reported in the Marburg's variant of MS[184]. Moreover, peripheral blood neutrophils from MS patients were found pre-activated in active MS compared to inactive MS and control donors[185,186], suggesting that neutrophil functions in the periphery are substantially altered during MS relapses.

Neutrophil-attracting chemokines can be detected in several EAE models[187-189] and neutrophils have been shown to amplify in peripheral tissues and to infiltrate into inflammatory CNS lesions of SJL/J and BALB/c mice upon EAE induction[187,190,191]. Although the number of CNS-infiltrating neutrophils is low in some models, treatment with an anti-Gr1 antibody, which primarily depletes neutrophils, or impairment of the recruitment of neutrophils to the CNS completely abrogates EAE in BALB/c and SJL/J models[187,192]. Although administration of anti-Gr1 antibody does not only result in the depletion of neutrophils, and also targets a specific inflammatory subset of monocytes and some T cells[175,193], these studies suggest a potential role for neutrophils in the induction of EAE. The functional mechanism by which neutrophils contribute to the development of EAE is so far unknown.

1.4 Damage and repair mechanisms in multiple sclerosis

The lesions observed in the CNS of MS patients are typically characterised by a demyelinated core separated by a very sharp border from normally myelinated surrounding tissue and are infiltrated by mononuclear cells[4]. This observation led to the primary description of MS as inflammatory demyelinating disease. Demyelination is probably the result of inflammatory

damage to oligodendrocytes and the myelin sheath[194,195] mediated by toxic cytokines, glutamate[196,197], radicals[198-200], antibodies[201-203] and microglia/ macrophages[204]. In demyelinated areas, saltatory conduction is inhibited and signal conduction is either slowed or no longer possible[23]. Oligodendrocyte precursor cells, which are present in the vicinity to lesions at all disease stages, can differentiate and remyelinate denuded internode areas[205]. Although the myelin sheath of remyelinated axons is thinner, conduction properties are often largely restored[206]. Remyelination is particular frequent in early MS stages and can even be detected in acute lesions[207], but remyelination efficiency seems to vary between different CNS regions and among patients[208]. In later stages of disease, remyelination efficiency decreases leaving an increasing number of lesions chronically demyelinated[209].

Inflammatory demyelination is still considered the primary disease pathology today, but axonal loss has been identified as the major cause of irreversible disability in MS patients[3,210]. Although the loss of nerve fibers in lesions has been described early in MS-research[211], these observations were disregarded until the end of the 20th century. Over the disease process, axonal damage and loss occur in the setting of acute inflammatory demyelination in active lesions[3] probably mediated by the inflammatory milieu described above[212] and as consequence of chronic demyelination, which challenges energy-demanding compensatory mechanisms and ultimately leads to ion imbalance and excitotoxicity[23,213-216]. It is also controversial, whether progressive neurodegeneration in SP-MS is exclusively resulting from chronic demyelination or still additionally triggered by inflammatory processes[212,217].

In contrast to axons in fish and tailed amphibians, mammalian embryonic CNS axons or axons of the peripheral nervous system (PNS), axons of the adult mammalian CNS have limited capabilities to regenerate axons after injury[218]. Spontaneous regeneration of peripheral nerves is mediated by activation of their intrinsic growth capacity by injury-related signals and facilitated by a permissive environment[219]. Adult CNS axons are thought to possess this intrinsic regenerative capacity too, but axonal regrowth is prevented by an inhibitory environment[220-222]. The major factor contributing to this environment is CNS myelin[223]. After injury, inhibitory proteins contained in myelin debris are responsible for axonal regeneration failure in the adult CNS. Additionally, chemorepulsive guidance molecules like semaphorins and ephrins are still expressed in the adult CNS and could therefore also contribute to the inhibition of axonal regrowth after injury[224].

Moreover, CNS injury results in the formation of a glial scar, which is composed of various inhibitory extracellular matrix molecules deposited by reactive astrocytes. This structure

forms a mechanical and biochemical barrier to regenerating axons[225,226]. In MS, glial scars are prominent features of inflammatory lesions and can be observed as a uniform and even very early event consequent to autoimmune demyelination[227,228]. Besides providing a non-permissive environment for axonal regeneration, reactive astrogliosis and glial scars might be additionally relevant for tissue stabilization in acute CNS inflammation[229].

1.5 Nogo and Nogo receptor interactions in CNS injury

Myelin-associated proteins mediate inhibition of axonal outgrowth over receptors expressed on axons. But the impairment of regeneration is not the only functional role these ligand-receptor systems play in CNS injury.

1.5.1 Myelin-associated inhibitory proteins and receptor complexes

CNS white matter, consisting of oligodendrocytes and myelin, is a non-permissive substrate for neurite outgrowth[230-232] and mediates growth cone collapse[233]. Three myelin-associated proteins contributing to this effect have been identified: the immunoglobulin superfamily myelin-associated glycoprotein (MAG)[234,235], the reticulon (RTN) family transmembrane protein Nogo[236-238] and a glycosylphosphatidylinositol (GPI)-anchored protein containing a series of tandem leucine-rich repeats (LRR), named oligodendrocyte myelin glycoprotein (OMG)[239].

MAG (siglec 4a) is a sialic acid-binding transmembrane protein with a putative role in the long-term maintenance and organization of the myelin sheath[240]. MAG is expressed in myelin-forming cells, namely Schwann cells in the PNS and oligodendrocytes in the CNS, but the expression level in the CNS is much higher[241]. MAG was the first myelin component for which inhibition of neurite outgrowth was demonstrated[234,235], and it plays a bifunctional role: it promotes axonal outgrowth in young neurons during brain development, but inhibits neurite outgrowth in adult neurons, concomitant with a decrease in neuronal cAMP levels[242-244].

Nogo (Reticulon 4, RTN4) was originally identified as the target antigen of a monoclonal antibody (IN-1)[236-238], which neutralized the growth inhibitory properties of myelin[245] and improved axonal regeneration after partial spinal cord injury[246,247]. From the nogo gene *Rtn4*, three major protein isoforms, Nogo-A, -B and –C are generated via alternate splicing and differential promoter usage[237,248]. The inhibitory action of Nogo on neurite growth is mediated by at least two domains[249], a N-terminal region specific for the Nogo-A isoform (Amino-Nogo) and an extracellular 66 amino acid loop (Nogo-66) between two hydrophobic segments

in the C-terminal domain that is common to all three isoforms. Between the two inhibitory domains, Nogo-66 appears to be more potent in growth cone collapse assays and its effect is more neuron-specific[250]. Nogo-A is predominantly expressed in oligodendrocytes and subtypes of CNS neurons, but not in Schwann cells, and is the only isoform targeted by the IN-1 antibody, which supposedly binds to its N-terminal inhibitory domain[251]. Both inhibitory domains of Nogo-A have been detected on the cell surface[252], but the exact topology of Nogo-A in the cell membrane is unclear. Nogo-B, which is a shorter isoform of Nogo-A, is ubiquitously expressed; whereas Nogo-C, which contains a specific domain encoded by exon 5, is predominantely expressed in muscle tissue[249].

OMG is a glycosylphosphatidylinositol (GPI)-anchored protein containing a series of tandem leucine-rich repeats (LRR), which mediates its growth inhibitory function[253]. In the adult CNS, OMG is primarily expressed in neurons[254,255]. OMG is not found in compact myelin, but rather is expressed in the membrane surrounding the nodes of Ranvier, which is formed by oligodendrocyte-like cells where it prevents collateral sprouting[256].

Although the three myelin-associated inhibitory proteins do not share homologous domains, common receptor complexes mediate their growth inhibitory function. Nogo receptor (NgR1, NgR, RTN4R), a GPI-anchored LRR-containing cell surface glycoprotein was initially identified as a receptor for Nogo-66[250] and later found also to bind to MAG and OMG[239,257,258]. NgR1, which is lacking an intracellular signalling domain, transduces the growth-inhibitory signal via a membrane complex involving low-affinity p75 neurotrophin receptor ($p75^{NTR}$)[259,260] and the LRR- and immunoglobulin domain-containing protein (LINGO-1)[261]. Whereas LINGO-1 is an essential member of this complex, $p75^{NTR}$ can be replaced by the orphan tumor necrosis factor (TNF) receptor superfamiliy member 19 TROY[262]. Binding of Nogo-66, MAG or OMG to these receptor complexes results in the activation of RhoA and the inactivation of Rac1[263]. Activation of the RhoA kinase (ROCK) leads to growth cone collapse and inhibition of axonal growth by influencing the dynamics of the actin cytoskeleton. The modulation of the activity of members of the Rho familiy of GTPases by NgR-signalling is in line with the signalling pathways of many other CNS axonal guidance and growth-regulatory molecules[264].

NgR1 is the founding member of the three-member NgR family. Two homologous genes of NgR1, Reticulon 4 receptor-like 1 (*Rtn4rl1*) and Reticulon 4 receptor-like 2 (*Rtn4rl2*), coding for NgR3 (RTN4RL1) and NgR2 (RTN4RL2), have been identified[265-267]. Like NgR1, NgR2 and NgR3 are GPI-linked proteins that contain LRR domains. Whereas NgR2 was shown to

be a superior binding partner for MAG than NgR1[268], no interaction partner for NgR3 has been identified yet. In the adult, NgR1 and NgR2 are predominantly expressed in the CNS, but low expression can be detected in other tissues[265]. In the brain, NgR1 and NgR2 show overlapping, yet distinct distribution patterns. However, both NgR1 and NgR2 are expressed in several neuronal populations projecting into the spinal cord, including neurons projecting through the corticospinal and several different brainstem tracts[269].

Recently, paired immunoglobulin-like receptor B (PirB) has been identified as another receptor mediating inhibition of axonal growth by Nogo-66, MAG and OMG[270]. PirB belongs to the leukocyte immunoglobulin-like family of immunoreceptors (LIR), and functions as a inhibitory MHCI receptor in B cells, monomyelocytic cells, NK cells and DC[271,272]. In the brain, PirB is expressed on a subset of neurons in the cerebral cortex, hippocampus, cerebellum and olfactory bulb. In addition to mediating regeneration block, PirB was implicated in the regulation of activity-dependent plasticity, probably by recognizing neuronal MHCI[273].

A receptor recognizing the N-terminal inhibitory domain of Nogo-A has not been identified yet. The broad inhibition of cell spreading and growth by this domain is more likely mediated by the functional inhibition of certain integrins in the extracellular matrix, suggesting that a specific neuronal receptor may not exist[274].

1.5.2 Role of Nogo and Nogo receptors in multiple sclerosis

With axonal pathology being a major determinant of neurological disability in MS patients, blocking the action of axonal growth inhibitors could offer a new therapeutic opportunity, especially for patients suffering from progressive disease.

Being a component of the myelin sheath, Nogo was originally considered a potential myelin autoantigen. Indeed, some Nogo-derived peptides are weakly encephalitogenic in EAE susceptible mouse strains[275]. However treatment of immunized mice with Nogo-reactive $CD4^+$ T cell lines or by co-immunization with Nogo-derived peptides is protective in EAE[275,276]. In addition, mice-deficient for either Nogo-A[276] or Nogo-A/B/C[275] show an ameliorated clinical course of EAE, suggesting a benefical role for Nogo-blockade in autoimmune demyelinating diseases such as MS. Since co-immunization with Nogo-derived peptides induced a shift towards the production of anti-inflammatory, Th2-related cytokines in the myelin-specific T cell response, and treatment of EAE mice with anti-Nogo-A antibodies delayed the onset of the disease[276], it is unclear, whether anti-Nogo strategies

solely target its inhibitory function on axonal regrowth or if Nogo-A might have additional roles in the regulation of immune responses. Myelin-associated proteins like Nogo, MAG and OMG could exert immunoregulatory function via Nogo receptors, that are also expressed in immune cells[277-279]. Although Nogo receptors are only expressed at very low levels in lymphatic tissues[265], upregulation of NgR1 and NgR2 over time can be detected on phagocytic macrophages infiltrating after peripheral nerve injury[277]. NgR mediated activation of RhoA in these macrophages mediates repulsion upon contact with myelin, suggesting that upregulation of Nogo receptors after phagocytosis plays an important role in macrophage efflux from the site of injury after myelin debris has been cleared and repair mechanisms are initiated. In the CNS, a similar upregulation of Nogo receptors can be detected in microglia/ macrophages present after spinal cord injury[279] and in MS lesions[280], and a higher number of infiltrating macrophages is observed at the site of spinal cord injury in Nogo-A-deficient mice[281]. Recently, CNS myelin was shown to regulate the motility of activated T cells, B cells and monocytes in an NgR1-dependent manner[278]. This suggests that, similar to the PNS, microglia/ macrophage infiltration and spreading might also be regulated by Nogo receptor signalling in the CNS.

Adding another level of complexity, B lymphocyte stimulator (BLyS) was identified as an additional functional ligand for NgR1[282], suggesting a role for immune-derived molecules in the inhibition of axonal regeneration in the CNS.

In summary, myelin-associated axonal growth inhibitors such as Nogo, MAG and OMG can be considered putative targets for regenerative therapeutic strategies in MS. However, since Nogo and Nogo receptors appear to exert multi-functional roles in the nervous system and possibly also in the immune system, targeting Nogo-A in inflammatory demyelinating diseases such as MS might result in unanticipated side effects. Therefore further studies are needed to dissect the neurobiological from the immunological functions of Nogo and Nogo receptors.

2 AIMS

Experimental autoimmune encephalomyelitis (EAE), the established animal model of the human disease multiple sclerosis has been used widely to identify the pathogenetic mechanisms involved in the initiation of an autoimmune T cell response in the CNS. In this thesis, MOG 35-55-induced EAE in C57BL/6 mice was used to investigate the contribution of different immune cell types to the initiation and maintenance of a chronic autoimmune response in the CNS. Furthermore, the potential of regenerative strategies in the context of chronic CNS inflammation and their crosstalk with the immune response was investigated.

Specific aims:

1. **Characterisation of temporal dynamics of the inflammatory response in the CNS during EAE**

   In order to monitor the CNS-specific immune response, a flow cytometry-based method for the identification and quantification of CNS-infiltrating immune cells was developed. Two aspects of the CNS-specific inflammation were analysed:

   a. Characterisation of early events during the initiation of CNS inflammation

   b. Analysis of the inflammatory response in the CNS at later time points of chronic disease

2. **Analysis of the functional role of early CNS-infiltrating cells**

   The purpose of this part was to follow up on the results obtained from the flow cytometric characterisation of CNS inflammation described above. Having identified neutrophils as main components of early CNS inflammation during EAE, the functional role of these cells was further investigated. Therefore, the neutrophil-response to the induction of EAE was characterised and a neutrophil-specific depletion system was established.

3. **Functional role of Nogo receptors in chronic autoimmune inflammation in the CNS**

   Nogo receptors are considered the main mediators of myelin-associated inhibition of axonal regrowth after CNS injury. Additionally, Nogo receptors might also be involved in the regulation of inflammatory responses in the nervous system. Using NgR1- and NgR2-deficient animals, the potential of a regenerative approach targeting Nogo receptor mediated inhibition of axonal regrowth during chronic CNS inflammation was examined. Furthermore, potential immunomodulatory functions of Nogo receptors were investigated.

3 MATERIAL AND METHODS

3.1 Material

3.1.1 Reagents

Reagent	*Company*	*Cat. #*
Animal experiments		
Animal lancets	Goldenrod	GR-4mm
Freund's Adjuvans, incomplete	Difco Laboratories	263910
Ketanest® 25 mg/ml	Pfizer	7829486
Mouse/ rat MOG 35-55 peptide MEVGWYRSPFSRVVHLYRNGK-NH2	NeoMPS	
Mycobacterium tuberculosis H37Ra	Difco Laboratories	231141
Pertussis toxin, bordetella pertussis	Calbiochem	516560
Rompun® 2%	Bayer	1320422
Cell isolation and cell culture		
2-mercaptoehanol	Invitrogen	31350010
[methyl-^{3}H]-Thymidine	Amersham	TRK300
Anti-CD3 (clone 145-2C11)	eBioscience	16-0031
Anti-Ly-6G Microbead Kit	Miltenyi Biotech	130-092-332
Brefeldin A	eBioscience	00-4506
$CD4^{+}$ T cell Isolation Kit II	Miltenyi Biotech	130-091-041
Collagenase A, from Clostridium histolyticum	Roche	10103578001
DNaseI, from bovine pâncreas	Roche	11284932001
Dulbecco's Phosphate Buffered Saline (PBS), 10x	Gibco	H15-011
Dulbecco's Phosphate Buffered Saline (DPBS), 1x	Gibco	H15-002
Ethylenediaminetetraacetic acid (EDTA), 0.5M	Fluka	GA11296
Ionomycin	Sigma-Aldrich	I0634
L-Glutamine, 200mM	Gibco	25030

Mouse/ rat MOG 35-55 peptide	NeoMPS	
Percoll	GE Healthcare	17-0891-01
Phorbol myristyl acetate (PMA)	Sigma-Aldrich	P1585
RPMI 1640	Gibco	61870
Serum, fetal bovine	PAA	A15-104
Trypan blue solution, 0.4%	Sigma Aldrich	T8154

Histology/ immunohistochemistry

3,3 diaminobezidine tetrahydrochloride (DAB)	Sigma-Aldrich	D5637
Antibody diluent reagent solution	Zymed	00.3218
Bielschowsky for neurofibrils, Kit	Bio-Optica	NIO 04-040805
Eukitt	Kindler	
Eosin, yellow	Merck	1159350100
Ethanol, ≥99,8 %, 2.5l	Roth	9065.2
Ethanol, absolute, denatured	Th.Geyer	RW/ETV99
Fluoromount G	Southern Biotech	0100-01
H 33258 (bisBenzimide)	Sigma-Aldrich	B1155
Hämalaun (Mayer)	AppliChem	A0884
Hämalaun (Harris)	AppliChem	A0884
Histofine simple stain Max PO	Nichirei Bioscience	414154 F
Hydrogen peroxide	Merck	1.07209
Isopentane	Roth	3747.1
Normal donkey serum	Chemicon	S30-100ML
Normal goat serum	DAKO	X 0907
Para-formaldehyde	AppliChem	A3813
Sucrose	Roth	4621.2
Tissue Freezing Médium	Leica	0201 08926
Triton X-100	Roth	3051.2
TO-PRO-3	Molecular Probes	T3605
Xylol	SDS	0750021
Xylol replacement XEM-200	Vogel	ND-HS-200
Zinc formalin solution	Thermo Shandon	3313-RAS

Flow cytometry

FACS Clean	BD Biosciences	340345
FACS Flow, 20l	BD Biosciences	342003
FACS Lysing Solution	BD Biosciences	349202
FACS Rinse	BD Biosciences	340246
Fixation Buffer	eBioscience	00-8333
FoxP3 Staining Buffer Set	eBioscience	00-5523
LIVE/DEAD®Fixable Aqua Dead Cell Stain Kit	Molecular Probes	L34957
Permeabilisation Buffer, 10x	eBioscience	00-8333-53
Sodium azide	Roth	K305.1
TruCOUNT® tubes	BD Biosciences	340334

DNA isolation and genotyping PCR

dNTP set, 100mM Solution	Fermentas	R0189
DreamTaq DNA Polymerase 500U	Fermentas	EP0702
Invisorb Spin Tissue Mini Kit	Invitek	10321002

RNA isolation/ cDNA synthesis/ real-time-PCR

DEPC	Sigma-Aldrich	D5758
dNTP set, 100mM Solution	Fermentas	R0189
LiChrosolv, ultra pure water	VWR International	1.15333. 2500
Master Mix, qPCR Plus for SYBR Green	Eurogentec	RTSN2X03
M-MLV Reverse Transcriptase 50000U, 200U/µl	Promega	M170B
M-MLV RT 5x Buffer, 1ml	Promega	M531A
Random hexamers 5'-phosphate (pd(N)6)	GE Healthcare	27-2166-01
RNAeasy mini Kit	Qiagen	74104
RNAsin RNase inhibitor 2500U, 40U/µl	Promega	N211A
TriZOL	Invitrogen	15596-026

Other reagents

1,4-dithiothreitol (DTT)	Roth	6908.1
2-mercaptoethanol	Roth	4227.3
Acrylamide/ bisacrylamide (30%/ 0.8%)	Roth	3029.1

Agarose	Invitrogen	15510-027
Agfa developer G 153	PMA Bode	WG0074VJ
Agfa fixer G 354	PMA Bode	WG0171VK
Albumin standard ampules, 2 mg/ ml	Pierce	23209
Ammomiumperoxodisulfate (APS)	Roth	9592.3
BETAPLATE SCINT	Perkin-Elmer	1205-440
Bovine serum albumin (BSA)	PAA	K45-001
Bradford reagent Roti-quant	Roth	KO15.3
Bromphenolblue	Merck	L516544
Buffer solution pH = 4.0	Roth	A517.1
Buffer solution pH = 7.0	Roth	P713.1
Buffer solution pH = 10	Roth	P716.1
Citric acid	Merck	244
Carbon dioxide 100%	TMG GmbH	
Carbon dioxide 90%, Oxygen 10%	TMG GmbH	
EDTA disodium salt, dihydrate	Roth	8043.2
Ethidium bromide	Roth	2218.1
Glacial acetic acid	Roth	6755.2
Glycerol	AppliChem	A1123
HEPES	Roth	9105.2
Hydrochloric acid	Roth	4625.2
Immobilion western HRP substrate	Millipore	WBKL50100
Isopropanol	Roth	6752.4
Milkpowder	Roth	T145.2
Nonidet p40 substritute (NP40)	Fluka	74385
Orange G	Roth	O318.1
Protease inhibitor cocktail (100x)	Serva	39102.01
Potassium acetate (KAc)	Roth	T874.1
Saline (0.9%)	Braun	12211753
Sakura GLC	Sakura	468253
Sodium chloride	AppliChem	A1149,5000
Sodium citrate	Sigma-Aldrich	S-4641
Sodium-dodecyl-sulfate (SDS)	Roth	2326.2

Sodium-hydroxyde	Roth	6771.2
Sucrose	Roth	4621.2
TEMED	Roth	2367.3
Tris	AppliChem	A1086
Xylene Cyanol	Fluka	95600

3.1.2 Antibodies

Flow cytometry

Antigen	*Label*	*Clone*	*Company*	*Cat. #*
CD3e	PE-Cy5.5	145-2C11	eBioscience	35-0031
CD3e	PerCP-Cy5.5	145-2C11	BDPharmingen	551163
CD3e	PacificBlue	500A2	BDPharmingen	558214
CD4	PE	GK1.5	eBioscience	12-0041
CD4	PE-Cy7	GK1.5	eBioscience	25-0041
CD4	APC-eFluor780	RM4-5	eBioscience	47-0042
CD4	eFluor450	RM4-5	eBiocience	48-0042
CD8a	PacificBlue	5-3-6.7	eBioscience	57-0081
CD11b	FITC	M1/70	eBioscience	11-0112
CD11b	FITC	M1/70	BDPharmingen	557396
CD11b	PerCP-Cy5.5	M1/70	BDPharmingen	550993
CD11b	APC	M1/70	eBioscience	17-0112
CD11c	PE-Cy7	N418	eBioscience	25-0114
CD11c	APC	N418	eBioscience	17-0114
CD16/32 (Fc-Block)	-	93	eBioscience	12-0161
CD25	Alexa488	PC61.5	eBioscience	53-0251
CD25	APC	PC61.5	eBioscience	17-0251
CD40	APC	1C10	eBioscience	17-0401
CD44	APC	IM7	eBioscience	17-0441
CD45	PE-Cy7	30-F11	eBioscience	25-0451
CD45	APC-Cy7	30-F11	BDPharmingen	557659

CD45	APC-eFluor780	30-F11	eBioscience	47-0451
CD45R (B220)	PE-Cy5.5	RA3-6B2	eBioscience	35-0452
CD62L	PE-Cy7	MEL-14	eBioscience	25-0621
CD64	Alexa647	X54-5/7.1	BDPharmingen	558539
CD69	FITC	H1.2F3	eBioscience	11-0691
CD69	PE-Cy7	H1.2F3	eBioscience	25-0691
CD80	FITC	16-10A1	eBioscience	11-0801
CD80	PE	16-10A1	eBioscience	12-0801
FoxP3	PE	FJK-16S	eBioscience	12-5773
Gr-1	FITC	RB6-8C5	eBioscience	11-5931
Gr-1	PacificBlue	RB6-8C5	eBioscience	57-5931
Gr-1	eFluor450	RB6-8C5	eBioscience	48-5931
IFN-γ	PE	XMG1.2	eBioscience	12-7311
IL-17A	Alexa647	eBio17B7	eBioscience	51-7177
Ly-6G	PE	1A8	BDPharmingen	551461
Ly-6G	V450	1A8	BDPharmingen	560603
MHCII (b, d, p, k)	FITC	M5/114.15.2	eBioscience	11-5321
NK1.1	PE	PK136	eBioscience	12-5941
NK1.1	PE-Cy7	PK136	BDPharmingen	552878
Neutrophils	FITC	7/4	AbDSerotec	MCA771GA
Vα3.2 TCR	FITC	RR3-16	BDPharmingen	553219
Vβ11 TCR	PE	RR3-15	BDPharmingen	553198

Primary antibodies for immunohistochemistry

Antigen	*Isotype*	*Clone*	*Company*	*Cat. #*
APC	msIgG2b	CC-1	Calbiochem	OP80
CD3e	rabIgG	-	Dako	A0452
CD3e	arHamIgG1	145-2C11	eBioscience	14-0031
CD3e	ratIgG2b	17A2	BDPharmingen	555273
CD3e	ratIgG2a	KT3	AbDSerotec	MCA500GA
CD4	ratIgG2b	GK1.5	eBioscience	14-0041

CD45	ratIgG2b	30-F11	BDPharmingen	557659
GFAP	msIgG2b	4A11	BDPharmingen	556327
GFAP	chIgY	-	Chemicon	AB5541
Gr-1	ratIgG2b	RB6-8C5	eBioscience	14-5931
Iba1	rabIgG	-	Wako	019-19741
Ly-6G	ratIgG2a	1A8	BioXcell	BE0075
MBP	ratIgG2a	-	Chemicon	MAB386
NeuN	msIgG1	A60	Chemicon	MAB377
Neurofilaments	msIgG1	SMI-32	Covance	SMI-32P
Non-phosphorylated Neurofilaments	msIgG1	SMI-31	Covance	SMI-31R
Phosphorylated				
Nogo-A	msIgG1	11C7	Novartis	
Nogo-R	ratIgG2b	202604	R&D	MAB1659

Secondary antibodies for immunohistochemistry

Antigen	*Label*	*Host*	*Company*	*Cat. #*
chIgY	Cy2	Donkey	Jackson	703-225-155
arHamIgG	Cy2	Goat	Jackson	127-225-160
msIgG	Cy3	Goat	Jackson	127-225-160
rabIgG	Dy488	Donnkey	Jackson	711-486-144
rabIgG	Cy3	Donkey	Jackson	711-165-152
ratIgG	Cy2	Donkey	Jackson	712-225-153
ratIgG	Cy3	Donkey	Jackson	712-166-150

Antibodies for western blot

Antigen	*Label*	*Host*	*Company*	*Cat. #*
Nogo-A/B/C	-	Rabbit	Chemicon	AB566P
rabIgG	HRPO	Goat	Jackson	111-035-144

Neutrophil depletion

Antibody	*Clone*	*Company*	*Cat. #*
Anti-Ly-6G	1A8	BioXcell	BE0075-1
RatIgG2a isotype control	2A3	BioXcell	BE0089

3.1.3 Primers

Primer	*Sequence*	*Company*
Real-Time PCR		
18S-RNA-fwd	5'-CGG CTA CCA CAT CCA AGG A -3'	Biomers
18S-RNA-rev	5'-GCT GGA ATT ACC GCG GCT -3'	Biomers
NgR1-fwd2	5'-AGG CTG CTG GCA TGG GTG TTA T -3'	Biomers
NgR1-rev2	5'-GCT GGC TAG AGG CTG GGA TGC -3'	Biomers
NgR2-fwd1	5'-CTG CTG CAA GGT CCT GCC -3'	Biomers
NgR2-rev1	5'-AAG GAA GGG CCA GGA GTG TC -3'	Biomers
Nogo-A-fwd	5'-GGC TCA GTG GAT GAG ACC CTT -3'	Biomers
Nogo-A-rev	5'-AGG AGG GTA TCA CAG GCT CAG AT -3'	Biomers
Genotyping		
bpA2	5'-TGG GCT CTA TGG CTT CTG AG -3'	Biomers
Neo-start	5'-ATG GGA TCG GCC ATT GAA CAA -3'	Biomers
NgRH1-fwd2	5'-TTG TCT GCA GAG CAC CTT CCA -3'	Biomers
NgRH1-rev	5'-TTC TCT GTG TAA CAG CCT TGG G -3'	Biomers
NR3F1	5'-TCG GCA CAT CAA TGA CTC TCC-3'	Biomers
NR3R3	5'-TAT GTA CAC ACA CCT GGT GGC -3'	Biomers

3.1.4 Buffers, solutions and media

4% PFA	Dissolve 4 g PFA in 100 ml 80°C Phosphate Buffer 0.1M cool to 4°C

6x SDS sample buffer	7 ml 4x stacking gel buffer 3 ml glycerol 4 g SDS 2 ml 2-mercaptoethanol 1 mg bromphenolblue add ddH_2O to 100 ml volume store 1 ml aliquots at -20°C
Blocking Solution	0.15% Triton X-100 5% normal donkey serum in PBS
Blocking Solution for DAB-IHC	5% goat serum 45% Tris buffered saline pH = 7.6 (TBS) 0.1% Triton X-100 in antibody diluent reagent solution
Citrate buffer	10 mM citric acid/ sodium citrate pH = 6.0
Collagenase/ DNase Solution	1 mg/ ml Collagenase A 0.1 mg/ ml DNaseI in D-MEM
DAB solution	0.05% DAB (w/v) 0.1% H_2O_2 in TBS
Decalcification buffer	20% EDTA in ddH_2O pH = 7.2-7.4
Electrophoresis buffer for SDS-PAGE (5x)	15.1 g Tris base 72.0 g glycine in 1000 ml ddH_2O pH = 8.3
Eosin staining solution	50 ml of 3% Eosin (w/v) in ddH_2O 390 ml 96% ethanol 2 ml glacial acetic acid

FACS Buffer	0.1% BSA 0.02% NaN3 in 1x PBS
Homogenization Buffer	20 mM HEPES 100 mM KAc 40 mM KCl 5 mM EGTA 5 mM MgCl2 adjust to pH = 7.2 and freshly add: 1:100 protease inhibitor cocktail 5 mM DTT 1 mM PMSF
MACS/ Sorting Buffer	0.5% BSA 2 mM EDTA in 1x PBS
Mouse complete medium	10% fetal bovine serum 2 mM L-Glutamine 50 µM 2-Mercaptoethanol in RPMI
Na_2HPO_4 0.2M	28.4 g Na_2HPO_4 anhydrous in 1000 ml ddH_2O
NaH_2PO_4 0.2M	13.9 g NaH_2PO_4 in 500 ml ddH_2O
Phosphate Buffer 0.1M	57 ml NaH_2PO_4 0.2 M 243 ml Na_2HPO_4 0.2 M 600 ml ddH_2O
Red Blood Cell (RBC) Lysis Buffer	0.15 M NH_4Cl 10 mM $KHCO_3$ 0.1 mM Na_2EDTA in ddH_2O pH = 7.2-7.4

Separating gel buffer (4x)	1.5 M Tris/ Cl in ddH_2O pH = 8.8
Separating-gel (7%) for SDS-PAGE	3.5 ml acrylamide/ bisacrylamide (30%/ 0.8%) 3.75 ml separating gel buffer (4x) 7.6 ml ddH_2O 150 µl 10% SDS 50 µl 10% APS 10 µl TEMED
Stacking gel buffer (4x)	0.5 M Tris/ Cl in ddH_2O pH = 6.8
Stacking gel for SDS-PAGE	650 µl acrylamide/ bisacrylamide (30%/ 0.8%) 1.25 ml stacking gel buffer (4x) 3 ml ddH_2O 50 µl 10% SDS 25 µl 10% APS 5 µl TEMED
TBS	50 mM Tris/ Cl 150 mM NaCl pH = 7.5
TBS-NP-40	0.2% NP-40 in TBS
Western blot transfer buffer	1x electrophoresis buffer 0.2 % SDS

3.1.5 Laboratory animals

Wildtype C57BL6/J were obtained from the Jackson Laboratory and bred in the animal facility of the University Medical Center Eppendorf. These mice were further used as background strains for embryo transfer of imported transgenic animals (see below). Mice are further referred to as WT animals.

Il17ra$^{-/-}$ mice were obtained from collaboration with Dr. Christoph Hölscher (Research center Borstel) and AMGEN GmbH, Munich.

Rtn4r$^{-/-}$ mice (B6.129S7/SvEvBrd-Rtn4r^{tm1Matl})^{283} and *Rtn4rl2*$^{-/-}$ mice (B6-TgH(NgRH1)^{143Npa})^{284} were obtained from a collaboration with Prof. Dr. Christine Bandtlow, Medical University Innsbruck, Austria, and Novartis Pharma Research, Basel, Switzerland. These mice are further referred to as *Ngr1*$^{-/-}$ mice (NgR1-deficient mice) for *Rtn4r*$^{-/-}$ mice, *Ngr2*$^{-/-}$ mice (NgR2-deficient mice) for *Rtn4rl2*$^{-/-}$ mice and *Ngr1/2*$^{-/-}$ mice (NgR1/2-deficient mice) for *Rtn4r/ Rtn4rl2* double mutant mice.

3.1.6 Equipment

ABI Prism 7900	Applied Biosystems
Beta counter, 1450 Microbeta	Perkin-Elmer
Blotter, BlueBlot Wet 100	Serva
Centrifuges	Eppendorf and Heraeus
Cryostat, JungCM3000	Leica
Developer, Curix 60	AGFA
Electrophoresis Unit, SE260 mighty small II	Hoefer (#SE260-10A-.75)
FACS Aria cell sorter	BD Bioscience
Filtermat Cassettes	Perkin-Elmer
FlexCycler	AnalytikJena
Freezers	Liebherr and Sanyo
Freezing Container, Nalgene Cryo 1°C	Roth
Fridges	Liebherr
Gamma irradiator, Biobeam 2000 (Cs-137;49.2 TBq)	Eckert & Ziegler
Harvester 96 MACH III M	Tomtec
Heat Sealer 1295-012	Wallac
Incubator, Hera Cell 240	Thermo Scientific
LSRII FACS analyser	BD Bioscience
MACS MultiStand	Miltenyi Biotech
Magnet, MACS Mini and Midi	Miltenyi Biotech
Microscope CKX41	Olympus
Microscope CX21	Olympus
Microscope, epifluorescence, Axioskop 40	Zeiss
Microscope, laser scanning (LSM)	Leica
Nitrogen tank	Tec-lab

Nanodrop Nd-1000	Peqlab
Rotators	GLW
Pipets	Gilson, eppendorf
Pipette help, accu jet	Hassa
Pump Reglo	Ismatec
Racks	Roth
Scale	Mettler PM 4000
Shandon Coverplate Cassette	Thermo Scientific
Shandon Coverplates	Thermo Scientific
Superfrost Plus Slides	VWR
Sterile bank, MSC-Advantage	Thermo Scientific
Thermomixer	Eppendorf
UV Transilluminator	Peqlab
Wallac Victor 1420 multilabel plate reader	Perkin-Elmer
Water bath with shaker	GFL
Western blot accessories (comb, spacer, glass plates)	Serva

3.1.7 Consumables

Adapter w/w	Braun	
Cell culture flasks	Sarstedt	
Cell culture plates	Greiner, Sarstedt	
Cell strainer (40, 70 and 100 µm)	BD	
Cover slips (15 – 50mm)	Menzel	
Columns for magnetic cell isolation	Miltenyi Biotec	
Eppendorf tubes	Eppendorf	
FACS tubes, 5 ml	Sarstedt	55.1579
Falcon tubes, 15 and 50 ml	BD	
Filtermat A (GF/C)	Perkin-Elmer	1450-421
Filtermat bag	Perkin-Elmer	1450-432
Gel blotting paper	Schleicher/ Schuell	
Hyperfilm ECL, 18 x 24 cm	Amersham	
Immobilon-P transfer membrane, PVDF, 0.45 µm	Millipore	

Liquid reservoir for mutlichannel pipettes	Roth
Multiplay-PCR plate, 96 well, half margin	Sarstedt
Pipette tips	Sarstedt
Pipettes (2, 5, 10 and 25 ml)	Greiner, Sarstedt
Syringes and needles	BD and Braun
Syringe filter, 0.22µm	Roth
Sealing gape for PCR plates, optically clear	Sarstedt
Tissue Base Molds	ThermoFischer

3.1.8 Software

AxioVision 4.6	Zeiss
FACSDiVa analysis software	BD Biosciences
FlowJo FACS analysis software	TreeStar Inc.
ImageJ	NIH, Bethesda
Leica Imaging Software	Leica
PRISM Graphpad	Graphpad Software Inc.

3.2 Methods

3.2.1 Genotyping of NgR-deficient animals

Genetic deletion of *Ngr1* and/ or *Ngr2* was determined by PCR. Genomic DNA was isolated from mouse tail biopsies using Invisorb Spin Tissue Mini Kit according to manufacturer's instructions. DNA was eluted using 200 µl elution buffer and used as template for genotyping PCRs (see tables 1, 2). For *Ngr1*, the primers NR3F1, NR3R3 and bpA2 were used, resulting in a 325 bp amplicon for the wildtype allele and a 210 bp amplicon for the targeted allele. For *Ngr2*, two PCR reactions, containing either NgRH1-fwd2 and NgRH1-rev or Neo-start and NgRH1-rev were used to detect the wildtype or targeted allele, respectively. A 500 bp amplicon was expected for the wildtype allele and a 1000 bp amplicon for the targeted allele. PCR products were resolved by electrophoresis on a 2% agarose gel, stained with ethidium bromide and visualized on a UV transilluminator.

Table 1 Genotyping PCR for *Ngr1* and *Ngr2* alleles.

Sample volume	**25 µl**
10x DreamTaq™ buffer	2.5 µl
25 mM $MgCl_2$	1.5 µl
Primers (10 µM)	Each 1.5 µl
dNTPs (10 mM)	0.5 µl
DreamTaq™	0.3 µl
Template	1 µl
ddH_2O	14.7 / 13.7 µl

Table 2 PCR program for *Ngr1*$^{-/-}$ and *Ngr2*$^{-/-}$ genotyping.

95°C	3 min	
95°C	30 s	40 cycles
68°C	45 s	
72°C	1 min	
72°C	10 min	
4°C	∞	

3.2.2 Induction of EAE

All animal experiments were performed in accordance with the guidelines of the local authorities. For this work, the following licences had been approved:

25/07 Role of Myelin-associated inhibitory proteins in EAE

07/08 Nogo-receptor-deficient animals and EAE

28/09 Pathogenetic relevance of inflammatory processes in the animal model of multiple sclerosis

Induction of active EAE

For induction of active EAE, 8-12 week old female mice were immunized subcutaneously on two spots at the flanks with 100 µl of a stable emulsion of 200 µg MOG 35-55 in CFA supplemented with 2 mg/ ml *Mycobacterium tuberculosis* H37Ra. Immunized animals were administered 300 ng of pertussis toxin intravenously the same day and intraperitoneally two

days later. EAE developed after approximately 10 days and was scored daily based on a 5-point EAE scale (0: no disease symptoms; 1: limp tail; 2: hind limb paresis; 3: partial hind limb paralysis; 3.5: complete hind limb paralysis; 4: hind limb paralysis and fore limb paresis; 5: moribund or dead). Food and water access for severly disabled animals was assured. Mice with complete hind limb paralysis continuing over 3 days or which suffered from tetraparalysis were euthanized.

Antibody-mediated depletion of neutrophils

In order to investigate the functional role of neutrophils for the development of active EAE, animals were treated with the neutrophil-specific antibody anti-Ly-6G (1A8) to deplete neutrophils. After initial dose-finding experiments, animals received repetitive injections of 100 µg anti-Ly-6G intraveneously every other day over the indicated time periods.

3.2.3 Histological analyses

Perfusion

Mice were anesthesized by intraperitoneal injection of 85 mg Ketamin (Ketanest®) and 13 mg Xylazin (Rompun®) per kg body weight and then transcardially perfused with 5 ml ice-cold PBS followed by 50 ml of ice-cold 4% PFA over 10 min using a peristaltic pump. Brain, spinal cord and optic nerves were prepared and processed as described below.

Tissue processing for cryosections

Prepared tissue was post-fixed in 4% PFA for 30 min at 4°C and then transferred into 30% sucrose for two to three days. Cervical, thoracic and lumbal spinal cord as well as cerebellum and forebrain were separated, embedded in tissue freezing medium and frozen in isopentane cooled on dry ice. Frozen tissue blocks were stored at -80°C. Cryosections of 14 or 20 µm were sliced at -17°C, hoisted onto slides and stored again at -80°C until further use.

Tissue processing for paraffin sections

Brains and cords were removed and fixed in zinc formalin solution for at least 48 h. Vertebral columns were incubated in decalcification buffer for 14 days. Paraffin embedding, histological stainings (Hematoxylin/ eosin and Bielschowsky silver impregnation) as well as immunohistochemistry for myelin basic protein (MBP) shown in this work were performed at the department of Neuropathology at the University Medical Center Eppendorf. Tissue was cut into 5 µm sections and mounted onto glass slides. Prior to staining procedures, paraffin was removed by incubating slides for 10 min in xylol, followed by 30 to 60 s in different

concentrations of ethanol (100%, 96%, 90%, 80%, 70%, 50%). Sections were further washed for 5 min in ddH_2O.

Hematoxylin/ eosin staining

Deparafinized sections were incubated in Hematoxylin (Harris) for 5 min, washed in ddH_2O, differentiated in 0.2% hydrochloric acid and incubated for additional 5 min in tab water. Sections were transferred into 70% ethanol, costained with eosin for up to 3 min, washed three times in 100% ethanol and three times in Xylol. Stained slices were mounted in Sakura GLC.

Bielschowsky silver impregnation

For the visualization of nerve fibres, axons and neurofibrillary tangles, sections are treated with ammoniacal silver which is then reduced to visible metallic silver.

Deparaffinized sections were stained with Bielschowsky for neurofibrils kit according to manufacturer's instructions. Briefly, sections were incubated in a humified chamber with 10 drops of reagent A for 5 min at 40°C, washed two times in ddH_2O and subsequently incubated with 10 drops of reagent B for another 20 min at 40°C. Sections were immediately transferred into a reducing reagent, consisting of reagents C-F diluted in 50 ml ddH_2O, and incubated for 2 min at RT. Slides were washed two times in ddH_2O and further incubated in 10 drops of reagent G for 3 min at RT. Slides were washed two times in ddH_2O, dehydrated in different concentrations of ethanol (70%, 95%, 100%), incubated in xylol for 2 min and embedded in eukitt.

Immunohistochemistry on paraffin sections

Deparrafinized sections were incubated with 0.3% H_2O_2 for 15 min to block endogenous peroxidase activity. The slides were then treated in a microwave oven (750 W) 15 min in 10 mM citrate buffer (pH 6.0) for demasking of antigens. Sections were cooled to RT and buffered in TBS for 5 min. For immunofluorescent staining with anti-Nogo-A, sections were treated according to the protocol described for cryostat sections. For DAB-developed immunohistochemistry, sections were incubated with rat-anti-MBP in blocking buffer over night at 4°C. Histofine universal immuno-peroxidase polymer anti-rat was applied after washing with TBS and incubated for 60 min at RT. The peroxidase reaction was detected using diaminobenzidine as chromogen. Slides were incubated with DAB-solution for 1-5 min until staining had developed. For costaining with alum-hematoxylin, slides were washed for 10 min in ddH_2O, stained for 20 s in Mayer's hematoxylin and incubated for further 5 min in

tab water. Slides were washed two times in ddH_2O, dehydrated in different concentrations of ethanol (70%, 95%, 100%), incubated in xylol for 2 min and embedded in eukitt.

Immunohistochemistry on cryosections

Cryosections were incubated in blocking solution for 1 h at RT, washed once in PBS and incubated with the indicated primary antibodies diluted in PBS over night at 4°C. Sections were washed three times in PBS for 5 minu and incubated in fluorescently labeled secondary antibodies diluted in PBS for 1 h at RT. Nuclei were stained with H 33258. Stained sections were washed three times in PBS for 5 min and mounted in Fluormount G.

Quantification of neuronal and axonal damage

For neuronal quantification, cryosections of cervical spinal cords were stained for neuronal cell bodies with anti-NeuN-antibody according to the above described protocol. Ventral horn motor neurons were counted in 6 ventral horns/ animal on 20x epifluorescence images using ImageJ.

For quantification of axonal densities, cryosections of cervical spinal cords were stained for axons with antibodies against phosphorylated and non-phosphorylated neurofilament (SMI-31 and SMI-32) according to the above described protocol. Confocal images (63x) of corticospinal tract and dorsal column were taken and axonal densities were analysed in these regions by counting at least 500 axons per region with ImageJ.

3.2.4 Cell isolation

All procedures were carried out at 4°C if not indicated otherwise.

Isolation of lymphocytes from lymph nodes and spleen

Single cell suspensions from lymph nodes and spleens were prepared by homogenizing the tissues through a 40 µm cell strainer. Cells were pelleted by centrifugation (300 g, 7 min, 4°C) and splenic red blood cells were lysed in red blood cell lysis buffer for 7 min at 4°C. Cells were washed once in PBS and resuspended in buffer or medium depending on further use.

Isolation of CNS-infiltrating immune cells

For the isolation of CNS-infiltrating immune cells, mice were sacrificed by CO_2 inhalation and immediately transcardially perfused with ice-cold PBS. Brain and spinal cord were removed, minced with blades and digested in Collagenase/ DNAseI solution for 45 min at 37°C. Tissue was triturated through a 40 µm cell strainer. The homogenized tissue was washed in PBS (300 g, 10 min, 4°C). Immune cells including microglia were separated from myelin, other glia and neuronal cells by centrifugation over a discontinuous percoll gradient. For that, the homogenized tissue was resuspended in 30% isotonic percoll, transferred into a 15 ml Falcon tube 78% isotonic percoll was carefully layered underneath. The gradient was centrifuged (1500 g, 30 min, 4°C) and CNS-infiltrating immune cells were then recovered from the gradient interphase. The isolated cell fraction was washed two times in PBS and subsequently resuspended in buffer or medium depending on further use.

Isolation of bone marrow cells

Bone marrow was prepared from femurs and tibiae of 6-8 week old C57BL/6 mice. Bones were removed, disinfected with 70% ethanol and cleaned from muscle tissue. Tips of bones were cut with scissors and bone marrow was flushed out using a 23 gauge syringe. Single cells were dissociated with a 1000 µl pipette and subsequently cleaned from remaining pieces of bones by passing through a 100 µm cell strainer. Cells were pelleted by centrifugation (300 g, 7 min, 4°C) and red blood cells were lysed for 2 min at 4°C. Cells were washed once in PBS and then resuspended in buffer or medium depending on further use.

Magnetic isolation of $CD4^+$ T cells

$CD4^+$ T cells were isolated from splenocytes or isolated CNS-infiltrating cells using $CD4^+$ T cell isolation kit II according to manufacturer's instructions. Briefly, cell suspensions were incubated with a cocktail of biotinylated antibodies sparing only $CD4^+$ T cells, followed by magnetic anti-biotin-microbeads. Subsequently, $CD4^+$ T cells were isolated by separation over a MACS® column which is placed in a magnetic field. The magnetically labeled cells are retained on the column, whereas the unlabeled $CD4^+$ T cells are collected in the flow through.

Magnetic isolation of neutrophils

Neutrophils were isolated from bone marrow cells using anti-Ly-6G microbead kit according to manufacturer's instructions. Briefly, cells were incubated with biotinylated anti-Ly-6G antibodies and anti-biotin-microbeads, by which Ly-6G-expressing cells are magnetically labeled. Subsequently, Ly-6G-expressing cells are separated from unlabeled cells using a

MACS® column placed in a magnetic field. The magnetically labeled Ly-6G-expressing cells are retained on the column, while unlabeled cells are collected in the flow through. After removal of the column from the magnetic field, the retained Ly-6G-expressing cells are eluted.

3.2.5 *In vitro* experiments

^{3}H Thymidine incorporation assay

For the analysis of T cell proliferation, lymph node cells from immunized animals were cultured in 96 well plates at $2x10^5$ cells/ well in mouse complete medium and stimulated with different concentrations of MOG 35-55 peptide or anti-CD3 (145-2C11). After 2 days, cells were pulsed with 1 µCi ^{3}H-Thymidine per well for 16 h. Cells were harvested and spotted on filtermats according to manufacturer's instructions. Spotted filtermats were dried for 2 h at 60°C, sealed in bags containing 5 ml betaplate scintillation liquid and assembled in filtermat cassettes. Incorporated activity/ 96 well was assessed in a beta counter in counts per minute (cpm). Stimulation index of applied peptides or antibodies was calculated by dividing the mean incorporated activity of stimulated wells by the mean of unstimulated control wells.

3.2.6 Flow cytometry

Whole blood surface staining

EDTA-treated whole blood was diluted to 50 µl with FACS buffer and stained with the indicated antibodies for 20 min at 4°C. Red blood cells were lysed in 1 ml FACS lysing solution for 10 min at RT, centrifuged (350 g, 5 min, RT) and resuspended in 400 µl FACS buffer before flow cytometric analysis.

Surface staining

Isolated cell fractions were resupended in FACS buffer at 10×10^6 cells/ ml. Fc receptors were blocked with 1:1000 anti-CD16/32 for 10 min at 4°C. 50 µl cell suspension were stained with indicated antibodies for 20 min at 4°C. Cells were washed with 1 ml FACS buffer (350 g, 5 min, 4°C) and resuspended in 400 µl FACS buffer for flow cytometric analysis.

Quantification of CNS-infiltrating immune cells using TruCount® beads

TruCOUNT® tubes release a known number of fluorecently labeled beads upon contact with liquid. During flow cytometric analysis, the absolute number of cells can be determined by comparing the number of analysed cellular events to analysed bead events. Isolated CNS-

infiltrating cells were resuspended in 1 ml FACS buffer. 100 µl cell suspension was transferred to TruCOUNT® tubes and incubated with anti-CD16/32 (1:1000) and anti-CD45-PE-Cy7 or anti-CD45-APC-Cy7 antibody for 20 min at 4°C. The stained sample was diluted with 300 µl FACS buffer and immediately analysed. The total number of CNS-infiltrating immune cells was calculated based on the analysed number of CD45 positive events and an analysed number of 10 000 fluorecently labeled beads: Number of $CD45^+$ cells = (number of beads/ analysed number of beads) × analysed number of $CD45^+$ events × dilution.

Intracellular staining for detection of FoxP3

Staining of the nuclear transcription factor FoxP3 was performed using FoxP3 staining buffer set according to manufacturer's instructions. After surface staining, cells were centrifuged (350 g, 5 min, 4°C), followed by fixation in 100 µl freshly prepared Fix/ Perm solution for 1 h. Cells were washed with 1 ml permeabilization buffer and subsequently stained with anti-FoxP3-PE for 1 h. Cells were again washed and resuspended in 400 µl FACS buffer for flow cytometric analysis.

Intracellular cytokine staining (ICS) of T cells

Cells were restimulated with 100 ng/ml PMA and 1 µg/ml ionomycin for 5 h in mouse complete medium. After 2 h of restimulation, 1:300 brefeldin A was added for the remaining time period to prevent the secretion of expressed cytokines. The stimulated cells were centrifuged, resuspended in FACS buffer and stained with antibodies against surface markers according to the surface staining protocol. Fixation and permeabilisation was performed with IC fixation and permeabilization buffer according to the manufacturers instructions. Intracellular cytokines were stained with anti-IL17A-Alexa647 and anti-IFN-γ-PE for 20 min at RT. Stained cells were washed with permeabilization buffer (1500 rpm, 5 min, RT) and resuspended in 300 µl FACS buffer.

Immunophenotyping of CNS-infiltrating cells

Using the protocols described above, the following stainings were performed in order to quantify and phenotype CNS-infiltrating immune cells (see table 3).

The establishment of the immunophenotyping of different immune cells using a 7-color flow cytometric staining was initially performed with the practical help of Johannes Neumann. Results from this initally developed antibody cocktail cell types, which were obtained by Johannes Neumann under my supervision, contribute to the results on B cell frequency and numbers in the analysis of the temporal dynamic of CNS inflammation in this work.

Table 3 Immunophenotyping of CNS-infiltrating cells. CNS-infiltrating cells were isolated according to 3.2.4 and stained with the indicated antibodies for flow cytometric analysis. If not indicated otherwise, cells were stained according to the surface staining protocol.

	FITC/ Al488	PE	PerCP-Cy5.5/ PE-Cy5.5	PE-Cy7	APC/ Al647	APC-Cy7	Pacific Blue
Cell types	CD11b	CD4	B220	NK1.1	CD11c	CD45	CD8a
Cell types I	CD11b	Ly-6G	B220	NK1.1	CD11c	CD45	CD3e
Cell types II	Gr1	Ly-6G	CD11b	NK1.1	CD11c	CD45	CD3e
T cell activation/ Treg	CD69	FoxP3[A]	CD3e	CD4	CD25	CD45	CD8a
T cell differentiation	CD11b	IFN-γ[B]	CD3e	CD4	IL-17A[B]	CD45	CD8a
APC maturation control			CD11b	CD11c		CD45	Ly-6G
APC maturation I	MHCII		CD11b	CD11c		CD45	Ly-6G
APC maturation II		CD80	CD11b	CD11c	CD40	CD45	Ly-6G

[A] According to FoxP3 staining protocol; [B] According to ICS protocol

In order to be able to identify CNS-infiltrating neutrophils, the antibody cocktails cell types I and cell types II were established. While antibody cocktail cell types I allows the identification of B cells in the isolated cell fraction, the pan-B cell antibody anti-B220 was removed in favor of a double identification of neutrophils using both anti-Gr1 and anti-Ly-6G in the cocktail cell types II. For the expression analysis of maturation markers on APC, all three APC maturation antibody cocktails were used in parallel. Expression of MHCII, CD80 and CD40 were analysed in comparison to the described control staining.

Analysis of surface-IL-17 on $CD4^+$ T cells

$CD4^+$ T cells were isolated from splenocytes or CNS-infiltrating cells by magnetic isolation (see 3.2.4) 14 days after induction of EAE. Isolated cells were stimulated with 100 ng/ ml PMA and 1 µg/ ml ionomycin for 16 h in mouse complete medium at 37°C and 5% CO_2. In order to prevent the secretion of cytokines, a part of the cells was additionally treated with brefeldin A. In order to analyse surface expression, stimulated cells were stained with anti-CD3-PacificBlue, anti-CD4-PE and anti-IL-17A-Alexa647. Dead cells with permeable cell membrane were excluded from the analysis using LIVE/DEAD® fixable aqua dead cell stain kit according to manufacturer's instructions. Briefly, cells were washed once in PBS and then stained with LIVE/DEAD® acqua fixable cell stain dye diluted 1:1000 in PBS for 30 min at 4°C. Cells were then either analysed or subsequently fixed and permeabilized to stain intracellular cytokines as described above.

3.2.7 RNA isolation, cDNA synthesis and real-time PCR

RNA isolation from tissue

For RNA isolation, target tissues were removed from animals sacrificed by CO_2 inhalation and immediately frozen in liqud nitrogen. Tissue was homogenized in 1 ml TriZOL reagent per 100 µg in a 2 ml glass vial using a teflon douncer and incubated for 15 min on ice to settle remaining tissue at the bottom of the tube. TriZOL extract was transferred to a new eppendorf tube. In order to extract RNA, 0.2 ml of chloroform per ml TriZOL was added, the sample was gently mixed, incubated for 10 min on ice and centrifuged (20 000 g, 15 min, 4°C). The upper aqueous phase was transferred to a new Eppendorf tube, RNA was precipitated with 0.5 ml isopropanol/ ml TriZOL and centrifuged (20 000 g, 15 min, 4°C). The RNA pellet was washed once with 75% ethanol and air-dried for 10 min at room temperature. Isolated RNA was dissolved in DEPC-treated ddH_2O for 10 min at 55-60°C. RNA concentration was determined photometrically.

cDNA synthesis

For cDNA synthesis, 2.5 µg of isolated RNA was denatured in the presence of random hexamer primers for 10 min at 70°C and cooled on ice. Reverse transcription was carried out using M-MLV reverse transcriptase according to manufacturer's instructions. The reaction was incubated for 10 min at room temperature, followed by 50 min at 42°C. M-MLV was inactivated by a 15 min incubation at 70°C.

Real-time PCR

cDNA was diluted at least 1:10 for expression analysis. Gene expression was analysed by Real Time-PCR performed in the Applied Biosystem ABI Prism 7900 Sequence Detection System. The primer sets used are listed above. Samples were run in duplicates. Real-Time monitoring of DNA amplification was performed by SYBR®Green incorporation. 18S rRNA was used as endogenous control and relative gene expression was calculated by the ΔΔCt method using appropriate cDNA as calibrator.

3.2.8 Western blot

Spinal cord homogenization

Animals were sacrificed by CO_2-inhalation and spinal cord tissue was removed and immediately frozen in liquid nitrogen until further use. Frozen tissue was transferred into a 2 ml glass vial and supplemented with 1ml ice-cold homogenization buffer. Tissue was

pottered with 8 strokes and 800 rpm/ min using a teflon douncer. The crude homogenisate was centrifuged in a 1.5 ml Eppendorf tube (1000 g, 10 min, 4°C) and the supernatant was transferred into a fresh Eppendorf tube and frozen at -20°C.

Determination of protein concentration

Protein concentration of spinal cord homogenates was determined after Bradford. 50 µl of standard proteins, 1:10 diluted homogenate or homogenization buffer (control) were supplemented with 850 µl ddH_2O and 200 µl Roti-Quant reagent. Samples were mixed and optical absorbance was measured at 595 nm. Different concentrations of BSA were used as standard proteins.

SDS-PAGE

Spinal cord homogenisates containing 25 µg protein were supplemented with 6x SDS sample buffer and denatured for 5 min at 95°C. Proteins were resolved on a 7% SDS-polyacrylamide-gel by electrophoresis (30 mA).

Western blot

Proteins were transferred onto a PVDF-membrane by wet-blot electrophoresis (30V, 16h). The blotted membane was blocked for 30 min in 3% milk/ TBS-NP-40 and subsequently incubated with anti-Nogo-A/B/C antibody (1:1000 in 1.5% milk/ TBS-NP-40) for 2 h at RT. The labeled membrane was washed three times with TBS-NP-40 for 5 min each, and then incubated with goat-anti-rabbit-HRPO (1:10 000 in 1.5% milk/ TBS-NP-40). The labeled membrane was washed three times with TBS-NP-40 for 15 min each, and subsequently developed with chemoluminescent HRP substrate.

3.2.9 Statistical analysis

Statistical analysis of EAE disease courses was performed using two-way ANOVA combined with a Bonferroni post-analysis using PRISM Graphpad. Two-tailed unpaired student's t-test was used to compare CNS-infiltrating cells between NgR1/2-deficient mice and WT littermates, anti-Ly-6G treated and isotype control treated animals as well as gene expression results obtained by real-time PCR.

4 RESULTS

4.1 Dynamic of inflammatory processes during MOG 35-55-induced EAE in C57BL/6 mice

4.1.1 Clinical course of MOG 35-55-induced EAE

Immunization of C57BL/6 mice with the encephalitogenic peptide MOG 35-55 in CFA results in the development of CNS inflammation accompanied by symptoms of motor disability (Fig. 1).

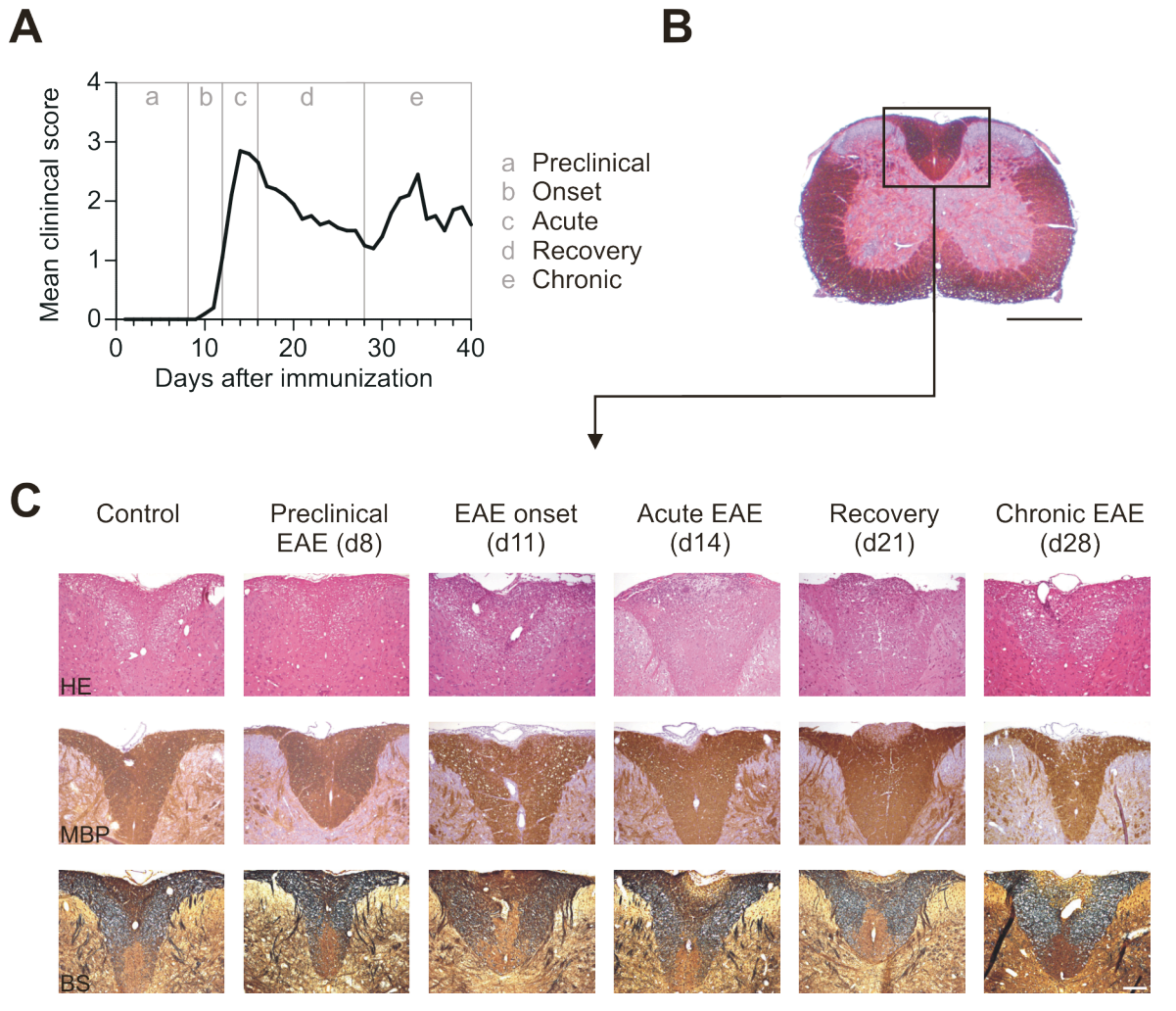

Fig. 1 Spinal cord pathology of MOG 35-55-induced EAE in C57BL/6 mice. (A) Disease course of MOG 35-55-induced EAE in C57BL/6 mice. The disease can be divided in 5 stages (a-e): Preclinical EAE, EAE onset, acute EAE, recovery and chronic EAE. (B,C) Histopathological analyses of cervical spinal cord sections were performed at the different disease stages. (B) Cross section of cervical spinal cord stained for MBP. Scale bar represents 500 µm. (C) Representative hematoxylin/ eosin (HE) stainings of nuclei and cell bodies, immunohistochemistry for MBP and Bielschowsky silver impregnation staining (BS) of neurofibrils are shown for dorsal white matter region (n=3). Scale bars represent 100 µm.

Approximately ten days after immunization, immunized animals develop first clinical symptoms and observed disease severity peaks at days 14-16, followed by a partial recovery from clinical disability and subsequently a chronic sustained deficit (Fig. 1A). This chronic disease phase is only moderately stable with intermittant spontaneous relapses which normally occur approximately 30 days after immunization. Histologically, the observed CNS inflammation affects mainly the spinal cord (Fig. 1B), although inflammation can also be detected in the cerebellum and optic nerves (data not shown). Already during the preclinical period after immunization, some infiltrating cells can be detected in the spinal cord. After onset of clinical symptoms, massive infiltrates are visible in the tissue. Following partial recovery from disability and during chronic disease, inflammation declines considerably, but small infiltrates can still be detected. CNS inflammation during EAE is accompagnied by demyelination and axonal loss. Whereas the initial loss of MBP that can be detected during acute disease is partially reversed during recovery, axonal loss that can be detected in the corticospinal tract (CST) and dorsal column (DC) of animals in acute disease is irreversible and still clearly visible during chronic disease (Fig. 1C).

4.1.2 Temporal dynamics of immune cell infiltration into the CNS during EAE

Flow cytometric quantification of CNS-specific inflammation

In order to characterise the temporal dynamics of CNS-infiltration by immune cells during EAE, a flow cytometry-based absolute quantification method was established (Fig. 2). Infiltrating cells were isolated from the CNS at different time points after EAE induction (Fig. 2A) and the isolated cell fraction was stained with the leukocyte marker CD45 to identify cells of hematopoetic origin in the isolated cell preparation. Combined flow cytometric analysis of $CD45^+$ cells with TruCOUNT® beads allowed the calculation of the total number of immune cells isolated from the CNS of single animals (Fig. 2B). Within $CD45^+$ cells, different infiltrating immune cell types in this population were identified further using a multi-color staining approach (Fig. 2C). Based on different expression levels of CD45, initially infiltrating cells ($CD45^{high}$) were separated from CNS-resident microglia ($CD11b^+CD45^{int}$). In the $CD45^{high}$-expressing cells, the majority of cells are of myeloid origin expressing CD11b. In order to identify reliably different cell types in this fraction, a sequential gating strategy was used.

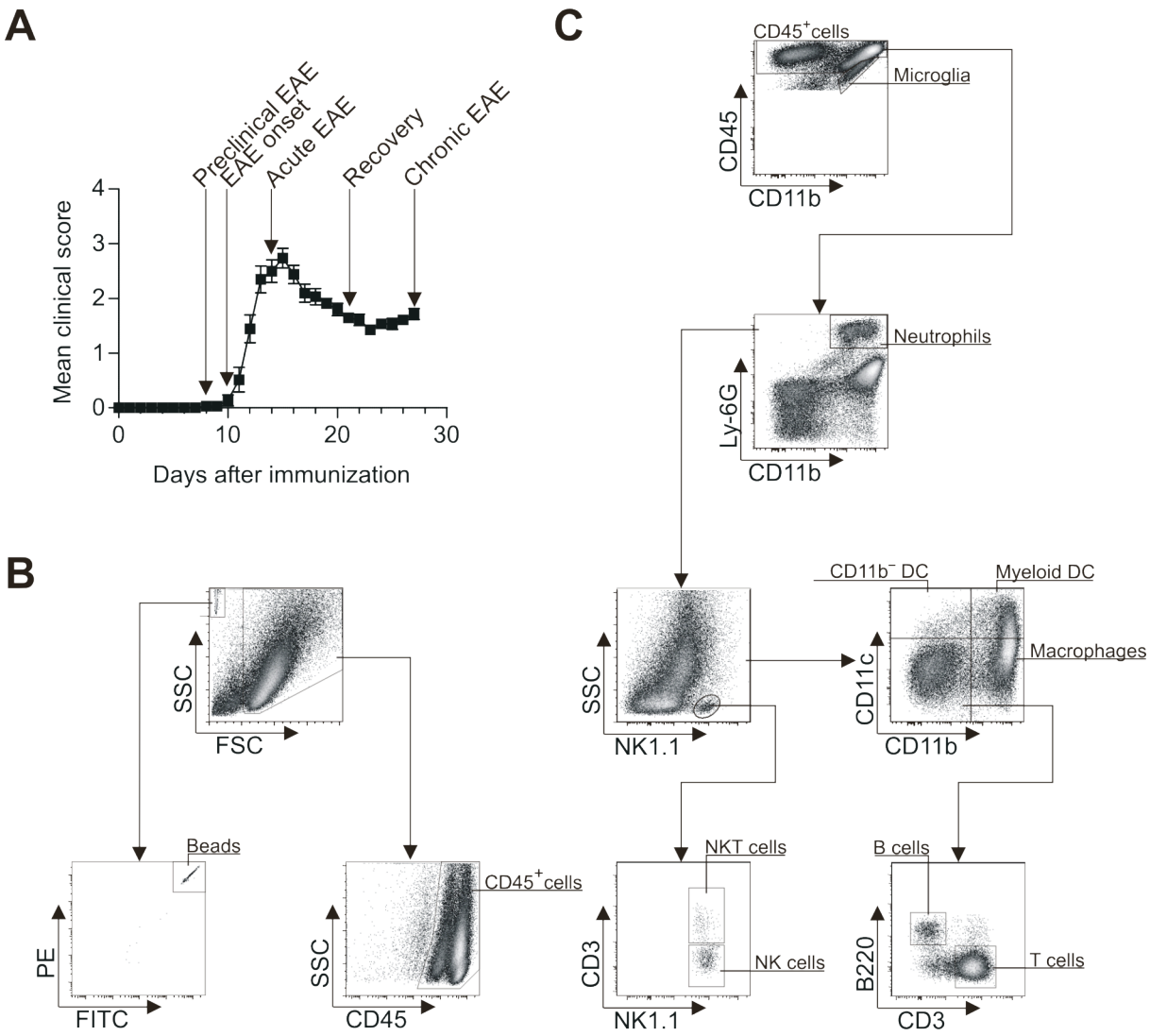

Fig. 2 Flow cytometric identification and quantification of CNS-infiltrating cells over the course of EAE. (A) Mean clinical disease course of analysed animals and time points of analyses are shown for animals, which completed the observation period. Mean clinical scores are mean ± sem, (n=14). (B) $CD45^+$ CNS-infiltrating immune cells were quantified using TruCount® beads. Separation of beads and cells based on size (FSC) and granularity (SSC) is shown in the upper panel, selection of fluorescent beads and $CD45^+$ cells is shown in the lower panel. (C) CNS-infiltrating immune cell types were identified by a sequential gating strategy. Identification of microglia ($CD45^{int}CD11b^+$), neutrophils ($CD45^{high}Ly\text{-}6G^+$), NK cells ($CD45^{high}Ly\text{-}6G^-NK1.1^+CD3^-$), NKT cells ($CD45^{high}Ly\text{-}6G^-NK1.1^+CD3^+$), $CD11b^-$DC ($CD45^{high}Ly\text{-}6G^-NK1.1^-$ $CD11c^+CD11b^-$), myeloid DC ($CD45^{high}Ly\text{-}6G^-NK1.1^-$ $CD11c^+CD11b^+$), macrophages ($CD45^{high}Ly\text{-}6G^-NK1.1^-CD11c^-CD11b^+$), B cells ($CD45^{high}Ly\text{-}6G^-$ $NK1.1^-CD11c^-CD11b^-B220^+$) and T cells ($CD45^{high}Ly\text{-}6G^-NK1.1^-CD11c^-CD11b^-CD3^+$) are shown from a representative experiment.

First, neutrophils ($CD11b^+Ly\text{-}6G^+$) were identified followed by NK1.1-expressing cells in the residual $Ly\text{-}6G^-$ population, since both populations express markers later used for the identification of dendritic cells and macrophages. NK1.1-expressing cell can be further subdivided in NK cells ($NK1.1^+CD3^-$) and NKT cells ($NK1.1^+CD3^+$), which display T cell characteristics, i.e. TCR-CD3 complexes in addition to NK markers. Next, in the $NK1.1^-$ population, macrophages ($CD11b^+CD11c^-$) and two main subsets of dendritic cells, namely

myeloid DC ($CD11b^+CD11c^+$) and $CD11b^-$DC ($CD11b^-CD11c^+$) were separated. Finally, T cells ($CD3^+$) and B cells ($B220^+$) were identified in the $CD11b^-CD11c^-$ population.

Temporal dynamics of CNS infiltration

Based on the multi-color flow cytometric stainings described in 3.2.6 (see table 3), the CNS-infiltration of different immune cell types was quantified at several time points after disease induction (Table 4).

Table 4 Calculated numbers of CNS-infiltrating cells. Mean number of isolated CNS-infiltrating cells ± sd. Numbers of analysed animals/ cell type are shown in brackets (n).

	Control	Preclinical EAE	EAE onset	Acute EAE	Recovery	Chronic EAE
$CD45^+$ Cells	345 000 ± 15 000 (12)	356 000 ± 101 000 (19)	1 444 000 ± 741 000 (8)	3 450 000 ± 546 000 (8)	945 000 ± 239 000 (16)	871 000 ± 477 000 (14)
$CD45^{high}$ Cells	40 000 ± 15000 (12)	75 000 ± 30 000 (19)	1 024 000 ± 647 000 (8)	2 562 000 ± 442 000 (8)	408 000 ± 126 000 (16)	449 000 ± 412 000 (14)
Microglia	293 000 ± 90 000 (8)	277 000 ± 61 000 (13)	379 000 ± 106 000 (8)	701 000 ± 109 000 (8)	440 000 ± 109 000 (15)	328 000 ± 132 000 (8)
Macro-phages	13 000 ± 4 000 (8)	27 000 ± 10 000 (13)	348 000 ± 180 000 (8)	827 000 ± 215 000 (8)	117 000 ± 34 000 (15)	152 000 ± 120 000 (8)
Myeloid DC	4 000 ± 1 000 (8)	10 000 ± 3 000 (13)	188 000 ± 124 000 (8)	773 000 ± 210 000 (8)	79 000 ± 30 000 (15)	178 000 ± 230 000 (8)
T cells	7 000 ± 3 000 (8)	15 000 ± 4 000 (13)	220 000 ± 194 000 (8)	455 000 ± 102 000 (8)	166 000 ± 57 000 (15)	166 000 ± 57 000 (8)
Neutrophils	4 000 ± 2 000 (8)	35 000 ± 13 000 (13)	142 000 ± 63 000 (8)	291 000 ± 180 000 (8)	39 000 ± 29000 (15)	76 000 ± 70 000 (8)
$CD11b^-$ DC	1 000 ± 500 (8)	2 000 ± 800 (13)	47 000 ± 31 000 (8)	99 000 ± 23 000 (8)	27 000 ± 10 000 (15)	23 000 ± 19 000 (8)
NK cells	7 000 ± 3 000 (8)	7 000 ± 2 000 (13)	27 000 ± 16 000 (8)	51 000 ± 15 000 (8)	15 000 ± 5 000 (15)	15 000 ± 9 000 (8)
NKT cells	500 ± 200 (8)	1 000 ± 300 (13)	8 000 ± 7 000 (8)	16 000 ± 5 000 (8)	6 000 ± 2 000 (15)	6 000 ± 3 000 (8)
B cells	9 000 ± 4 000 (5)	7 000 ± 3 000 (5)	9 000 ± 5 000 (5)	25 000 ± 24 000 (5)	10 000 ± 5 000 (5)	9 000 ± 12 000 (4)

During EAE, the CNS is subject to extensive inflammation. Over the disease course, numbers of $CD45^+$ cells correlate well with clinical severity, as they increase from a background level of approximately 3.5×10^5 cells in non-diseased animals to 1.5×10^6 cells at disease onset and then to more than 3×10^6 cells at acute EAE. When animals partially recover from the initial inflammatory attack and progress into chronic disease, the number of $CD45^+$ cells decreases significantly, but a remaining inflammatory infiltrate of about 1×10^6 cells can still be detected. The correlation of the number of CNS-infiltrating cells with disease severity was

detected for all investigated cell types (Fig. 3A). However, the composition of the inflammatory infiltrate in the CNS is changing considerably over the disease course (Fig. 3B).

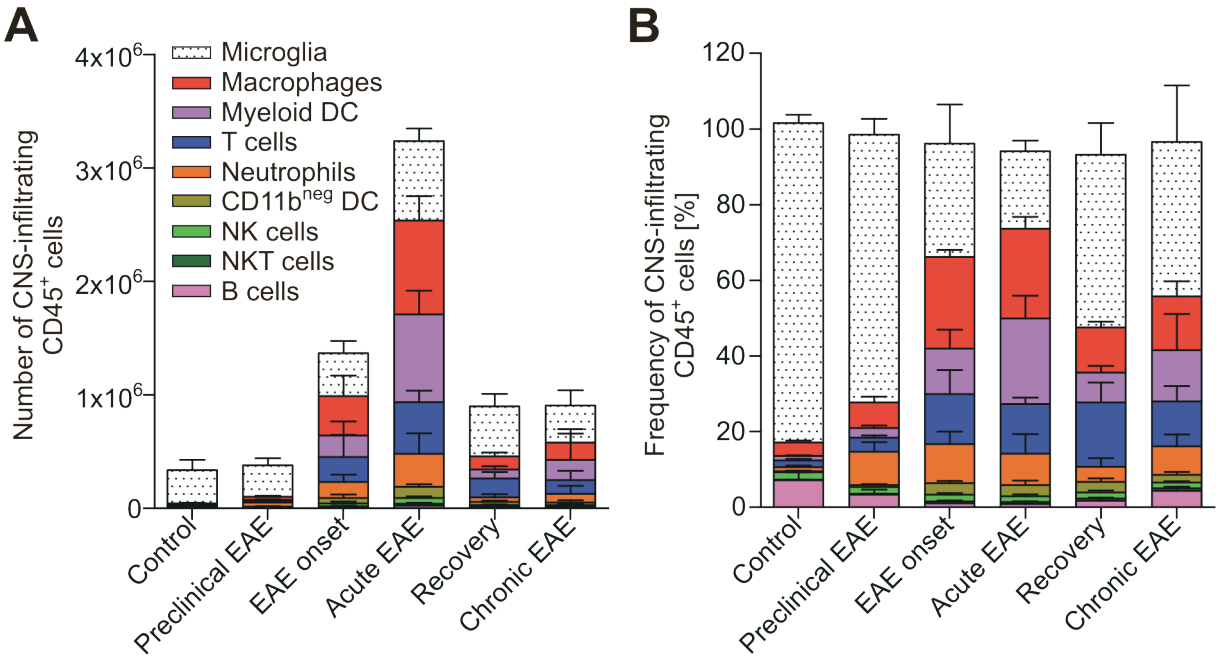

Fig. 3 Temporal dynamics of CNS-infiltration by immune cells. (A) Mean calculated numbers of investigated CNS-infiltrating cell types. Results for individual cell types are stacked. (B) Frequency of investigated immune cell types within CNS-infiltrating cells. $CD45^+$ cells are set to 100%. Results are shown as mean ± sd. Numbers of analysed animals is indicated in table 4.

In healthy control animals, microglia constitute 85% of CNS-resident $CD45^+$ cells, whereas the remaining 15% are distributed among all investigated immune cell types. Numbers of microglia do not increase before the onset of clinical symptoms and are only significantly increased during acute disease, when microglia expand about two-fold reaching a maximum quantity of about 7×10^5. At this point, microglia are one of the main components of CNS-infiltrating cells. After recovery and during chronic disease, numbers of microglia are only slightly elevated over levels in control animals.

Compared to healthy controls, the number of CNS-infiltrating $CD45^{high}$ cells is already elevated two-fold during preclinical EAE, indicating that infiltration into the CNS starts already two to three days before the onset of clinical symptoms. Neutrophils, macrophages and T cells are the main cell types involved in this early infiltration. Neutrophils show characteristics of early inflammatory cells with almost ten-fold expansion already in the preclinical phase. Although their numbers increase further after the onset of disease, the proportion of neutrophils among CNS-infiltrating cells does not expand further and even declines during acute EAE. In contrast, numbers and frequency of macrophages and T cells increase after onset of clinical symptoms. At this time point, CNS-infiltration of professional

APC like myeloid DC can also be detected. During acute disease, the main components of the inflammatory infiltrate are then macrophages, myeloid DC and T cells. A significant contribution of CD11b$^-$ DC, NK cells and NKT cells to CNS inflammation could also be detected, whereas numbers of B cells were only elevated in animals suffering from very severe EAE associated with hind limb paralysis. Recovery from severe EAE and the transition to chronic disease were mainly associated with a decrease in the numbers of macrophages and myeloid DC, although both populations are still contributing to the inflammatory infiltrate during chronic disease. Interestingly, T cells constitute one of the main cell types among CNS-infiltrating cells during recovery and the main cell type during chronic disease.

In summary, the immune response in the CNS during preclinical EAE is dominated by innate immune cells like neutrophils and macrophages, whereas after the onset of disease, T cells and professional APC contribute more and more to CNS inflammation. After recovery and during chronic disease, the inflammatory response declines, but a substantial amount of infiltrating cells remains in the CNS during this period.

4.1.3 Activation of CNS-infiltrating immune cells over the disease course

Antigen-presenting cells show signs of chronic activation

In order to investigate the potential of APC to present antigen and costimulatory signals to T cells, the expression of MHCII and the costimulatory molecules CD80 and CD40 on microglia, macrophages and DC was investigated (Fig. 4). Therefore these four populations were identified with a multi-color flow cytometric staining according to Fig. 2B and the expression of maturation markers was investigated in comparison to control stainings (see table 3). High expression of MHCII can be detected from disease onset and remains high over the whole observation period in all investigated cell populations (Fig. 4A). CNS-resident microglia from healthy control animals do not express MHCII, while expression is seen on a small fraction of resident macrophages and DC. Already at onset of clinical symptoms, MHCII–expression on mDC reaches maximal levels, while the expression on microglia, macrophages and CD11b$^-$ DC increases further during acute disease. During recovery from the initial clinical attack and during chronic disease, only microglia show a significantly lower MHCII-expression compared to acute disease, while expression levels on macrophages and DC remain stable. Interestingly, CD11b$^-$ DC isolated during recovery and in chronic disease express even higher levels of MHCII than during acute disease.

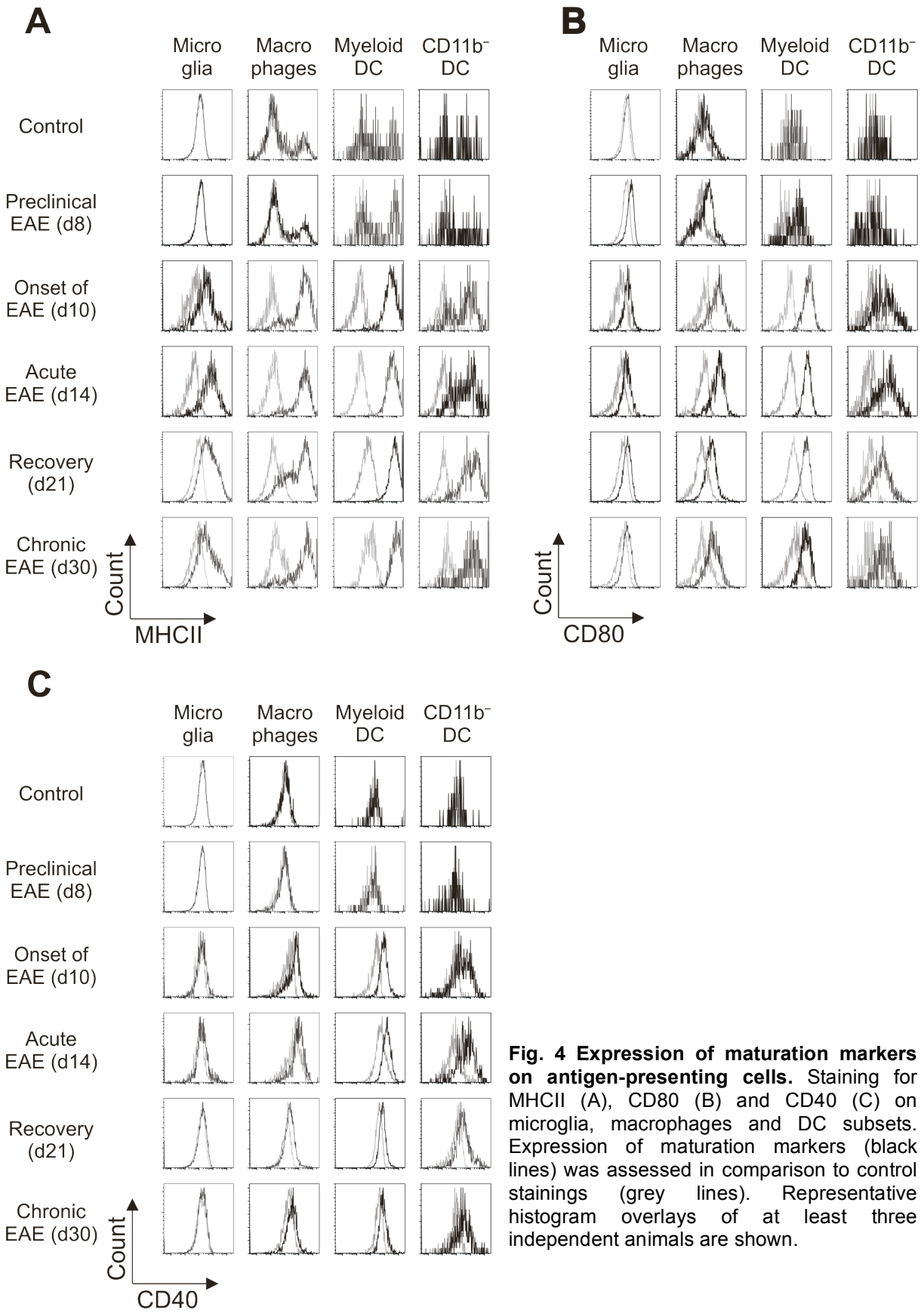

Fig. 4 Expression of maturation markers on antigen-presenting cells. Staining for MHCII (A), CD80 (B) and CD40 (C) on microglia, macrophages and DC subsets. Expression of maturation markers (black lines) was assessed in comparison to control stainings (grey lines). Representative histogram overlays of at least three independent animals are shown.

In contrast to MHCII-expression, elevated levels of CD80, by which APC provide a costimulatory signal to T cells, can even be detected in preclinical EAE (Fig. 4B). Already at this disease stage microglia reach their maximum expression, while further upregulation of CD80 on macrophages and DC can be observed at disease onset and during acute disease. During recovery and in chronic disease all investigated cell populations express reduced, but stable levels of CD80. Concerning CD40, by which APC receive maturation signals from T cells, only little expression could be detected on microglia and macrophages, however, DC expressed high CD40 levels during disease (Fig. 4C). On both populations, a significant upregulation of CD40 is visible at onset of disease, which increases further on $CD11b^-$ DC during acute disease. During recovery and chronic disease, macrophages, mDC and $CD11b^-$ DC maintain a reduced, but stable CD40 expression.

In summary, microglia, macrophages and DC upregulate surface molecules such as MHCII, CD80 and CD40, which are involved in the presentation of antigen and activation of CNS-infiltrating $CD4^+$ T cells. However, DC subsets show constitutive expression of these molecules as well as the highest upregulation during acute disease. After recovery and during chronic disease all investigated cell types retain elevated expression levels of maturation markers indicating chronic activation.

Dynamics of T cell activation

In order to characterise the dynamics of T cell activation, CNS-infiltrating $CD4^+$ regulatory and effector T cells as well as $CD8^+$ T cells were quantified and T cell activation was determined by analysing the expression of CD69 as a marker of recent activation as well as the IL-2 receptor α chain (CD25; Fig. 5). T cells were identified as $CD45^{high}CD3^+$ population and then further subdivided into $CD8^+$ T cells and $CD4^+$ T cells (Fig. 5A). Based on the constitutive expression of CD25 and the transcription factor FoxP3, regulatory T cells were identified as $CD4^+CD25^+FoxP3^+$ T cells, whereas $CD4^+$ effector T cells were gated as $CD4^+FoxP3^-$ T cells. $CD4^+$ T cells account for the majority of CNS-infiltrating T cells (85%) and infiltrate already at disease onset at near maximal amounts (Fig. 5B). In contrast, $CD8^+$ T cells infiltrate in smaller numbers (Fig. 5C). The further increase of $CD4^+$ T cells during acute disease is mainly due to the infiltration of regulatory T cells at that time point (Fig. 5D), whereas $CD4^+$ effector T cell levels are not significantly altered between onset and acute disease. This leads to a change in the ratio of $CD4^+$ regulatory T cells to $CD4^+$ effector T cells from 1:30 during preclinical EAE and during disease onset to 1:15 during acute disease.

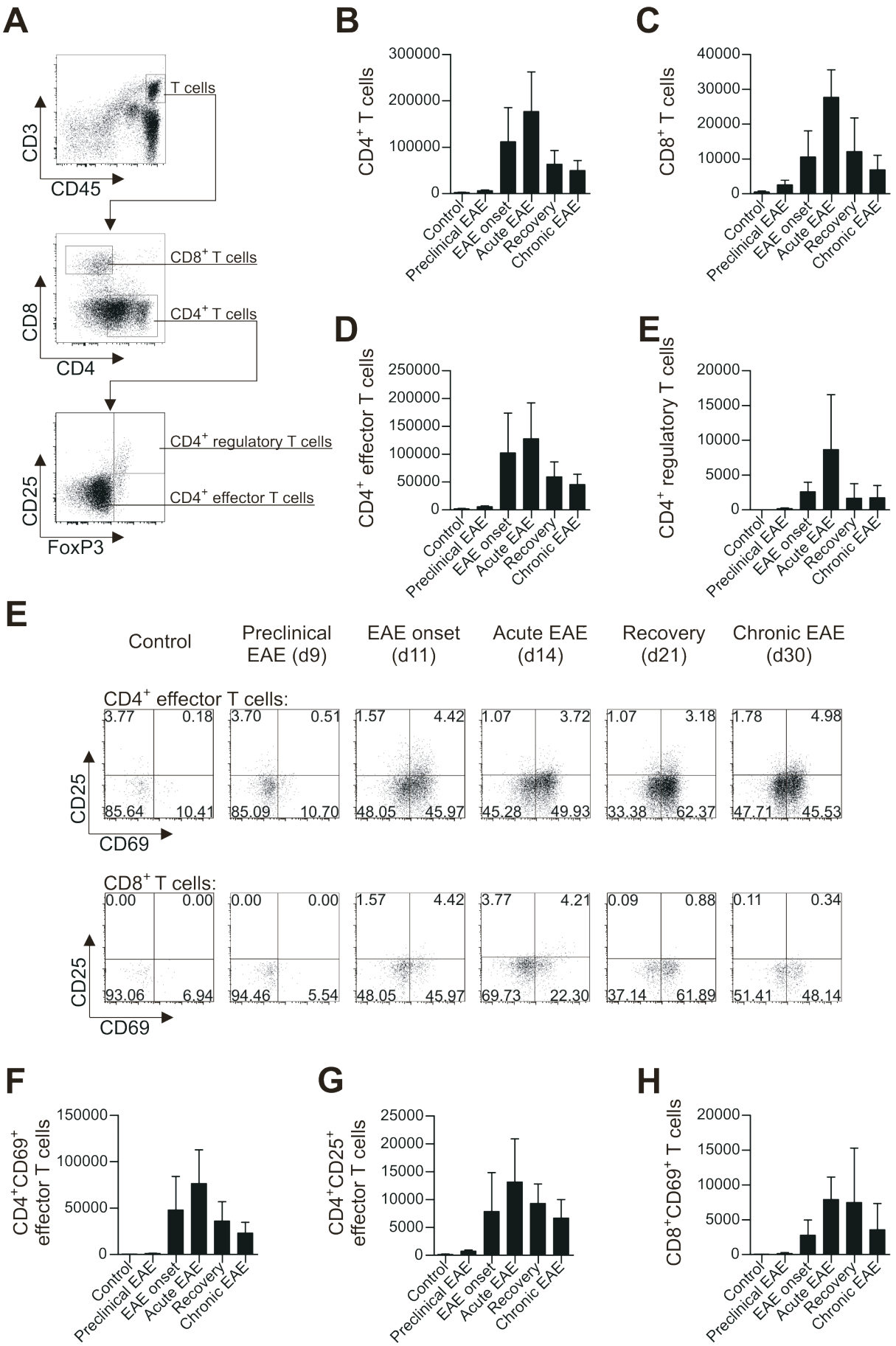
A
T cells
CD3
CD45
CD8+ T cells
CD4+ T cells
CD8
CD4
CD4+ regulatory T cells
CD4+ effector T cells
CD25
FoxP3
B
CD4+ T cells
C
CD8+ T cells
D
CD4+ effector T cells
E
CD4+ regulatory T cells
Control
Preclinical EAE
EAE onset
Acute EAE
Recovery
Chronic EAE
E
Control
Preclinical EAE (d9)
EAE onset (d11)
Acute EAE (d14)
Recovery (d21)
Chronic EAE (d30)
CD4+ effector T cells:
3.77 0.18 85.64 10.41
3.70 0.51 85.09 10.70
1.57 4.42 48.05 45.97
1.07 3.72 45.28 49.93
1.07 3.18 33.38 62.37
1.78 4.98 47.71 45.53
CD8+ T cells:
0.00 0.00 93.06 6.94
0.00 0.00 94.46 5.54
1.57 4.42 48.05 45.97
3.77 4.21 69.73 22.30
0.09 0.88 37.14 61.89
0.11 0.34 51.41 48.14
CD25
CD69
F
CD4+CD69+ effector T cells
G
CD4+CD25+ effector T cells
H
CD8+CD69+ T cells

Fig. 5 Quantification of CNS-infiltrating T cell subsets and expression of activation markers. (A) CNS-infiltrating T cells ($CD45^{high}CD3^{+}$) are subdivided into $CD8^{+}$ T cells ($CD45^{high}CD3^{+}CD4^{-}CD8^{+}$), $CD4^{+}$ T cells ($CD45^{high}CD3^{+}CD8^{-}CD4^{+}$), $CD4^{+}$ effector T cells ($CD45^{high}CD3^{+}CD8^{-}CD4^{+}FoxP3^{-}$) and $CD4^{+}$ regulatory T cells ($CD45^{high}CD3^{+}CD8^{-}CD4^{+}FoxP3^{-}CD25^{+}$). (B-E) Calculated numbers of CNS-infiltrating $CD4^{+}$ T cells (B), $CD8^{+}$ T cells (C), $CD4^{+}$ effector T cells (D) and $CD4^{+}$ regulatory T cells (E) are shown. (F) Expression of activation markers on $CD4^{+}$ effector T cells (upper panel) and $CD8^{+}$ T cells (lower panel) was analysed. (G-I) Calculated numbers of CNS-infiltrating $CD4^{+}$ effector T cells expressing either CD69 (G) or CD25 (H) and $CD8^{+}$ T cells expressing CD69 (I). Dotplots of representative animals are shown. Calculated numbers of CNS-infiltrating cells are mean ± sd ($n \geq 3$).

During recovery, T cell numbers decrease significantly, but T cell infiltration is still visible. Interestingly the ratio of $CD4^{+}$ regulatory T cells to $CD4^{+}$ effector T cells again declines to 1:30.

Starting at onset of disease signs of recent T cell activation can be detected over the whole disease course (Fig. 5E). The proportion of $CD4^{+}$ effector T cells and $CD8^{+}$ T cells expressing CD69 is steadily increasing until animals recover from the initial attack, when about 60% of both T cell populations are activated. The frequency of $CD69^{+}$ T cells then drops slightly during chronic disease. At the onset of clinical symptoms a small proportion of $CD4^{+}$ T cells starts to express CD25 (4%), whereas no clear $CD25^{+}$ population can be distinguished in the $CD8^{+}$ T cell population. The frequency of CD25-expressing $CD4^{+}$ effector T cells is then maintained over the whole disease process. In absolute numbers, CNS-infiltrating activated $CD4^{+}$ effector T cells expressing either CD69 or CD25 can be detected at almost maximal amounts already at onset of disease (Fig. 5F, G) and do not increase significantly during acute disease. During recovery from the initial attack, numbers of activated $CD4^{+}$ effector T cells decrease, but a significant fraction of activated $CD4^{+}$ effector T cells remains in the CNS during chronic disease. In contrast to $CD4^{+}$ effector T cells the infiltration of activated $CD8^{+}$ T cells into the CNS is slightly shifted to later time points (Fig. 5H) reaching maximal amounts of activated $CD8^{+}$ T cells during acute disease. During recovery the amount of activated $CD8^{+}$ T cells in the CNS remains stable, and numbers of $CD69^{+}CD8^{+}$ T cells only drop during chronic disease.

In the inflamed CNS, Th17 cells persist longer than Th1 cells

In order to quantitate the relative contribution to T cell infiltration by the two major T helper subsets Th1 and Th17 into the CNS, IFN-γ and IL-17 production by CNS-infiltrating $CD4^{+}$ and $CD8^{+}$ T cells was determined by intracellular cytokine staining followed by flow cytometric analysis (Fig. 6). For this, isolated CNS-infiltrating cells were restimulated *in vitro* in the presence of brefeldin A, which inhibits the secretory pathway of protein synthesis and therefore leads to intracellular accumulation of otherwise secreted proteins such as cytokines.

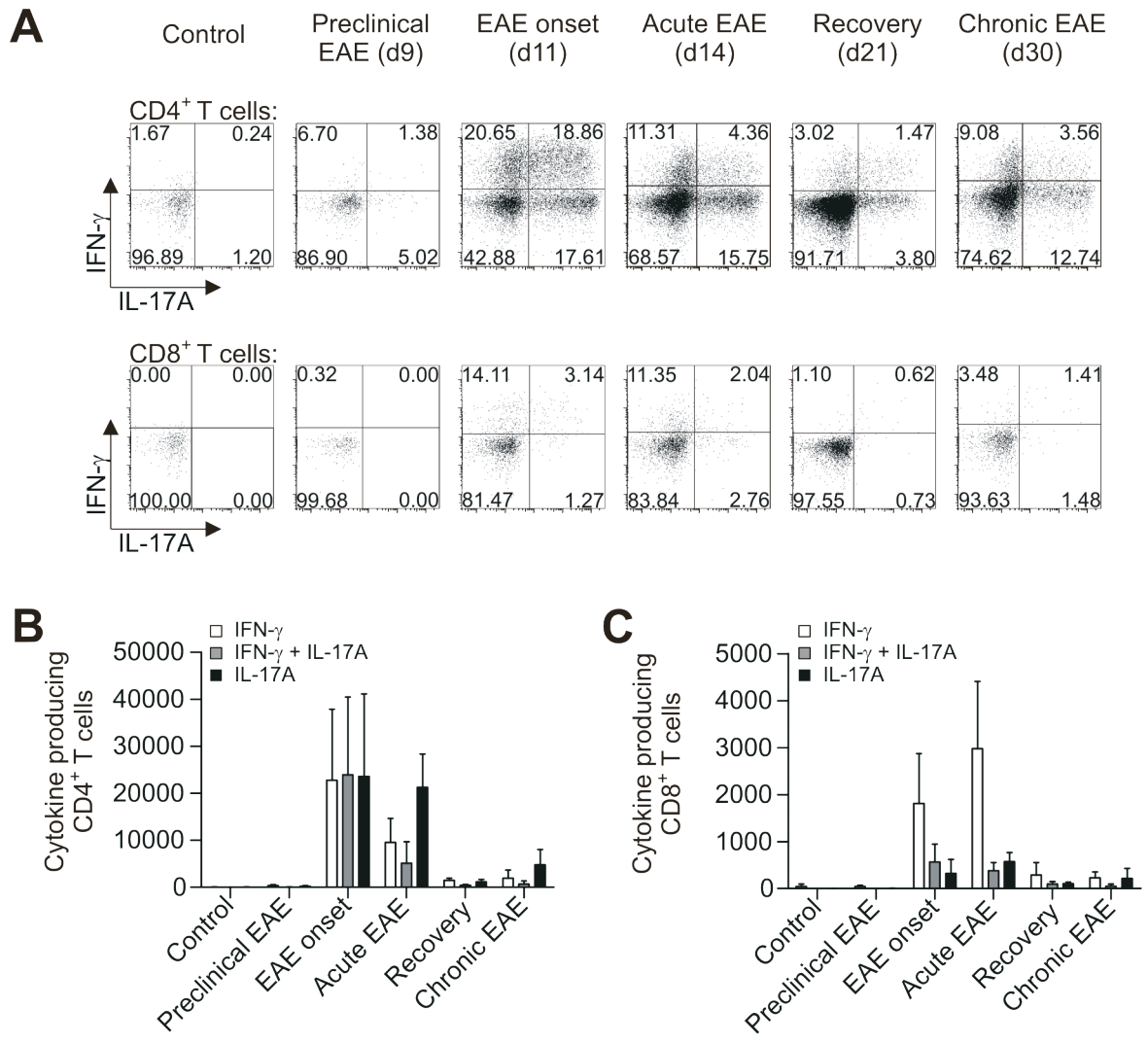

Fig. 6 Quantification of cytokine production by CNS-infiltrating CD4$^+$ and CD8$^+$ T cells. (A) Representative intracellular cytokine stainings of CNS-infiltrating CD4$^+$ T cells (upper panel) and CD8$^+$ T cells (lower panel). (B-C) Calculated numbers of cell producing IFN-γ (white bars), IL-17A (black bars) or both cytokines (grey bars) are shown for CD4$^+$ T cells (B) and CD8$^+$ T cells (C). Results are mean ± sd (n≥4).

CD4$^+$ and CD8$^+$ T cells were identified according to the gating strategy shown in Fig. 5A. During disease, production of IL-17 and IFN-γ can be detected in CD4$^+$ and CD8$^+$ T cells (Fig. 6A). Already before the onset of clinical symptoms, CNS-infiltrating CD4$^+$ T cells start to produce IL-17 and IFN-γ, which they do in comparable amounts (~6%). At onset of clinical symptoms, cytokine-production by CD4$^+$ T cells is maximal, with ~60% of cells producing either IL-17 or IFN-γ. At this time point, neither Th1 nor Th17 cell differentiation is favoured, since comparable amounts CD4$^+$ T cells produce IL-17, IFN-γ or both cytokines. During acute disease, overall cytokine production decreases, and the balanced Th responses shift towards a Th17 response, as IFN-γ-producing CD4$^+$ T cells decline. In contrast, the number and frequency of IL-17-producing CD4$^+$ T cells remains stable (Fig. 6B). During recovery,

IL-17 producing CD4$^+$ T cells decline. When cytokine production during chronic disease increases again, IL-17-producing CD4$^+$ T cells dominate again. Concerning CD8$^+$ T cells, only a small fraction appears to produce IL-17, while most of them produce IFN-γ (Fig. 6A). Cytokine-producing CD8$^+$ T cells are only detectable after the onset of clinical symptoms and increase further during acute disease (Fig. 6C). During recovery and chronic disease, only a small fraction of CD8$^+$ T cells produces IL-17 or IFN-γ in the CNS.

In summary, the Th response in the CNS changes during the disease course from a response predominantly involving both Th1 and Th17 cells in equal amounts to an inflammatory response, which is substantially less pronounced, but mainly composed of Th17 cells.

4.1.4 Th17 cells can be identified by expression of surface IL-17A

Since the detection of cytokine-producing T cells requires the accumulation of cytokines in the cell and subsequent fixation and permeablilization for intracellular staining, these cells are of no further use for functional assays. Surprisingly, IL-17A could be detected on the cell surface of *in vitro* restimulated CD4$^+$ T cells (Fig. 7).

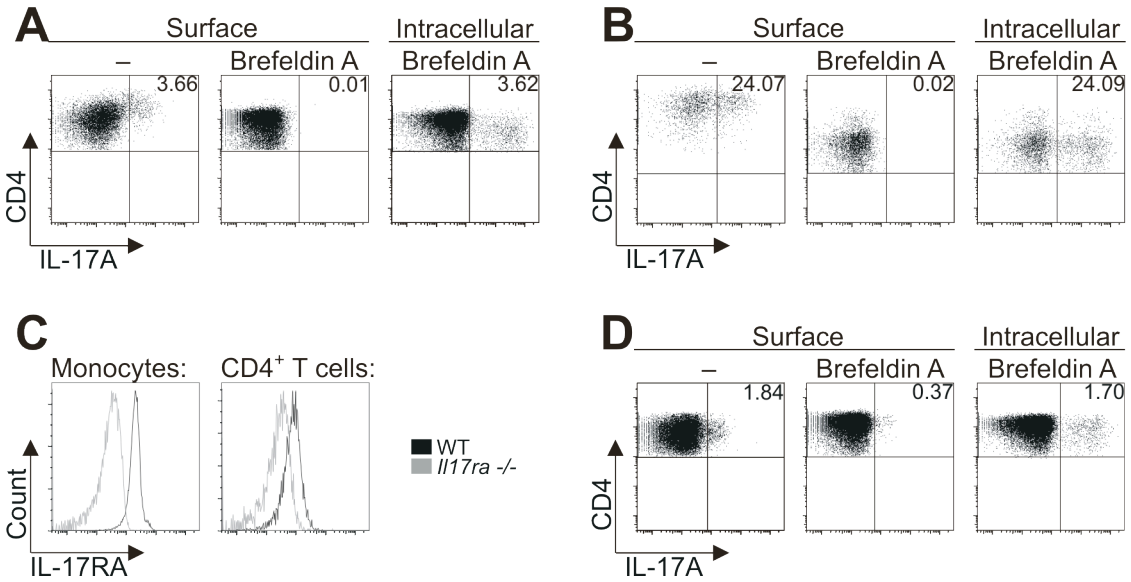

Fig. 7 IL-17A is displayed on the surface of Th17 cells, but not bound to IL17R. (A-B) CD4$^+$ T cells were isolated from splenocytes (A) or CNS-infiltrating cells (B) during EAE and restimulated *in vitro* with PMA and ionomycin and stained 16 h later for IL-17A without cell permeabilization (left, middle) or after permeabilization (right). Brefeldin A was added where indicated. The frequency of CD4$^+$ T cells expressing surface-IL17A or intracellular IL-17A is indicated. (C) Expression of IL-17RA on splenocytes was analysed on WT (black lines) compared to IL-17RA-deficient mice (grey lines). Histogram overlays show monocytes (CD11b$^+$, left) and CD4$^+$ T cells (CD3$^+$CD4$^+$, right). (D) CD4$^+$ T cells from IL17RA-deficient mice were isolated from splenocytes during EAE and stained for surface and intracellular IL-17A as described above. Representative results from at least three animals are shown.

In order to detect surface expression of IL-17A, $CD4^+$ T cells were purified from splenocytes and CNS-infiltrating cells during acute EAE. Purified $CD4^+$ T cells were restimulated with PMA and ionomycin and stained for IL-17A at the cell surface and intracellularly. Compared to IL-17A-producing $CD4^+$ T cells identified by intracellular cytokine staining, a similar amount of $CD4^+$ T cells expressed IL-17A on the surface of splenic $CD4^+$ T cells (3.66 and 3.62%) (Fig. 7A) and CNS-infiltrating $CD4^+$ T cells (24.07 and 24.09%) (Fig. 7B). $CD4^+$ T cells stimulated in the presence of brefeldin A were completely devoid of surface IL-17A in both cases (Fig. 7A,B), suggesting that surface-IL-17A expression is specific and allows the reliable identification of living IL-17A-producing $CD4^+$ T cells.

Cytokines can be displayed on the cell surface either bound to a receptor or directly anchored to the cell membrane by a transmembrane domain. Since no transmembrane domain is reported for IL-17A, the role of IL-17 receptor (IL-17RA) in expression of surface IL-17A was assessed using IL-17RA-deficient mice. IL-17RA is expressed on myeloid cells like monocytes and on $CD4^+$ T cells in WT animals (Fig. 7C). Nevertheless, surface IL-17A can still be detected on $CD4^+$ T cells isolated from immunized IL-17RA-deficient animals (Fig. 7D). Again, the proportion of surface IL-17A-expressing $CD4^+$ T cells was comparable to IL-17A-producing $CD4^+$ T cells identified by intracellular cytokine staining (1.84 and 1.70%). This suggests that IL-17A displayed on the cell surface of $CD4^+$ T cells is not bound to IL-17RA.

4.2 Neutrophil granulocytes in EAE

Since neutrophils appeared early during the infiltration of the CNS by immune cells and since the role of neutrophils is relatively underexplored in EAE and MS, their functional role in the development and progression of EAE was characterised further. Therefore, the neutrophil-response and its involvement during induction of EAE was characterised and a neutrophil-specific depletion system was established.

4.2.1 Identification and isolation of mouse neutrophils

In different disease models including EAE the anti-Gr-1 antibody RB6-8C5[285] has been employed in phenotypical and functional studies of neutrophils for their detection and depletion. This antibody recognizes not only the neutrophil-specific surface protein Ly-6G, but also Ly-6C, a molecule that is expressed by several other immune cells, like plasmacytoid DC and subsets of monocytes and T cells[175,193]. Therefore, anti-Gr-1 (RB6-8C5) is clearly not

suitable for neutrophil specific targeting. Since Ly-6C^{high}-expressing monocytes have been shown to be essential for development of EAE[286,287], results from depletion studies using anti-Gr-1 in EAE are unprecise and need to be revisited. In order to specifically detect and deplete neutrophils during EAE, the monoclonal anti-Ly-6G antibody 1A8[193] was used, which does not recognize Ly-6C (Fig. 8).

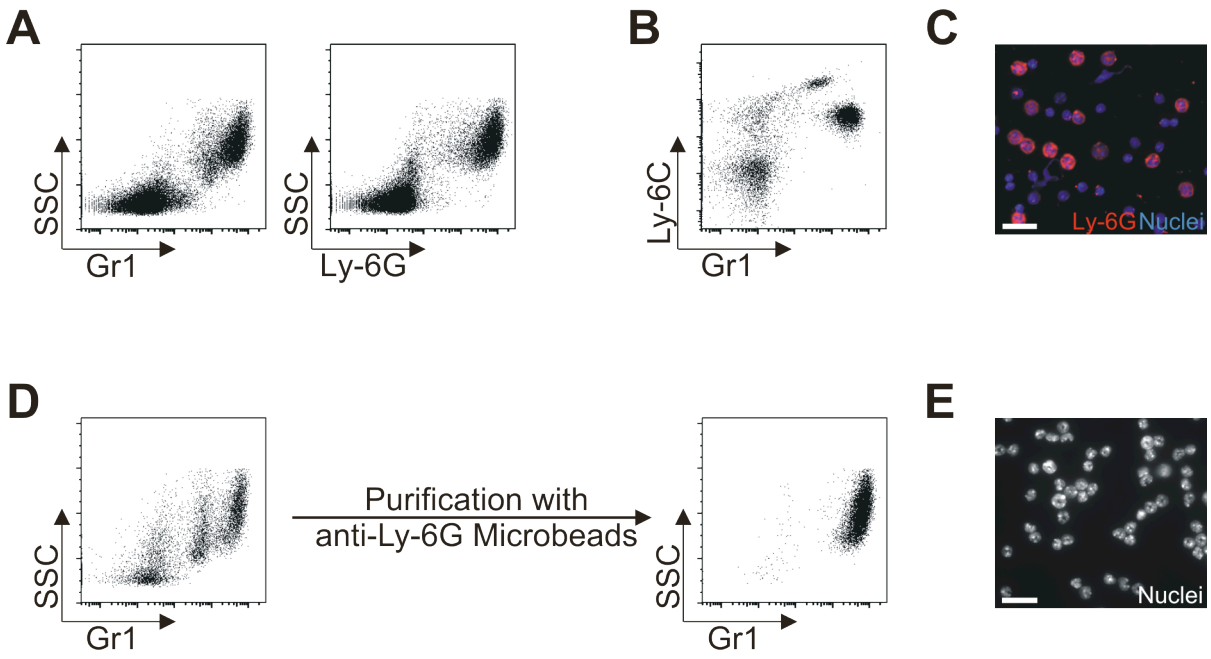

Fig. 8 Anti-Ly-6G antibody 1A8 specifically detects neutrophils. (A) Flow cytometric analysis of splenocytes isolated eight days after immunization using anti-Gr1 (RB6-8C5, left) or anti-Ly-6G (1A8, right). (B) Double staining of anti-Gr1 and anti-Ly-6C on peripheral blood cells eight days after immunization. (C) Immunofluorescent staining using rat-anti-Ly-6G/ anti-rat-Cy3 on cytospins from splenocytes isolated eight days after immunization. (D) Purification of Gr1^{high}-expressing cells from bone marrow cells by magnetic separation using anti-Ly-6G microbeads. (E) Nuclei of purified Gr1^{high}-expressing cells were stained with Hoechst 33258. Scale bars represent 20 µm.

In the peripheral blood of mice that have been immunized with MOG 35-55 in CFA, staining with anti-Gr-1 antibody RB6-8C5 leads to the detection of two populations of Gr1^{int} and Gr1^{high}-expressing cells, whereas the anti-Ly-6G antibody 1A8 labels only one population (Fig. 8A). This double recognition by anti-Gr-1 is clearly due to the corecognition of Ly-6C^{high}-expressing cells (Fig. 8B). Accordingly, immunofluorecence staining with anti-Ly-6G specifically labels cells with a segmented nucleus, which is typical for neutrophils (Fig.8C). In addition, affinity purification using anti-Ly-6G microbeads allows the specific isolation of Gr1^{high}-expressing cells out of mixed cell populations like bone marrow cells (Fig. 8D). This purified cell fraction shows a morphology, which is characteristic for neutrophils (Fig. 8E).

4.2.2 Characterisation of neutrophil involvement during EAE

The presence of pathogen-associated molecular patterns (PAMP) and of pro-inflammatory cytokines like GM-CSF, TNF-α and IFN-γ leads to a neutrophil response in the affected organism. This response includes an increased release of neutrophils from the bone marrow and the secretion of rective oxygen species, proteases and cytokines from the activated neutrophil[164]. *In vitro* activation of Neutrophils by heat-inactivated mycobacteria leads to an increased surface staining of CD11b and loss of L-selectin (CD62L) (Fig. 9). Both proteins are involved in the migration and extravasation of neutrophils into inflamed tissues[288], changes in surface expression therefore indicate neutrophil activation and extravasation.

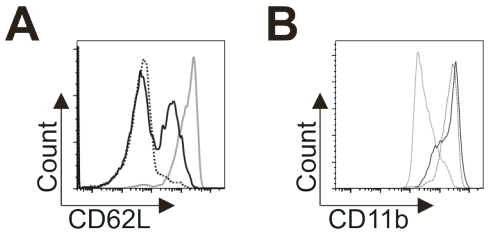

Fig. 9 Changes in surface marker expression upon neutrophil activation. Bone marrow neutrophils were stimulated with 50 µg/ ml heat-inactivated *M. tuberculosis* particles. Surface expression of CD62L (A) and CD11b (B) was investigated after 6 h (black line) and 24 h (dotted line) and compared to unstimulated cells (grey line).

In order to investigate neutrophil release from the bone marrow as well as neutrophil activation, the frequency of $Gr1^{high}$-expressing neutrophils was analysed in peripheral blood, spleen and mesenteric lymph nodes (mesLN) at several time points after immunization until development of acute disease (Fig. 10A). The proportion of neutrophils in peripheral blood and spleen increases steadily after immunization, whereas only a marginal number of neutrophils are detected in mesLN. Activation of neutrophils in peripheral compartments was assessed by staining for CD11b (data not shown) and CD62L (Fig. 10B). Whereas surface expression of CD11b remains unchanged in both compartments, up to 20% of neutrophils loose CD62L-surface expression in the peripheral blood before the onset of clinical symptoms. In the spleen, CD62L expression decreases accordingly, but is minimal at onset of disease. During the preclinical stage of the disease at day eight, when neutrophils show first signs of activation in the peripheral blood, the first neutrophils infiltrate into the CNS (Fig. 10C). At that time point, only a small number of other infiltrating cells can be detected, and neutrophils constitute up to 40% of infiltrating $CD45^{high}$-expressing cells. After the onset of clinical symptoms, additional infiltration of other immune cells like T cells can also be detected.

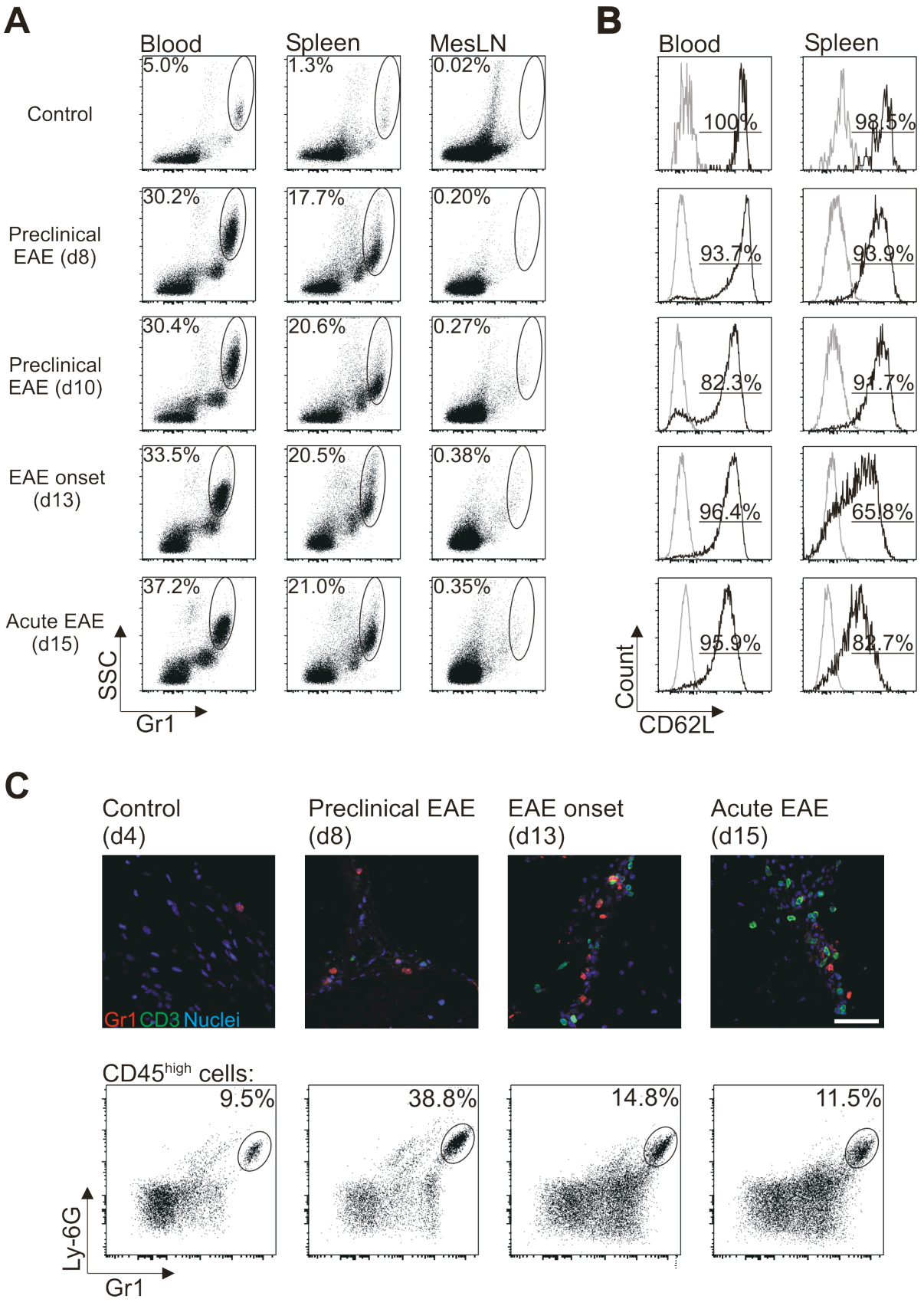
A
Blood
Spleen
MesLN
Control
5.0%
1.3%
0.02%
Preclinical EAE (d8)
30.2%
17.7%
0.20%
Preclinical EAE (d10)
30.4%
20.6%
0.27%
EAE onset (d13)
33.5%
20.5%
0.38%
Acute EAE (d15)
37.2%
21.0%
0.35%
SSC
Gr1
B
Blood
Spleen
100%
98.5%
93.7%
93.9%
82.3%
91.7%
96.4%
65.8%
95.9%
82.7%
Count
CD62L
C
Control (d4)
Preclinical EAE (d8)
EAE onset (d13)
Acute EAE (d15)
Gr1 CD3 Nuclei
CD45high cells:
9.5%
38.8%
14.8%
11.5%
Ly-6G
Gr1

Fig. 10 Neutrophil response after immunization with MOG 35-55 in CFA. Peripheral blood and single cell suspensions obtained from spleen, mesenteric lymph nodes (mesLN) and CNS-infiltrating cells were analysed by flow cytometry at indicated time points after immunization. (A) Neutrophils were identified as $Gr1^{high}$-expressing cells within $CD45^{+}$ cells in peripheral blood, spleen and mesLN. The frequency of $Gr1^{high}$-expressing neutrophils within CD45+ cells is indicated. (B) Surface expression of CD62L was analysed on $CD45^{+}Gr1^{high}$-expressing cells in peripheral blood and splenocytes. Representative histogram overlays of anti-CD62L-staining (black line) and control staining (grey line) are shown. The precentage of $CD45^{+}Gr1^{high}$-expressing cells expressing high amounts of CD62L is indicated (C) CNS-infiltration of neutrophils was analysed by immunohistochemistry using anti-Gr1 combined with the pan-T cell staining anti-CD3 (upper panel). Scale bar represents 50 µm. The frequency of $Gr1^{high}Ly\text{-}6G^{+}$ neutrophils in CNS-infiltrating $CD45^{high}$cells was analysed by flow cytometry (lower panel). Representative results of at least three animals are shown.

Although neutrophil infiltration into the CNS further increases after disease onset, the proportion of neutrophils within infiltrating $CD45^{high}$-expressing cells decreases considerably.

4.2.3 Antibody-mediated depletion of neutrophils ameliorates actively induced EAE

The functional role of early neutrophil infiltration into the CNS during EAE was approached by neutrophil-depletion studies using the anti-Ly-6G antibody 1A8.

Anti-Ly-6G treatment results in a transient, but specific depletion of neutrophils

In order to establish antibody-mediated neutrophil depletion, anti-Ly-6G was administered once six days after immunization and the temporal development of neutrophil numbers and the depletion specificity in the peripheral blood of treated animals was analysed by flow cytometry (Fig. 11). Single administration of anti-Ly-6G leads to a transient reduction of neutrophils in the peripheral blood of treated animals (Fig. 11A). After an initial decrease of neutrophil numbers from 30% before treatment to below 5% after two days, depletion is efficient for two more days. Five days after treatment with anti-Ly-6G neutrophil numbers increase again and reach normal levels six days after treatment. In order to investigate the specificity of the depletion, the frequencies of Ly-6C-expressing cells like $Ly\text{-}6C^{high}$-expressing monocytes, monocytes and T cells were investigated concomitant to neutrophil depletion (Fig. 11B-E). Although neutrophil numbers are decreased considerably upon treatment, no change is observed in any of the other populations.

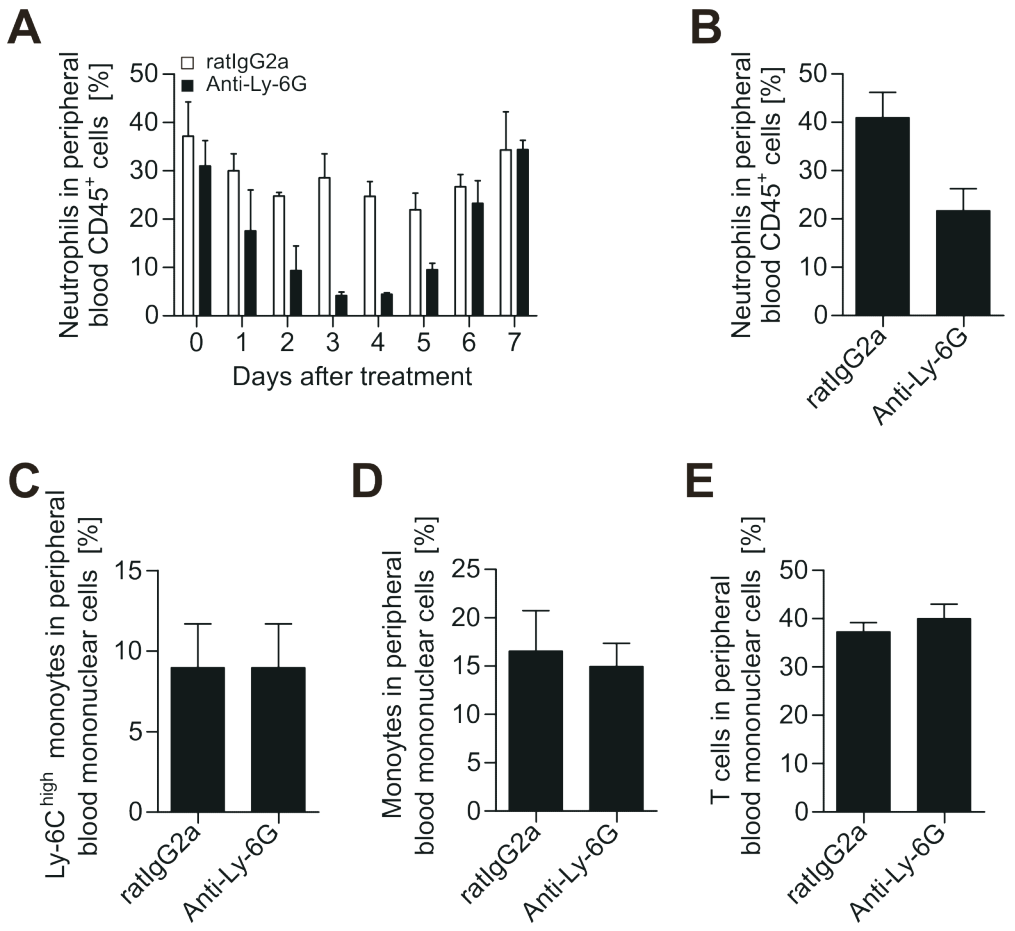

Fig. 11 Treatment with anti-Ly-6G antibody 1A8 specifically depletes neutrophils. (A) Time course of neutrophil depletion upon a single administration of 100 µg anti-Ly-6G i.v. six days after immunization. Neutrophils were identified as $Gr1^{high}$-expressing cells within peripheral blood $CD45^+$ cells by flow cytometry. Anti-Ly-6G treated animals (black bars) were analysed in comparison to isotype control treated animals (white bars). (B-E) Flow cytometric analysis of depletion specificity 48 h after a single administration of 50 µg anti-Ly-6G i.v.. The frequency of neutrophils ($Gr1^{high}Ly\text{-}6C^{int}$; B), $Ly\text{-}6C^{high}$-expressing monocytes ($Gr1^{int}Ly\text{-}6C^{high}$; C), monocytes ($Ly\text{-}6C^{low/int}CD11b^+$; D) and T cells ($CD3^+$; E) was analysed within peripheral blood $CD45^+$ cells. Results are mean ± sd. (n≥3)

Neutrophils are essential for the development of EAE

In order to investigate the functional role of the early infiltration of neutrophils into the CNS during EAE, animals were treated with anti-Ly-6G or corresponding isotype control (ratIgG2a) before and at the onset of clinical symptoms (Fig. 12). Since antibody-mediated depletion of neutrophils results only in a transient reduction of neutrophil numbers in the peripheral blood, immunized animals were either treated once or every other day with anti-Ly-6G. A transient depletion of neutrophils results in a delayed onset of disease (Fig. 12A), whereas continous depletion of neutrophils is able to completely abrogate the development of clinical EAE (Fig. 12B).

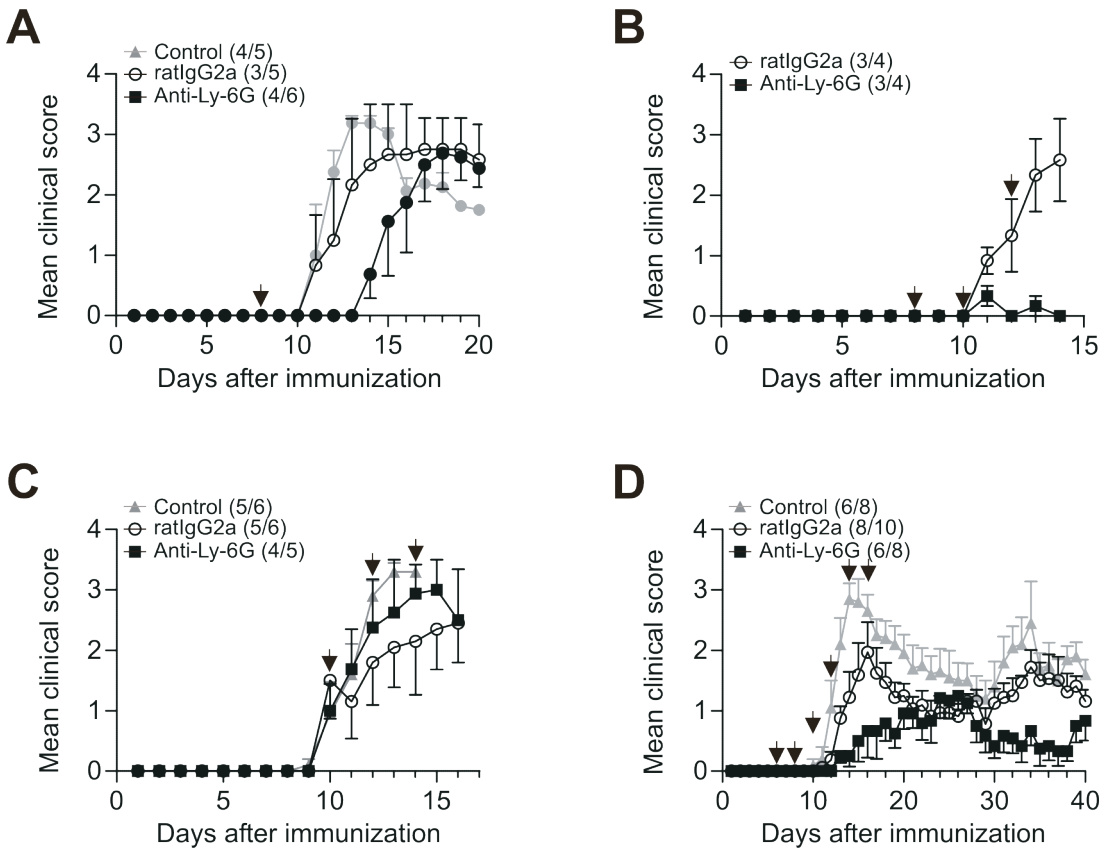

Fig. 12 Antibody-mediated neutrophil depletion during preclinical EAE inhibits disease initiation. At indicated time points after EAE induction (black arrows) animals were treated with 100 µg anti-Ly-6G i.v. (black squares), corresponding isotype control ratIgG2a (open circles) or left untreated (grey triangles). Animals were either treated with a single injection only (A), or with repeated injections every second day (B-D). Results show mean clinical score of diseased animals ± sem. Disease incidences are shown in the legend.

In agreement with the early recruitment of neutrophils into the CNS already during preclinical EAE, depletion of neutrophils after the onset of clinical symptoms has no significant effect on disease incidence or severity (Fig. 12C). A long-term treatment with anti-Ly-6G is only efficient for maximal ten days (data not shown). Nevertheless, depletion of neutrophils for this time period results in an almost complete protection from EAE (Fig. 12D). Only two out of eight treated animals developed full-blown EAE, while the other treated animals only developed very mild clinical symptoms.

CNS-infiltrating neutrophils are important for the recruitment of professional APC and subsequent T cell activation

Since the used depletion approach should specifically target the early recruitment of neutrophils into the CNS, the peripheral T cell response and the inflammatory immune response in the CNS was analysed in the animals depicted in Fig. 12B (Fig. 13).

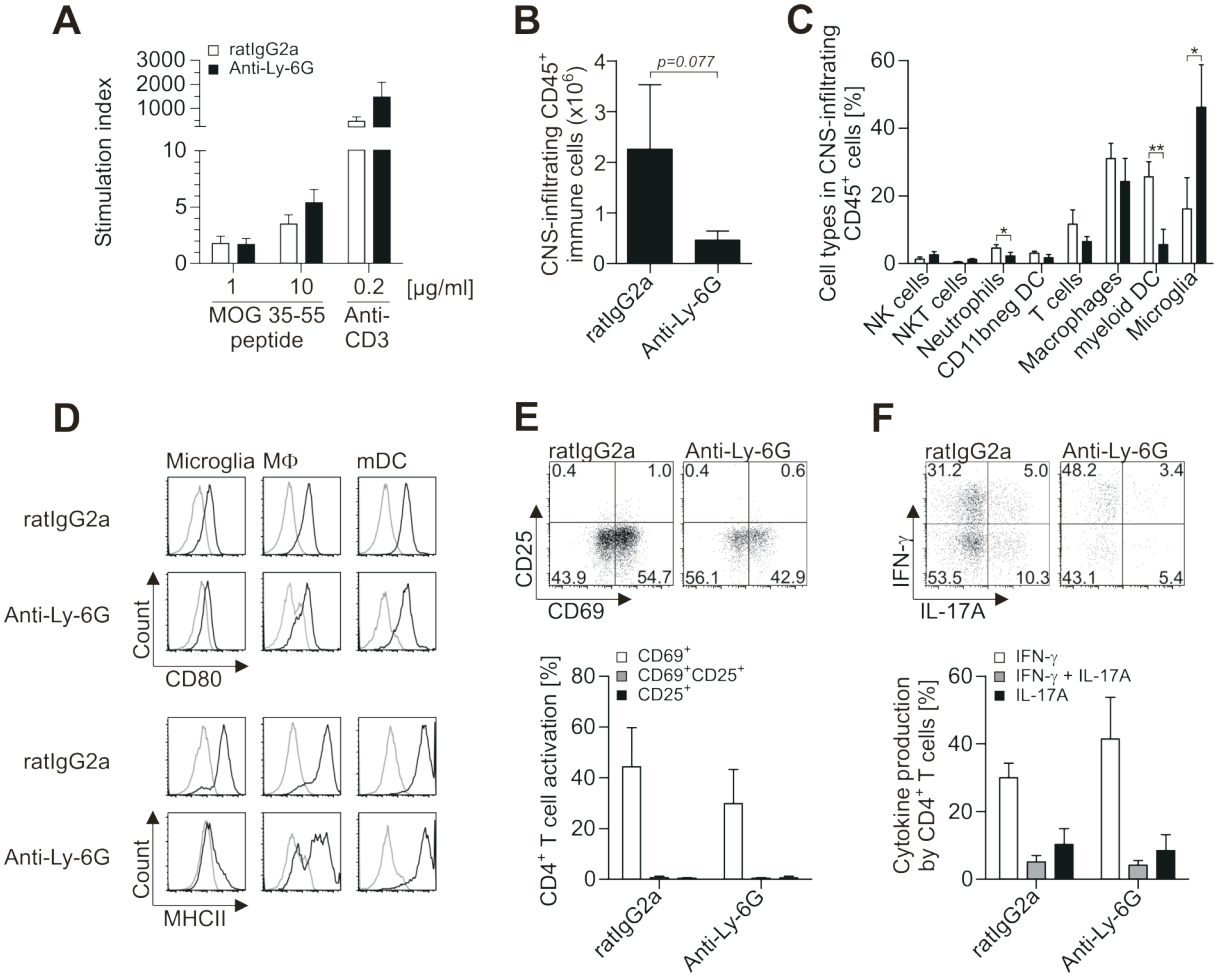

Fig. 13 Encephalitogenic immune response in anti-Ly-6G treated EAE. (A) Single cell suspensions from a pool of mesenteric, axial and brachial lymph nodes of anti-Ly-6G (black bars) or isotype control treated (white bars) animals (see Fig. 12B) were restimulated *in vitro* with either MOG 35-55 peptide or anti-CD3 (2C11) at indicated concentrations. Resulting T cell proliferation was assessed by ^{3}H-thymidine incorporation as described in 4.2.5. (B-F) CD45^{+} CNS-infiltrating cells were isolated and analysed by flow cytometry as described in 4.2.6 and table 3. CD45^{+} CNS-infiltrating cells from anti-Ly-6G and ratIgG2a treated animals were quantified by flow cytometry (B), and the frequency of different immune cell types (C), expression of maturation markers on microglia, macrophages (MΦ) and mDC (D), CD4^{+} effector T cell activation (E) and cytokine production by CD4^{+} T cells (F) was analysed. Results are mean ± sd. (n=3).

As expected, proliferation of peripheral T cells in response to MOG 35-55 or anti-CD3 does not decrease in animals treated with anti-Ly-6G compared to isotype control treated animals (Fig. 13A), suggesting that anti-Ly-6G treatment does not interfere with peripheral T cell priming. In depleted animals, even higher numbers of MOG-reactive T cells could be detected, which indicates that upon treatment peripheral T cells do not migrate into the CNS and accumulate in the periphery. For the analysis of CNS-inflammation, the quantitative flow cytometric approach described in 5.1.2 was used. In the CNS of treated animals, the number of infiltrating CD45^{+} cells is reduced by 80% (Fig. 13B). Interestingly, anti-Ly-6G treatment does not completely abrogate CNS-inflammation. The number of CNS-infiltrating CD45^{+}

cells (4.6×10^5) is elevated in comparison to healthy control animals (3.5×10^5, see also table 4). Every investigated immune cell type was decreased in absolute numbers in anti-Ly-6G treated animals, but only two populations also decreased in frequency, namely the targeted neutrophils and myeloid DC (Fig. 13C). Concomitant to the observed overall decrease in inflammation, the activation state of infiltrating immune cells was considerably reduced in treated animals (Fig. 13D-E). Microglia and macrophages (MΦ) showed less expression of maturation markers (Fig. 13D), suggesting less activation. However, CNS-infiltrating myeloid DC do not differ in maturation marker expression. Moreover, a lower proportion of $CD4^+$ T cells express the activation marker CD69 (Fig. 13E). Interestingly, the low number of infiltrating $CD4^+$ T cells in treated animals are more polarized towards Th1 cells when compared to CNS-infiltrating $CD4^+$ T cells in animals treated with isotype control (Fig.13F).

4.3 Role of Nogo/ Nogo receptor interactions for development and progression of EAE

A potential function of Nogo receptor-mediated interactions in the regulation of autoimmune CNS inflammation and the regeneration of the damaged CNS during EAE was addressed using NgR1-, NgR2- and NgR1/2-deficient mice.

4.3.1 Expression of Nogo and Nogo receptors over the course of EAE

The expression of Nogo and Nogo receptors in the CNS was examined in tissue samples from immunized animals prepared during acute disease (day 15) and chronic disease (day 30) and compared to tissue of healthy control animals (Fig. 14). Expression of Nogo-A was assessed by immunohistochemistry (Fig. 14A). In healthy control animals, Nogo-A expressing oligodendrocytes are present in high numbers in the white matter of the spinal cord. During acute disease, Nogo-A expressing cells are significantly reduced in the area of the inflammatory infiltrate, but remain easily identifiable in the surrounding tissue. During chronic disease, Nogo-A expressing cells can still be detected throughout the white matter, suggesting that Nogo-A-mediated inhibition of axonal regrowth can occur. Over the course of EAE, the overall expression of Nogo-A mRNA in the spinal cord is decreased by 20% although this decrease is not statistically significant ($p = 0.07$) (Fig. 14C). Growth-inhibitiory signalling via Nogo-receptors is mediated by Nogo-66, a domain which is also present in Nogo-B. Since Nogo-B can only be distinguished from Nogo-A by size, Nogo-B expression was assessed by western blot (Fig. 14B). In inflamed spinal cord tissue, Nogo-B expression

does not change significantly compared to healthy controls. Expression of Nogo-receptors NgR1 and NgR2 can only be measured by real-time PCR (Fig. 14D-E), since commercially available antibodies did not result in a specific detection of NgR1 or NgR2. Over the disease course, NgR1- or NgR2-mRNA expression does not change significantly in spinal cord tissue samples.

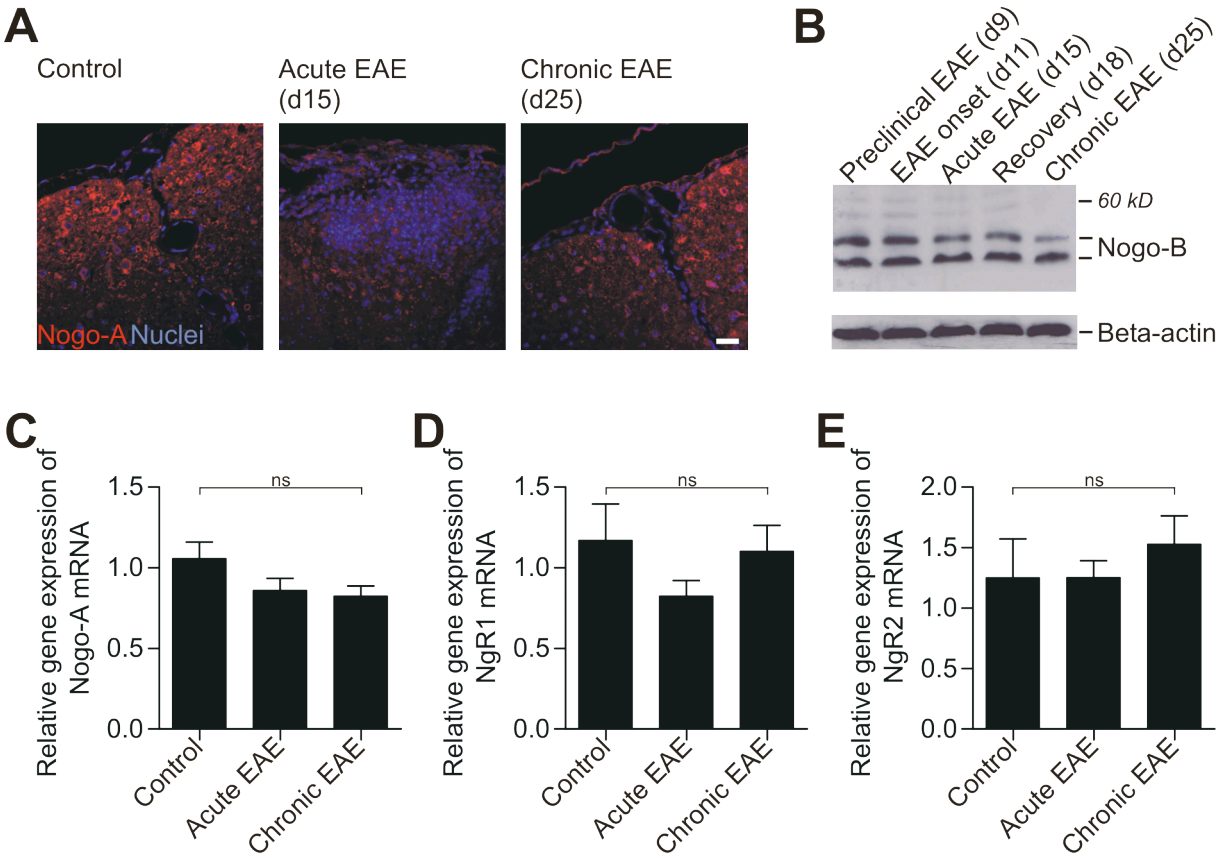

Fig. 14 Expression of Nogo and Nogo receptors in the inflamed CNS. (A) Cervical spinal cord sections from control animals or animals during acute and chronic EAE were stained with anti-Nogo-A (11C7). Scale bar represents 50 µm. (B) Western blot analysis of spinal cord homogenates prepared from animals at indicated time points after disease stained with anti-Nogo-A/B/C. Two forms of Nogo-B with a molecular mass of about 45 and 50 kDa are detected. (C-E) Real-time PCR analysis of spinal cord for Nogo-A mRNA (C), NgR1 mRNA (D) and NgR2 mRNA (E). Real-time PCR results are mean ± sem (n≥5).

4.3.2 Nogo receptor deficiency does not improve recovery during chronic EAE

Induction of EAE in NgR-deficient animals.

In order to investigate, whether the absence of NgR1 and NgR2-mediated signalling enhances recovery or alters the inflammatory response, EAE was induced in different NgR-deficient animals and their clinical course was compared to WT littermates (Fig. 15, table 5).

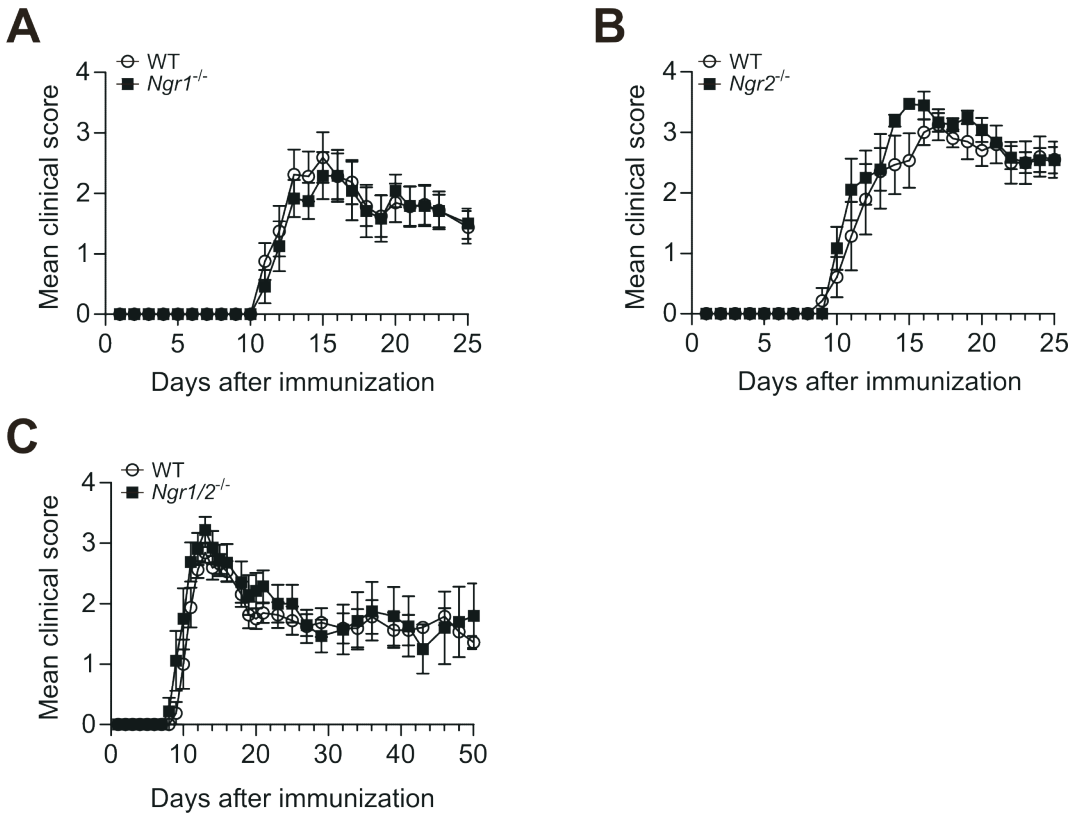

Fig. 15 Clinical course of EAE in Nogo receptor-deficient animals. EAE was induced in NgR1-deficient (A), NgR2-deficient (B) and NgR1/2-deficient animals (C), and disease course was observed in comparison to WT littermates for at least 30 days. n=3 for NgR1- and NgR1/2-deficient animals, n=1 for NgR2-deficient animals.

Although NgR2-deficient and NgR1/2-deficient animals show slightly increased mean clinical scores during acute EAE at days 13-15, the changes of the clinical course are not significant in either NgR1-deficient (Fig. 15A), NgR2-deficient (Fig. 15B) or NgR1/2-deficient animals (Fig. 15C) when compared to WT littermates. Furthermore, Nogo receptor-deficient animals do also not significantly differ from WT controls when analysed in respect to disease incidence, day of disease onset or maximal disease severity (Table 5), although NgR2-deficient and NgR1/2-deficient and animals show a slightly earlier disease onset and a slightly increased maximal clinical score.

Table 5 Course of EAE in NgR-deficient mice. Shown are the representative experiments presented in Fig.15. Results are mean ± sd.

	Incidence	Mean day of onset[A]	Mean maximal clinical score[A]
WT	7/8	11.4 ± 0.8	3.1 ± 0.5
Ngr1$^{-/-}$	6/8	11.7 ± 0.8	2.5 ± 0.8
WT	7/8	11.9 ± 2.5	3.6 ± 0.3
Ngr2$^{-/-}$	9/9	11.0 ± 2.5	3.8 ± 0.3
WT	8/11	10.0 ± 0.9	3.0 ± 0.3
Ngr1/2$^{-/-}$	9/10	9.6 ± 1.1	3.3 ± 0.6

[A] Diseased animals

Based on the known functions of Nogo receptor interactions with its ligands, it was expected that Nogo receptor deficiency could result in a slightly enhanced repair, which does not necessarily have to transmit into an alteration of clinical symptoms during chronic EAE. In order to determine if Nogo receptor-deficient mice show enhanced recovery at the cellular level, neuronal and axonal loss in NgR1/2-deficient animals were quantified (Fig. 16). Loss of ventral horn motor neurons (Fig. 16A, B) and axons in the dorsal column (Fig. 16C, D) as well as in the corticospinal tract (Fig. 16E, F) was examined in cervical spinal cord by immunohistochemistry. A significant loss of motor neurons and axons due to EAE can be detected in these regions, but the observed damage is similar in NgR1/2-deficient mice and WT controls. Thus, Nogo receptor deficiency does not result in enhanced recovery from EAE.

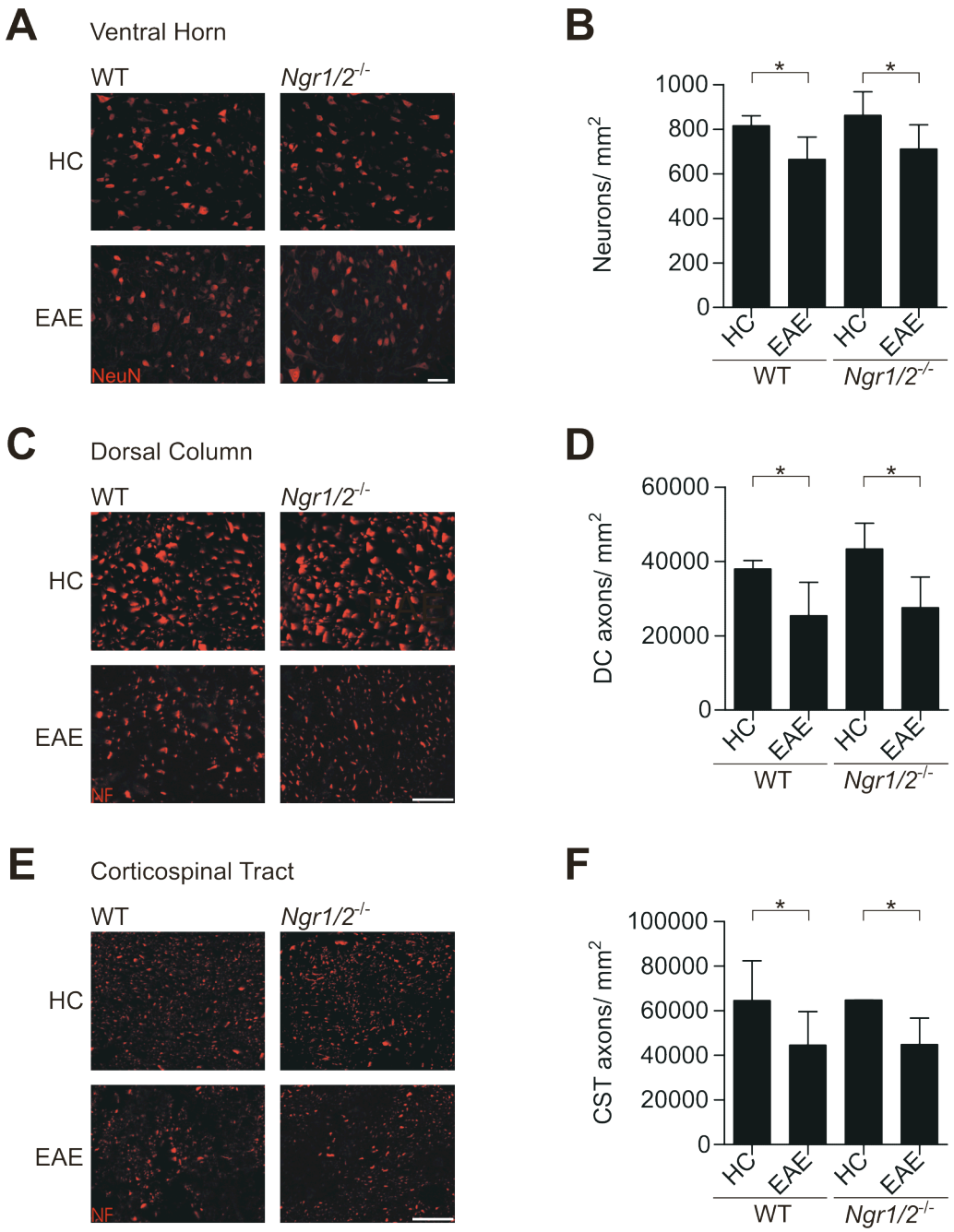

Fig. 16 Neuronal and axonal damage in NgR1/2-deficient animals. (A,B) Cell bodies of ventral horn motor neurons were stained with anti-NeuN antibody and neuronal nuclei were counted in spinal cord sections. Scale bar represents 50 µm. (C-F) Axons in the dorsal column (C,D) and corticospinal tract (E,F) were stained with anti-neurofilament (NF) antibodies SMI-31 and SMI-32 and quantified as described in 4.2.3. Scale bars represent 20 µm. Representative staining images are shown. Results are mean ± sd. n≥ 2 for healthy control animals and n≥7 for diseased animals. Statistical significance is indicated by * ($p \leq 0.05$).

4.3.3 Nogo receptor-deficiency results in an enhanced B cell response in the CNS

Since a potential role for Nogo receptors in the regulation of nervous system inflammation has been suggested[220], the CNS-specific inflammatory response of NgR1/2-deficient animals was examined by the quantitative flow cytometric approach described in 5.1.2 (Fig. 17).

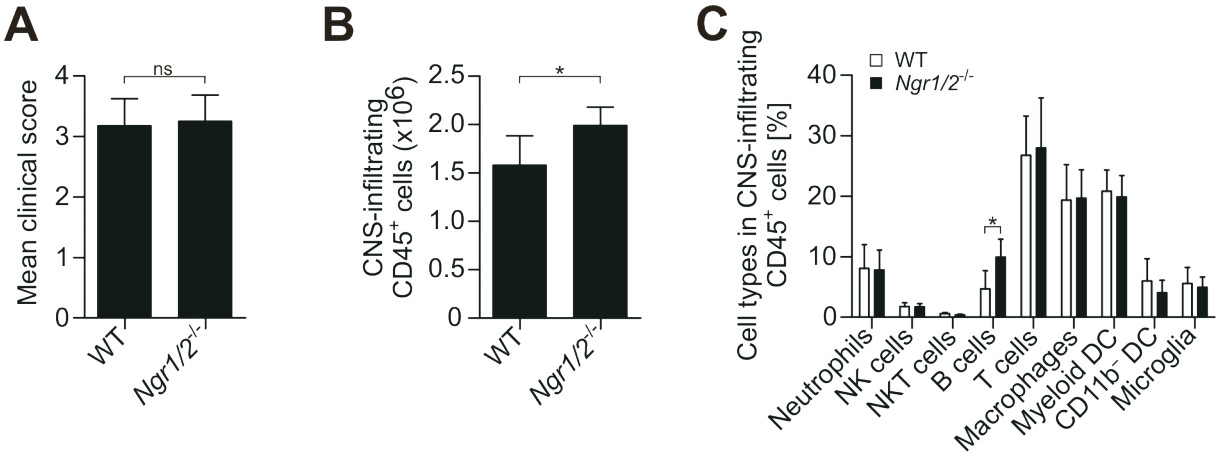

Fig. 17 CNS-specific immune response in NgR1/2-deficient animals. CNS-infiltrating cells from NgR1/2-deficient mice and wt littermates were isolated during acute EAE 14 days after immunization. (A) Mean clinical scores of analysed mice. (B-C) Quantification of $CD45^+$ CNS-infiltrating cells (B) and frequency of different immune cell types within $CD45^+$ cells was analysed by flow cytometry (C). Results are mean ± sd (n=7). Statistical significance is indicated by * ($p \leq 0.05$).

Surprisingly, although NgR1/2-deficient mice and WT littermates have comparable mean clinical scores (Fig. 17A), the numbers of $CD45^+$ CNS-infiltrating cells are significantly elevated (Fig. 17B). This increase is mainly due to an enhanced proportion of B cells within $CD45^+$ CNS-infiltrating cells. Compared to WT littermates, the observed frequency of B cells in $CD45^+$ CNS-infiltrating cells is doubled from 5% in wildtype to 10% in NgR1/2-deficient mice, whereas the contribution of all other investigated cell types to CNS inflammation during EAE is unchanged (Fig. 17C).

In summary, the deficiency in NgR1, NgR2 or both Nogo receptors does not lead to enhanced functional recovery during EAE, but results in an enhanced B cell infiltration into the CNS during acute EAE.

5 DISCUSSION

A multi-color flow cytometry-based method allows monitoring of tissue-specific inflammation.

In this work, a flow cytometry-based method for the absolute quantification of tissue-infiltrating cells was established to monitor the CNS-specific immune response in EAE , an established animal model of the human disease MS. Isolation of tissue-infiltrating immune cells and subsequent flow cytometric analysis is a well documented method for the phenotypic characterisation of tissue inflammation. However, such an analysis is often limited to a small number of parameters and only examines frequencies of e.g. infiltrating cells but not absolute numbers. By combining up to seven antibodies with different fluorescent tags, a detailed characterisation of CNS-infiltrating immune cells could be achieved. By using only seven different antibody cocktails the small number of cells that can be retrieved from the CNS of single animals were sufficient to phenotype all major immune cell types. Moreover, the combination of this flow cytometric analysis with TruCOUNT® beads, which were originally designed to quantify peripheral blood leukocytes, allowed the calculation of absolute numbers of isolated CNS-infiltrating cells. This method allowed a quick and reproducible characterisation of tissue inflammation in general, resulting not only in the determination of immune cell composition in the inflamed tissue, but also measuring the amount of inflammation by quantifying tissue-infiltrating cells in absolute numbers. A detailed picture of a tissue-specific immune response can be obtained by this method. Although this flow cytometric approach provides no information about the spatial distribution of inflammatory cells in the target tissue, it reflects the amount of tissue infiltration detected by immunohistochemistry as has been demonstrated here by the correlation between the quantified numbers of CNS-infiltrating neutrophils with data from immunohistochemical stainings. As soon as numbers of CNS-infiltrating neutrophils rise significantly over background levels with the flow cytometric quantification, infiltrating neutrophils can be detected in the perivascular spaces of spinal cord sections. In addition, this method was also used to monitor the temporal dynamic of post ischemic inflammation in an experimental model of stroke[289]. Equally, the characterisation of CNS inflammation obtained by this flow cytometric method correlated well with tissue infiltration seen by immunohistochemistry.

Therefore, the flow cytometry-based strategy described here represents a quick and reproducible screening method to characterise comprehensively the composition of tissue-

infiltrating immune cells and to quantitate their absolute numbers and relative distributions. In this work, it was used to detect CNS-specific inflammatory changes during different treatments and to compare genetically modified animals with WT controls.

The early CNS-specific immune response is mainly mediated by innate immune cells, particularly neutrophil granulocytes.

Using the flow cytometry-based quantification of CNS-infiltrating immune cells, the temporal dynamics of immune cell infiltration and activation was characterised over the course of EAE. Significantly elevated levels of CNS-infiltration by immune cells were already detectable two to three days before onset of disease. This preclinical immune response was mainly characterised by the infiltration of innate immune cells, particularly by neutrophil granulocytes. In addition, slightly elevated numbers of macrophages, myeloid DC and T cells were detectable. Only a small proportion of these early infiltrating cells expressed MHCII, but microglia, macrophages and myeloid DC started to express the costimulatory molecule CD80, probably in response to an early inflammatory environment in the CNS. The preclinical environment does not seem to favour T cell differentiation into a special direction, since equal amounts of $CD4^+$ T cells produce IFN-γ, IL-17 or both cytokines. Th1, Th1/17 and Th17 cells are then equally expanded and/ or recruited into the CNS until the onset of clinical symptoms, where they can be detected in similar numbers.

After immunization with CFA, which mimics pathogenic infection, the expression of immune cell attracting chemokines in the CNS is induced even in the absence of a specific adaptive immune response[290-292]. Similarily, peripheral immune cell activation and cytokine production lead to *de novo* expression of pro-inflammatory cytokines like IL-1β, IL-6 and TNF-α in glial cells in the CNS[293-295]. Therefore, the observed early recruitment of innate immune cells could in principal be antigen-independent, although the presence of few T cells in the CNS during preclinical EAE indicates a prior reactivation of MOG-35-55-specific T cells in the CNS. Accordingly, it has been described that the expression of neutrophil-attracting chemokines in the CNS is dependent on a immunization with a CNS antigen in CFA, but does not occur after immunization with CFA alone[292]. This suggests that the inital reactivation of a first-wave of CNS-infiltrating T cells leads to the production of attracting chemokines and the subsequent infiltration of neutrophils and macrophages into the CNS during preclinical EAE. Recruitment of neutrophils to the CNS is probably dependent on the chemokine receptor CXCR2 on neutrophils, since CXCR2-deficient mice have been shown to be protected from EAE and chemically induced demyelination in a neutrophil-dependent manner[187,296].

There are few reports describing early pathological changes in MS brains and the sequence of events involved in the formation of inflammatory lesions in the CNS still has to be clarified[297,298]. Since neutrophils are only minor components of the acute inflammatory lesion during EAE and mainly infiltrate early during lesion formation, it might be possible that the contribution of neutrophils to the formation of early lesions in MS has been missed so far. Pathological examinations of biopsy and post mortem tissue of MS brain can only cover one time point in each case and are mostly carried out in very acute or advanced disease. This limited availability of tissue samples from early or even preactive MS poses a major challenge to the identification of early inflammatory changes, such as neutrophil infiltration, in MS lesions.

Neutrophil granulocytes contribute to the initiation of CNS inflammation during MOG 35-55-induced EAE

Having identified neutrophils as main components of preclinical CNS inflammation during EAE, the functional role of these cells was further investigated. Using antibody-mediated depletion to target the recruitment of neutrophils during early CNS inflammation, this work demonstrates that neutrophils play a major role in the intiation of the CNS-specific immune response before the onset of clinical symptoms during EAE. Treatment of immunized animals with the anti-Ly-6G antibody 1A8, which specifically targets neutrophils, protected from EAE, when administered two to three days before onset of clinical symptoms, but not when administered after onset of disease. Due to the short half-life of neutrophils and their continous release from bone marrow[164], a single administration of antibody resulted in only a temporary depletion of neutrophils. After five days, neutrophil numbers in the peripheral blood increased to control levels. Correspondingly, a single administration of depleting antibody two days before onset of clinical symptoms delayed disease onset for three days. Treating animals every second day with anti-Ly-6G, neutrophil depletion could be prolonged for up to ten days. Subsequently neutrophil numbers in the peripheral blood increased irrespective of further treatment (data not shown), which is likely due to the development of neutralizing antibodies in treated animals. Interestingly, the course of ten days treatment resulted in an almost complete abrogation of EAE and 75% of anti-Ly-6G-treated animals did not develop severe EAE after treatment was discontinued. This observation suggests that when neutrophil recruitment to the CNS is inhibited, the beginning inflammatory response is stopped and cannot be initiated again even though neutrophil numbers rise in the periphery. Neutrophils therefore are essential to the initiation of a productive inflammatory response in

the CNS and to establishing the proinflammatory milieu required to cause EAE. In order to understand this step better, the CNS-specific immune response during acute EAE was characterised in anti-Ly-6G treated animals compared to animals treated with isotype control. The peripheral MOG-specific T cell response was not reduced in anti-Ly-6G treated animals, suggesting that antibody-mediated depletion of neutrophils by this approach does not interfere with peripheral T cell priming, but specifically targets neutrophil recruitment to the CNS. The analysis of the CNS-specific immune response revealed that apart from the protection from onset of disease, the CNS of anti-Ly-6G treated animals is not completely protected from inflammation, but that a limited inflammatory response still occurs in the CNS. Correspondingly, CNS-infiltrating T cells from neutrophil-depleted animals were less activated and APCs expressed lower levels of maturation markers. Interestingly, the restricted immune response of anti-Ly-6G treated animals showed an impaired recruitment of myeloid DC. This indicates that neutrophils might play a role in the recruitment of myeloid DC or their precursors from the peripheral blood to the CNS during preclinical EAE. In fact, neutrophils have been shown to be involved in the recruitment, activation and programming of APCs during microbial infections[164], e.g. by the expression of CC chemokine ligands (CCL), which recruit immature DC and monocytes during microbial infection[174]. In addition, neutrophil-derived products, which are released upon pathogen recognition e.g. proteases like cathepsin G, or microbicidal molecules like LL-37 and heparin-binding protein (HBP) have been reported to attract inflammatory monocytes[299,300]. Interestingly, these inflammatory monocytes, which express high amounts of Ly-6C, have been shown to be essential for the development of EAE[286,287]. Futhermore, these Ly-6C^{high} expressing monocytes are probably the precursors of the myeloid DC present in the CNS during EAE[286]. Therefore, it seems plausible that neutrophils, which infiltrate into the CNS during preclinical EAE, mediate the recruitment of Ly-6C^{high} expressing inflammatory monocytes which subsequently differentiate into professional APCs, probably myeloid DC, and amplify the myelin-specific T cell response.

Further experiments are needed to clarify if the above-described sequence of events occurs in the context of EAE and which neutrophil-derived factors are involved. The infiltration of Ly-6C^{high}-expressing monocytes into the CNS and their differentation into myeloid DC has to be monitored in anti-Ly-6G treated animals. Furthermore, functional studies targeting neutrophil-derived secretion products are required to identify the mechanism, by which

neutrophils mediate the recruitment of inflammatory monocytes during CNS inflammation in the context of EAE.

Chronic inflammation during MOG 35-55-induced EAE is characterised by chronically activated APC and Th17 cells

After partial recovery from acute EAE when microglia, macrophages, myeloid DC and T cells dominate the inflammatory response, the transition to chronic disease is mainly characterised by a decrease in the proportion of phagocytes and myeloid DC. Although T cell infiltration also declines, T cells are numerically the main contributors to chronic inflammation. Remarkably, these persisting T cells have the characteristics of chronic inflammatory cells, since they express markers of early activation, indicating recent restimulation. In addition, these T cells mainly produce IL-17A and low amounts of IFN-γ. In fact, after the onset of clinical symptoms, the frequency of Th1 cells decreases steadily resulting in a chronic inflammatory T cell response, which is mainly characterised by Th17 cells.

Th17 cells have indeed been reported to be better suited for mediating chronic inflammation than Th1 cells. Th17 cells are more resistant to restimulation-induced cell death than Th1 cells[301] and less susceptible to suppression by regulatory T cells[106]. Both mechanisms could be responsible for the observed continuous decline of the Th1 response. CNS-infiltrating $CD4^+$ effector T cells show signs of recent activation over the whole disease process, indicating frequent restimulation. Consequently, the observed decline in CNS-infiltrating Th1 cells might be due to their elimiation by restimulation-induced cell death. During acute disease, concomitant with the observed decline in Th1 cells in the CNS, numbers of $CD25^+FoxP3^+$ regulatory T cells rise. The observation that numbers of Th17 cells are stable at this disease stage indicates that T cell suppression mediated by CNS-infiltrating regulatory T cells might mainly affect Th1 cells. Indeed it has been shown, that CNS-infiltrating $FoxP3^+$ regulatory T cells are able suppress MOG-induced IFN-γ production in CNS-infiltrating effector T cells but do not block IL-17 production[302]. After the peak of the disease, the ratio of CNS-infiltrating $FoxP3^+$ regulatory T cells to $CD4^+$ effector T cells declines to levels present during preclinical EAE and at disease onset. Indeed, the suppressive function of $FoxP3^+$ regulatory T cells is vulnerable to inflammatory conditions and these cells can give rise to pro-inflammatory $FoxP3^-$ effector T cells[303-305]. Since a reciprocal differentiation of $FoxP3^+$ regulatory T cells and Th17 cells has been reported[80] and cytokines required for Th17 differentiation are highly expressed in the inflamed CNS[305], CNS-infiltrating regulatory T cells might differentiate into Th17 cells in the context of chronic EAE and also contribute to

the persistence of these cells in the CNS. A correlation between disease progression and an increasing proportion of Th17 cells in the CNS can also be detected in MS patients. Elevated numbers of IL-17 producing T cells can be detected in the CSF and parenchyma of MS patients during relapses[105,106] and the frequency Th17 cells in the CSF increases with disease progression. In contrast to the results obtained in the EAE model, Th1 cells greatly outnumber Th17 cells at least in the CSF at all times in MS patients[106].

In addition to the presence of recently activated T cells during chronic disease, remaining APCs also show signs of chronic activation. MHCII, CD80 and CD40 are still expressed at higher levels than in preclinical EAE. Consequently, these APCs should still be able to present antigens and stimulate specific T cells and may therefore contribute to initiating clinical relapses. Indeed, infiltrating DC mediate epitope spreading inside the CNS during EAE[306], resulting in a diversified myelin-specific T cell response.

In summary, the initial episode of autoreactive CNS inflammation induced by active immunization with MOG35-55 in CFA results in a persisting sub-acute inflammatory response characterised by chronic activation of APCs and T cells. This chronic immune response might then possibly in response to an environmental trigger elicit new relapses.

Surface expression of IL-17A is a marker for Th17 cells.

This work describes the detection of surface IL-17A on a subset of mouse $CD4^+$ T cells. Since the frequency of $CD4^+$ T cells expressing IL-17A on their surface correlated well with the proportion of $CD4^+$ T cells accumulating IL-17A intracellularly in the presence of a inhibitor of protein secretion, surface IL-17A-expressing $CD4^+$ T cells probably correspond to Th17 cells. Indeed, surface expression of other cytokines like IL-10 and IFN-γ has been described[307,308], but sensitivity enhancing staining methods have been necessary for their detection. In contrast, surface IL-17A can be detected by normal flow cytometric surface staining, although the staining sensitivity is less compared to the staining of intracellularly accumulated IL-17A. Identification of Th17 cells by their surface expression of IL-17A gives the opportunity to obtain living cells that allow further analysis. In the mouse this could circumvent the use of genetically labeled cells of IL-17A reporter mice. The discovery of surface IL-17A is yet most relevant for research on human Th17 cells. We were able to describe surface IL-17A as a specific marker for human Th17 cells[309], allowing the identification and purification of *ex vivo* Th17 cells.

IL-17A is probably not displayed on the cell surface bound to IL-17R, since IL-17A is still detectable on the surface of a $CD4^+$ T cell subset isolated from IL-17RA-deficient mice. Instead, IL-17A is probably displayed on the cell surface as a heterodimer with IL-17F, which possesses a putative transmembrane domain[309].

It is still unclear, if the surface expression of IL-17A has any functional relevance *in vivo*. During the analysis of IL-17A surface expression, it was observed that prior isolation of pure $CD4^+$ T cells is necessary to detect surface-IL-17A (data not shown). Therefore, IL-17A may only be displayed transiently on the surface of $CD4^+$ T cells *in vivo*, restricting IL-17A secretion to the local environment. Such a localized cytokine secretion could be involved in the prolongation of the interaction between a Th17 cell and IL-17R-expressing cells, e.g. APC or endothelial cells[310].

Functional role of Nogo receptors during CNS inflammation

Strategies targeting myelin-associated proteins that inhibit axonal regrowth, particularly blockade of Nogo-A, have been successfully applied in several nerve injury models and in EAE. However, whether and to what extent signalling via Nogo receptors is really mediating Nogo-A related inhibition of axonal regrowth is currently under debate. To address this issue, a potential function of Nogo receptors in autoimmune CNS inflammation and regeneration of the damaged CNS was examined by analysing NgR1-, NgR2- and NgR1/2-deficient mice.

In this work, the removal of NgR1- and NgR2-mediated inhibition of axonal regrowth did not result in enhanced repair and functional recovery from inflammation-induced axonal damage in EAE. Disease severity during chronic disease as well as the observed neuronal and axonal loss of ventral horn motor neurons and axons in corticospinal tract and dorsal column of the spinal cord were all similar between NgR1/2-deficient mice and WT littermates. The observed lack of improved regeneration is not due to a loss in expression of Nogo and Nogo receptors during chronic disease. Although Nogo-A mRNA decreases during chronic disease, probably due to an inflammatory-mediated loss of Nogo-A expressing oligodendrocytes, Nogo-A expression can still be detected widely around the injured spinal cord areas during chronic disease.

Genetic deletion of NgR1 alone has been reported to be insufficient to enhance regeneration of the corticospinal tract after spinal cord injury[283,311]. Although NgR1/2-deficient mice have not yet been tested in CNS injury models, the observed regeneration failure during EAE is probably not only due to a compensatory role of NgR2 in NgR1-deficient mice, since an

additional common receptor for Nogo-66, MAG and OMG, which is PirB, has been recently discovered[270]. Only with the blockade of both NgR1 and PirB, myelin-associated inhibition of cerebellar granule cells – which do not express NgR2 – could be overcome, suggesting that even genetic deletion of NgR1 and NgR2 might be insufficient to enhance regeneration not only in EAE, but also in other CNS injury models.

In addition to the redundant functions of receptors for myelin-associated growth inhibition, other mechanisms inhibit axonal regeneration as well[226]. Several growth-inhibitory cues like semaphorins and ephrins as well as the formation of a glial scar contribute to the inhibition of axonal regrowth after CNS injury. It has been suggested, that only combinatorial approaches targeting several mechanisms of inhibition will be able to promote functional repair in the CNS, but interestingly, scavenging of myelin-associated inhibitor proteins with a soluble Nogo-66 receptor can promote axonal sprouting and functional recovery after spinal cord injury[312]. This treatment probably does not only inhibit the binding of Nogo, MAG and OMG to NgR1, but also to other receptors. These data suggest that in spite of the existence of other inhibitory mechanisms, targeting myelin-associated inhibitors proteins is still a promising approach to promote recovery after CNS injury.

In the context of chronic CNS inflammation like in EAE, additional mechanisms might regulate axonal regrowth. Factors produced by CNS-infiltrating immune cells can either promote or inhibit axonal survival and growth[313]. On the one hand, CNS-infiltrating immune cells produce cytokines which are toxic for oligodendrocytes and neurons[194,212], but they also express neurotrophic factors, e.g. BDNF[314-317]. Furthermore, the pro-inflammatory cytokine IL-6 has been reported to stimulate the intrinsic regenerative capacity of neurons[219,318]. So far, the complex interactions between signalling molecules from immune system and the nervous system are only at the beginning to be understood.

Concerning myelin-associated inhibition of axonal regeneration, a bidirectional signalling between CNS cells and immune cells is also evident. Co-immunization with Nogo-A-derived peptides results in a shift from the encephalitogenic Th1 response towards a protective Th2 response and treatment of EAE with anti-Nogo-A antibodies primarily delays the onset of clinical symptoms during EAE[276], indicating that Nogo-A blockade can exert a immunoregulatory effect in EAE. Concerning Nogo receptors, the discovery of the B cell growth factor BLyS as functional ligand for NgR1[282] suggests, that NgR-mediated signalling in the CNS might be influenced by inflammatory changes.

The expression of Nogo receptors by immune cells provides an additional possibility of signalling between myelin-associated proteins like Nogo, MAG and OMG and immune cells expressing Nogo receptors[265] and a role for Nogo receptors has been suggested in the regulation of immune cell migration in the CNS[279]. In this dissertation, no changes were observed concerning the infiltration of microglia and macrophages for which this regulatory function has been proposed. In contrast, NgR1/2-deficient mice had a significantly higher amount of B cells in the acute inflamed CNS. However, this enhanced B cell response did not result in a significantly aggravated disease in MOG 35-55-induced EAE in C57BL/6 mice. Mouse models of EAE have the special limitation that their pathology only minimally involves B cells and antibody-mediated demyelination[112]. In fact, EAE induced by MOG 35-55 peptide has been shown to be independent of B cell functions[319]. During the analysis of the temporal dynamic of CNS inflammation, CNS-infiltration of B cells during MOG 35-55-induced EAE was only detected during acute disease that was associated with hind limb paralysis. This suggests that due to the fact that B cells do not play a major role in the pathogenesis of MOG 35-55-induced EAE in C57BL/6 mice, the observed enhancement of B cell infiltration into the CNS might not result in changes in disease severity. Nevertheless, the fact that inhibition of NgR-mediated signalling can result in an amplified B cell response might still be very important for MS, where the functional importance of B cells and antibodies in disease pathology is evident[12,50,320]. One possibility to gain further insights into the relevance of the observed increase in B cell infiltration into the CNS could be EAE induced by immunization of C57BL/6 mice with human MOG protein in CFA, which shows a B cell and antibody-dependent pathology[112,319].

The mechanism, by which the genetic deletion of NgR1 and NgR2 leads to an increase in CNS-infiltrating B cells, still needs to be examined. As described above, BLyS has been shown to exert growth inhibitory functions on CNS neurons by interacting with NgR1[282]. Therefore, the absence of this BLyS receptor on axons during acute EAE might lead to a higher availablilty of BLyS, which is secreted by astrocytes in the inflamed CNS[321], thereby stimulating survival and proliferation of CNS-infiltrating B cells. So far it is unknown, whether NgR1 is the only Nogo receptor which is able to bind to BLyS, or if this interaction takes place *in vivo*. Further experiments should clarify, whether the observed increase in CNS-infiltrating B cells is indeed due to enhanced BLyS levels in the CNS. Furthermore it needs to be examined, whether this effect is due to the absence of NgR1, NgR2 or both receptors.

Conclusion

A simplified scheme summarising results and their implications discussed here is shown in Fig.18. A detailed decription of the described processes is included in the figure legend.

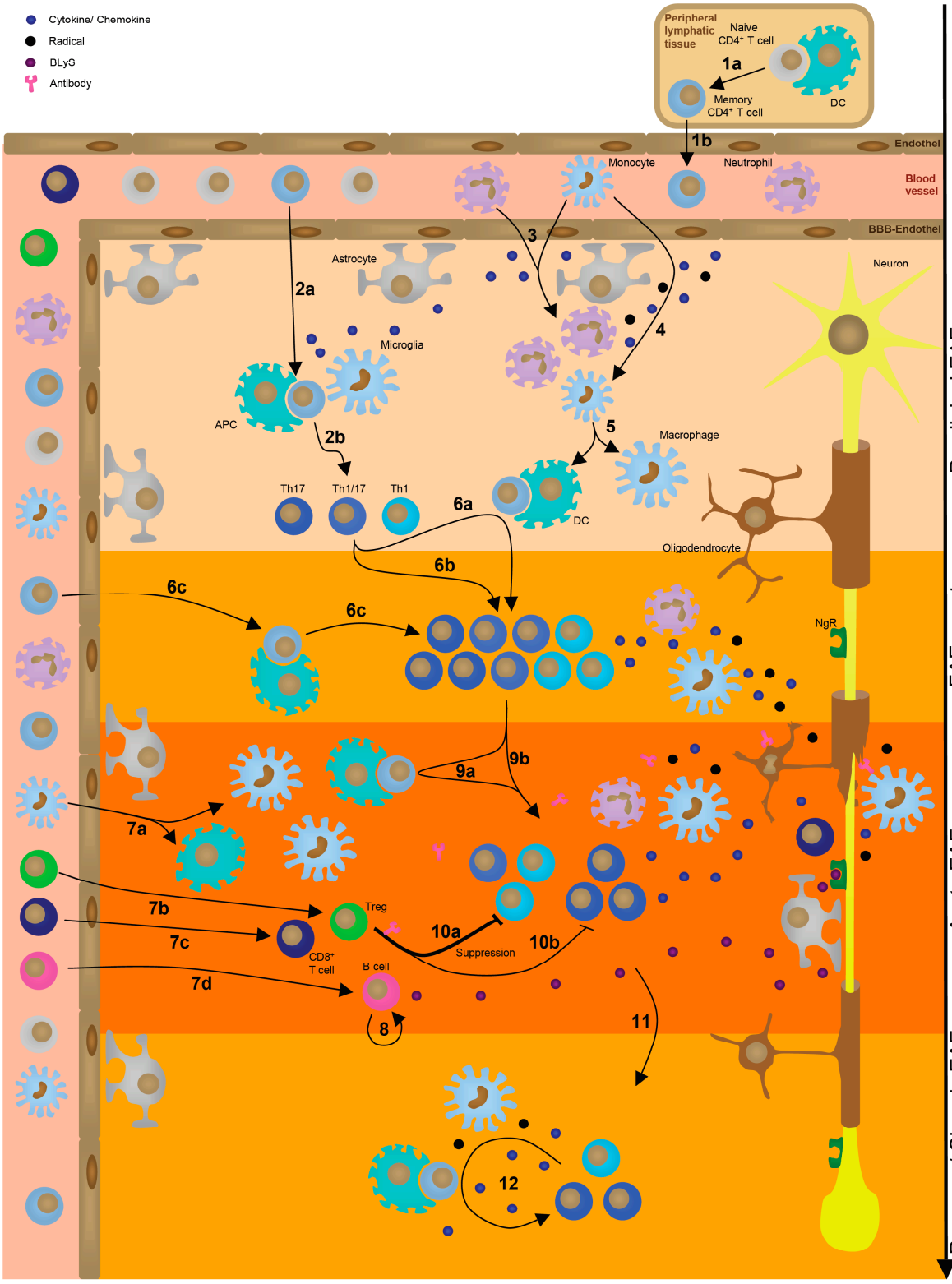

Fig. 18 Temporal course of CNS inflammation during EAE.

$CD4^+$ T cells are primed in the periphery by dendritic cells presenting myelin (or myelin-crossreactive) epitopes (**1a**). Primed memory $CD4^+$ T cells circulate in the blood (**1b**) and enter the CNS by crossing the blood-brain barrier (BBB) (**2a**) and can be reactivated by local MHCII-expressing APC presenting the respective antigen. The nature of this initially responsible APC is currently unknown. Upon this restimulation, $CD4^+$ T cells give rise to Th1, Th1/17 or Th17 cells (**2b**). The initial restimulation of T cells probably results in the production of soluble mediators like cytokines, chemokines, radicals and proteases (indicated by round symbols) by either T cells, APC or microglia, which result in changes in BBB-premeability and probably lead to the recruitment of early-infiltrating innate immune cells, particularly neutrophils (**3**). The recruitment of neutrophils during this preclinical stage of the disease seems to be responsible for an efficient recruitment of further immune cells, particularly monocytes and DC subsets (**4**). Directly or indirectly neutrophils could change the cytokine/ chemokine milieu in the CNS, resulting in the recruitment of monocyte (subsets), which then differentiate in the CNS into either professional APC like DC or into macrophages (**5**). Being efficient APC, CNS-infiltrating DC may contribute to the observed expansion of Th1, Th1/17 and Th17 (**6a**). Alternatively, recently restimulated Th cells may proliferate in response to the cytokine-milieu present (**6b**) or be newly recruited (**6c**). The production of toxic cytokines, radicals and proteases by T cells, DC, macrophages and neutrophils during this disease stage damages oligodendrocytes, myelin and axons and leads to the onset of clinical symptoms. After EAE onset, CNS inflammation further increases and more immune cells, e.g. monocytes, $CD8^+$ cytotoxic T cells, regulatory T cells (Treg) and antibody-producing B cells are recruited (**7a-d**). B cell survival and expansion may be regulated by the production of the B cell growth factor BLyS (small violet symbols), which is produced e.g. by astrocytes. Additionally, BLyS might function as a Nogo receptor (NgR)-ligand to restrict axonal regrowth. In NgR1/2-deficient mice, more BLyS might be available for B cells, leading to the observed increase in CNS-infiltrating B cells. (**8**). During acute EAE, the Th17 response is stable, while a decrease in the numbers of Th1 cells is observed (**9**). This is probably due to a enhanced susceptibility of Th1 cells to restimulation-induced cell death (**9a,b**) and to Treg-mediated suppression (**10a,b**). When the disease transmits into a recovery phase and finally into a chronic disease stage, CNS-infiltration declines (**11**). Nevertheless, remaining macrophages, DC and T cells, the latter ones mainly being Th17 cells, show signs of chronic activation, indicating frequent restimulation (**12**). This persisting chronically activated inflammatory response might be highly susceptible for environmental triggers and therefore be able to elicit new clinical relapses later during disease.

6 SUMMARY

In this work the temporal dynamics of immune cell infiltration into the CNS was characterised during experimental autoimmune encephalomyelitis (EAE), an established mouse model of the human disease Multiple Sclerosis (MS). This was done using a newly established flow cytometry-based method, which allowed the combined analysis of the amount and composition of CNS inflammation. Already two to three days before onset of EAE CNS-infiltrating immune cells can be detected. This preclinical CNS inflammation is mainly characterised by infiltration of innate immune cells, particularly neutrophil granulocytes. Subsequent antibody-mediated depletion of these cells using a neutrophil-specific antibody demonstrated that neutrophils play an important role during the initiation of the CNS-specific immune response during preclinical and early EAE. Mechanistically this is likely due to the recruitment of professional antigen-presenting cells (APC) like myeloid dendritic cells (DC).

Until the onset of clinical symptoms the T cell response in the CNS consists of equal proportions IFN-γ producing T-helper (Th) type 1 (Th1) cells and IL-17A-producing Th17 cells or a cell population that produces both cytokines. During the further course of EAE, however, the Th1 response declines steadily, concomitant with the infiltration of regulatory T cells. Irrespectively, the Th17 response stays stable during acute disease and only declines during recovery phase. In this phase CNS-infiltration decreases and the disease transits into a chronic-inflammatory stage, which is mainly characterised by chronically activated APC and T cells, the latter being mainly Th17 cells.

During this chronic disease stage of EAE, animals suffer from sustained disability, which mainly results from neuronal and axonal damage in the spinal cord. The myelin proteins Nogo, MAG and OMG are considered to mediate inhibition of nerve regeneration in the adult CNS via Nogo receptor (NgR)-mediated signalling. Blocking strategies targeting this pathway have been successfully applied in several nerve injury models, suggesting myelin-proteins and Nogo receptors as therapeutic targets to enhance regeneration in MS. Therefore, the aim of this work was to elucidate a potential function of NgR-mediated signalling in autoimmune CNS inflammation and regeneration of the damaged CNS. EAE was induced in NgR1-, NgR2- and NgR1/2-deficient mice, but had neither an effect on the clinical outcome during chronic EAE nor on the occurance of neuronal and axonal loss. Instead, the relief from NgR-

mediated signalling results in an enhanced B cell infiltration during the acute disease period in NgR1/2-double-deficient mice.

7 REFERENCES

1. Pearce, J.M. Historical descriptions of multiple sclerosis. *Eur Neurol* **54**, 49-53 (2005).
2. Charcot, J.M. Histologie de la sclérose en plaques. *Hop civils et militaires*, 140: 554-555 and 141: 557-558 and 143 566 (1868).
3. Trapp, B.D. et al. Axonal transection in the lesions of multiple sclerosis. *N Engl J Med* **338**, 278-85 (1998).
4. Noseworthy, J.H., Lucchinetti, C., Rodriguez, M. & Weinshenker, B.G. Multiple sclerosis. *N Engl J Med* **343**, 938-52 (2000).
5. Hein, T. & Hopfenmuller, W. [Projection of the number of multiple sclerosis patients in Germany]. *Nervenarzt* **71**, 288-94 (2000).
6. Alter, M., Leibowitz, U. & Speer, J. Risk of multiple sclerosis related to age at immigration to Israel. *Arch Neurol* **15**, 234-7 (1966).
7. Dean, G. Annual incidence, prevalence, and mortality of multiple sclerosis in white South-African-born and in white immigrants to South Africa. *Br Med J* **2**, 724-30 (1967).
8. Elian, M., Nightingale, S. & Dean, G. Multiple sclerosis among United Kingdom-born children of immigrants from the Indian subcontinent, Africa and the West Indies. *J Neurol Neurosurg Psychiatry* **53**, 906-11 (1990).
9. Ebers, G.C., Sadovnick, A.D. & Risch, N.J. A genetic basis for familial aggregation in multiple sclerosis. Canadian Collaborative Study Group. *Nature* **377**, 150-1 (1995).
10. McFarland, H.F. Correlation between MR and clinical findings of disease activity in multiple sclerosis. *AJNR Am J Neuroradiol* **20**, 1777-8 (1999).
11. Raine, C.S. & Scheinberg, L.C. On the immunopathology of plaque development and repair in multiple sclerosis. *J Neuroimmunol* **20**, 189-201 (1988).
12. Lucchinetti, C. et al. Heterogeneity of multiple sclerosis lesions: implications for the pathogenesis of demyelination. *Ann Neurol* **47**, 707-17 (2000).
13. Paty, D.W. & Li, D.K. Interferon beta-1b is effective in relapsing-remitting multiple sclerosis. II. MRI analysis results of a multicenter, randomized, double-blind, placebo-controlled trial. UBC MS/MRI Study Group and the IFNB Multiple Sclerosis Study Group. *Neurology* **43**, 662-7 (1993).
14. Jacobs, L.D. et al. Intramuscular interferon beta-1a for disease progression in relapsing multiple sclerosis. The Multiple Sclerosis Collaborative Research Group (MSCRG). *Ann Neurol* **39**, 285-94 (1996).
15. Randomised double-blind placebo-controlled study of interferon beta-1a in relapsing/remitting multiple sclerosis. PRISMS (Prevention of Relapses and Disability by Interferon beta-1a Subcutaneously in Multiple Sclerosis) Study Group. *Lancet* **352**, 1498-504 (1998).
16. Placebo-controlled multicentre randomised trial of interferon beta-1b in treatment of secondary progressive multiple sclerosis. European Study Group on interferon beta-1b in secondary progressive MS. *Lancet* **352**, 1491-7 (1998).
17. Neuhaus, O., Farina, C., Wekerle, H. & Hohlfeld, R. Mechanisms of action of glatiramer acetate in multiple sclerosis. *Neurology* **56**, 702-8 (2001).
18. Yednock, T.A. et al. Prevention of experimental autoimmune encephalomyelitis by antibodies against alpha 4 beta 1 integrin. *Nature* **356**, 63-6 (1992).
19. Hartung, H.P. et al. Mitoxantrone in progressive multiple sclerosis: a placebo-controlled, double-blind, randomised, multicentre trial. *Lancet* **360**, 2018-25 (2002).

20. Breuer, B. et al. A randomized, double-blind, placebo-controlled, two-period, crossover, pilot trial of lamotrigine in patients with central pain due to multiple sclerosis. *Clin Ther* **29**, 2022-30 (2007).

21. Bechtold, D.A. et al. Axonal protection achieved in a model of multiple sclerosis using lamotrigine. *J Neurol* **253**, 1542-51 (2006).

22. Stys, P.K. General mechanisms of axonal damage and its prevention. *J Neurol Sci* **233**, 3-13 (2005).

23. Waxman, S.G. Axonal conduction and injury in multiple sclerosis: the role of sodium channels. *Nat Rev Neurosci* **7**, 932-41 (2006).

24. Brand-Schieber, E. & Werner, P. Calcium channel blockers ameliorate disease in a mouse model of multiple sclerosis. *Exp Neurol* **189**, 5-9 (2004).

25. Friese, M.A. et al. Acid-sensing ion channel-1 contributes to axonal degeneration in autoimmune inflammation of the central nervous system. *Nat Med* **13**, 1483-9 (2007).

26. Smith, T., Groom, A., Zhu, B. & Turski, L. Autoimmune encephalomyelitis ameliorated by AMPA antagonists. *Nat Med* **6**, 62-6 (2000).

27. Pitt, D., Werner, P. & Raine, C.S. Glutamate excitotoxicity in a model of multiple sclerosis. *Nat Med* **6**, 67-70 (2000).

28. Kanwar, J.R., Kanwar, R.K. & Krissansen, G.W. Simultaneous neuroprotection and blockade of inflammation reverses autoimmune encephalomyelitis. *Brain* **127**, 1313-31 (2004).

29. Paul, C. & Bolton, C. Modulation of blood-brain barrier dysfunction and neurological deficits during acute experimental allergic encephalomyelitis by the N-methyl-D-aspartate receptor antagonist memantine. *J Pharmacol Exp Ther* **302**, 50-7 (2002).

30. Li, W. et al. Beneficial effect of erythropoietin on experimental allergic encephalomyelitis. *Ann Neurol* **56**, 767-77 (2004).

31. Ehrenreich, H. et al. Exploring recombinant human erythropoietin in chronic progressive multiple sclerosis. *Brain* **130**, 2577-88 (2007).

32. Goodman, A.D. et al. Sustained-release oral fampridine in multiple sclerosis: a randomised, double-blind, controlled trial. *Lancet* **373**, 732-8 (2009).

33. Husseini, L., Leussink, V.I., Kieseier, B.C. & Hartung, H.P. [4-Aminopyridine (Fampridine). A new attempt for the symptomatic treatment of multiple sclerosis]. *Nervenarzt* **81**, 203-11.

34. Haines, J.L. et al. Multiple susceptibility loci for multiple sclerosis. *Hum Mol Genet* **11**, 2251-6 (2002).

35. A meta-analysis of whole genome linkage screens in multiple sclerosis. *J Neuroimmunol* **143**, 39-46 (2003).

36. Dyment, D.A., Ebers, G.C. & Sadovnick, A.D. Genetics of multiple sclerosis. *Lancet Neurol* **3**, 104-10 (2004).

37. Olerup, O. & Hillert, J. HLA class II-associated genetic susceptibility in multiple sclerosis: a critical evaluation. *Tissue Antigens* **38**, 1-15 (1991).

38. Barcellos, L.F. & Thomson, G. Genetic analysis of multiple sclerosis in Europeans. *J Neuroimmunol* **143**, 1-6 (2003).

39. Fogdell-Hahn, A., Ligers, A., Gronning, M., Hillert, J. & Olerup, O. Multiple sclerosis: a modifying influence of HLA class I genes in an HLA class II associated autoimmune disease. *Tissue Antigens* **55**, 140-8 (2000).

40. Sawcer, S. et al. A high-density screen for linkage in multiple sclerosis. *Am J Hum Genet* **77**, 454-67 (2005).

41. Brynedal, B. et al. HLA-A confers an HLA-DRB1 independent influence on the risk of multiple sclerosis. *PLoS One* **2**, e664 (2007).

42. Chao, M.J. et al. HLA class I alleles tag HLA-DRB1*1501 haplotypes for differential risk in multiple sclerosis susceptibility. *Proc Natl Acad Sci U S A* **105**, 13069-74 (2008).

43. Friese, M.A. & Fugger, L. Pathogenic CD8(+) T cells in multiple sclerosis. *Ann Neurol* **66**, 132-41 (2009).

44. Gregory, S.G. et al. Interleukin 7 receptor alpha chain (IL7R) shows allelic and functional association with multiple sclerosis. *Nat Genet* **39**, 1083-91 (2007).

45. Lundmark, F. et al. Variation in interleukin 7 receptor alpha chain (IL7R) influences risk of multiple sclerosis. *Nat Genet* **39**, 1108-13 (2007).

46. Weber, F. et al. IL2RA and IL7RA genes confer susceptibility for multiple sclerosis in two independent European populations. *Genes Immun* **9**, 259-63 (2008).

47. Hafler, D.A. et al. Risk alleles for multiple sclerosis identified by a genomewide study. *N Engl J Med* **357**, 851-62 (2007).

48. Miller, D.H. et al. A controlled trial of natalizumab for relapsing multiple sclerosis. *N Engl J Med* **348**, 15-23 (2003).

49. Coles, A.J. et al. Alemtuzumab vs. interferon beta-1a in early multiple sclerosis. *N Engl J Med* **359**, 1786-801 (2008).

50. Hauser, S.L. et al. B-cell depletion with rituximab in relapsing-remitting multiple sclerosis. *N Engl J Med* **358**, 676-88 (2008).

51. Sospedra, M. & Martin, R. Immunology of multiple sclerosis. *Annu Rev Immunol* **23**, 683-747 (2005).

52. Burns, J., Rosenzweig, A., Zweiman, B. & Lisak, R.P. Isolation of myelin basic protein-reactive T-cell lines from normal human blood. *Cell Immunol* **81**, 435-40 (1983).

53. Pette, M. et al. Myelin basic protein-specific T lymphocyte lines from MS patients and healthy individuals. *Neurology* **40**, 1770-6 (1990).

54. Richert, J.R., McFarlin, D.E., Rose, J.W., McFarland, H.F. & Greenstein, J.I. Expansion of antigen-specific T cells from cerebrospinal fluid of patients with multiple sclerosis. *J Neuroimmunol* **5**, 317-24 (1983).

55. Chou, Y.K. et al. Response of human T lymphocyte lines to myelin basic protein: association of dominant epitopes with HLA class II restriction molecules. *J Neurosci Res* **23**, 207-16 (1989).

56. Martin, R. et al. Fine specificity and HLA restriction of myelin basic protein-specific cytotoxic T cell lines from multiple sclerosis patients and healthy individuals. *J Immunol* **145**, 540-8 (1990).

57. Ota, K. et al. T-cell recognition of an immunodominant myelin basic protein epitope in multiple sclerosis. *Nature* **346**, 183-7 (1990).

58. Olsson, T. et al. Autoreactive T lymphocytes in multiple sclerosis determined by antigen-induced secretion of interferon-gamma. *J Clin Invest* **86**, 981-5 (1990).

59. Bielekova, B. et al. Encephalitogenic potential of the myelin basic protein peptide (amino acids 83-99) in multiple sclerosis: results of a phase II clinical trial with an altered peptide ligand. *Nat Med* **6**, 1167-75 (2000).

60. Kabat, E.A., Wolf, A. & Bezer, A.E. Rapid Production of Acute Disseminated Encephalomyelitis in Rhesus Monkeys by Injection of Brain Tissue With Adjuvants. *Science* **104**, 362-363 (1946).

61. Wekerle, H., Kojima, K., Lannes-Vieira, J., Lassmann, H. & Linington, C. Animal models. *Ann Neurol* **36 Suppl**, S47-53 (1994).

62. Zamvil, S.S. & Steinman, L. The T lymphocyte in experimental allergic encephalomyelitis. *Annu Rev Immunol* **8**, 579-621 (1990).

63. Martin, R., McFarland, H.F. & McFarlin, D.E. Immunological aspects of demyelinating diseases. *Annu Rev Immunol* **10**, 153-87 (1992).

64. Ben-Nun, A., Wekerle, H. & Cohen, I.R. The rapid isolation of clonable antigen-specific T lymphocyte lines capable of mediating autoimmune encephalomyelitis. *Eur J Immunol* **11**, 195-9 (1981).

65. Pettinelli, C.B. & McFarlin, D.E. Adoptive transfer of experimental allergic encephalomyelitis in SJL/J mice after in vitro activation of lymph node cells by myelin basic protein: requirement for Lyt 1+ 2- T lymphocytes. *J Immunol* **127**, 1420-3 (1981).

66. Goverman, J. et al. Transgenic mice that express a myelin basic protein-specific T cell receptor develop spontaneous autoimmunity. *Cell* **72**, 551-60 (1993).

67. Lafaille, J.J., Nagashima, K., Katsuki, M. & Tonegawa, S. High incidence of spontaneous autoimmune encephalomyelitis in immunodeficient anti-myelin basic protein T cell receptor transgenic mice. *Cell* **78**, 399-408 (1994).

68. Bettelli, E. et al. Myelin oligodendrocyte glycoprotein-specific T cell receptor transgenic mice develop spontaneous autoimmune optic neuritis. *J Exp Med* **197**, 1073-81 (2003).

69. Waldner, H., Collins, M. & Kuchroo, V.K. Activation of antigen-presenting cells by microbial products breaks self tolerance and induces autoimmune disease. *J Clin Invest* **113**, 990-7 (2004).

70. Pollinger, B. et al. Spontaneous relapsing-remitting EAE in the SJL/J mouse: MOG-reactive transgenic T cells recruit endogenous MOG-specific B cells. *J Exp Med* **206**, 1303-16 (2009).

71. Madsen, L.S. et al. A humanized model for multiple sclerosis using HLA-DR2 and a human T-cell receptor. *Nat Genet* **23**, 343-7 (1999).

72. Quandt, J.A. et al. Unique clinical and pathological features in HLA-DRB1*0401-restricted MBP 111-129-specific humanized TCR transgenic mice. *J Exp Med* **200**, 223-34 (2004).

73. Gregersen, J.W. et al. Functional epistasis on a common MHC haplotype associated with multiple sclerosis. *Nature* **443**, 574-7 (2006).

74. Zhu, J., Yamane, H. & Paul, W.E. Differentiation of effector CD4 T cell populations (*). *Annu Rev Immunol* **28**, 445-89.

75. Kolls, J.K. & Linden, A. Interleukin-17 family members and inflammation. *Immunity* **21**, 467-76 (2004).

76. Stark, M.A. et al. Phagocytosis of apoptotic neutrophils regulates granulopoiesis via IL-23 and IL-17. *Immunity* **22**, 285-94 (2005).

77. Iwakura, Y., Nakae, S., Saijo, S. & Ishigame, H. The roles of IL-17A in inflammatory immune responses and host defense against pathogens. *Immunol Rev* **226**, 57-79 (2008).

78. Hsieh, C.S. et al. Development of TH1 CD4+ T cells through IL-12 produced by Listeria-induced macrophages. *Science* **260**, 547-9 (1993).

79. Wynn, T.A. Basophils trump dendritic cells as APCs for T(H)2 responses. *Nat Immunol* **10**, 679-81 (2009).

80. Bettelli, E. et al. Reciprocal developmental pathways for the generation of pathogenic effector TH17 and regulatory T cells. *Nature* **441**, 235-8 (2006).

81. Veldhoen, M., Hocking, R.J., Atkins, C.J., Locksley, R.M. & Stockinger, B. TGFbeta in the context of an inflammatory cytokine milieu supports de novo differentiation of IL-17-producing T cells. *Immunity* **24**, 179-89 (2006).

82. Curotto de Lafaille, M.A. & Lafaille, J.J. Natural and adaptive foxp3+ regulatory T cells: more of the same or a division of labor? *Immunity* **30**, 626-35 (2009).

83. Becher, B., Durell, B.G. & Noelle, R.J. Experimental autoimmune encephalitis and inflammation in the absence of interleukin-12. *J Clin Invest* **110**, 493-7 (2002).

84. Duong, T.T., St Louis, J., Gilbert, J.J., Finkelman, F.D. & Strejan, G.H. Effect of anti-interferon-gamma and anti-interleukin-2 monoclonal antibody treatment on the development of actively and passively induced experimental allergic encephalomyelitis in the SJL/J mouse. *J Neuroimmunol* **36**, 105-15 (1992).

85. Gran, B. et al. IL-12p35-deficient mice are susceptible to experimental autoimmune encephalomyelitis: evidence for redundancy in the IL-12 system in the induction of central nervous system autoimmune demyelination. *J Immunol* **169**, 7104-10 (2002).

86. Krakowski, M. & Owens, T. Interferon-gamma confers resistance to experimental allergic encephalomyelitis. *Eur J Immunol* **26**, 1641-6 (1996).

87. Voorthuis, J.A. et al. Suppression of experimental allergic encephalomyelitis by intraventricular administration of interferon-gamma in Lewis rats. *Clin Exp Immunol* **81**, 183-8 (1990).

88. Willenborg, D.O., Fordham, S., Bernard, C.C., Cowden, W.B. & Ramshaw, I.A. IFN-gamma plays a critical down-regulatory role in the induction and effector phase of myelin oligodendrocyte glycoprotein-induced autoimmune encephalomyelitis. *J Immunol* **157**, 3223-7 (1996).

89. Zhang, G.X. et al. Induction of experimental autoimmune encephalomyelitis in IL-12 receptor-beta 2-deficient mice: IL-12 responsiveness is not required in the pathogenesis of inflammatory demyelination in the central nervous system. *J Immunol* **170**, 2153-60 (2003).

90. Cua, D.J. et al. Interleukin-23 rather than interleukin-12 is the critical cytokine for autoimmune inflammation of the brain. *Nature* **421**, 744-8 (2003).

91. Chen, Y. et al. Anti-IL-23 therapy inhibits multiple inflammatory pathways and ameliorates autoimmune encephalomyelitis. *J Clin Invest* **116**, 1317-26 (2006).

92. Kroenke, M.A., Carlson, T.J., Andjelkovic, A.V. & Segal, B.M. IL-12- and IL-23-modulated T cells induce distinct types of EAE based on histology, CNS chemokine profile, and response to cytokine inhibition. *J Exp Med* **205**, 1535-41 (2008).

93. Bettelli, E., Oukka, M. & Kuchroo, V.K. T(H)-17 cells in the circle of immunity and autoimmunity. *Nat Immunol* **8**, 345-50 (2007).

94. Nicoletti, F. et al. Elevated serum levels of interleukin-12 in chronic progressive multiple sclerosis. *J Neuroimmunol* **70**, 87-90 (1996).

95. Drulovic, J. et al. Interleukin-12 and tumor necrosis factor-alpha levels in cerebrospinal fluid of multiple sclerosis patients. *J Neurol Sci* **147**, 145-50 (1997).

96. Comabella, M. et al. Elevated interleukin-12 in progressive multiple sclerosis correlates with disease activity and is normalized by pulse cyclophosphamide therapy. *J Clin Invest* **102**, 671-8 (1998).

97. van Boxel-Dezaire, A.H. et al. Decreased interleukin-10 and increased interleukin-12p40 mRNA are associated with disease activity and characterize different disease stages in multiple sclerosis. *Ann Neurol* **45**, 695-703 (1999).

98. Nicoletti, F. et al. Increased serum levels of interleukin-18 in patients with multiple sclerosis. *Neurology* **57**, 342-4 (2001).

99. Gutcher, I. & Becher, B. APC-derived cytokines and T cell polarization in autoimmune inflammation. *J Clin Invest* **117**, 1119-27 (2007).

100. Olsson, T. Cytokines in neuroinflammatory disease: role of myelin autoreactive T cell production of interferon-gamma. *J Neuroimmunol* **40**, 211-8 (1992).

101. Correale, J. et al. Patterns of cytokine secretion by autoreactive proteolipid protein-specific T cell clones during the course of multiple sclerosis. *J Immunol* **154**, 2959-68 (1995).

102. Hemmer, B. et al. Cytokine phenotype of human autoreactive T cell clones specific for the immunodominant myelin basic protein peptide (83-99). *J Neurosci Res* **45**, 852-62 (1996).

103. Bielekova, B. et al. Expansion and functional relevance of high-avidity myelin-specific CD4+ T cells in multiple sclerosis. *J Immunol* **172**, 3893-904 (2004).

104. Panitch, H.S., Hirsch, R.L., Haley, A.S. & Johnson, K.P. Exacerbations of multiple sclerosis in patients treated with gamma interferon. *Lancet* **1**, 893-5 (1987).

105. Tzartos, J.S. et al. Interleukin-17 production in central nervous system-infiltrating T cells and glial cells is associated with active disease in multiple sclerosis. *Am J Pathol* **172**, 146-55 (2008).

106. Brucklacher-Waldert, V., Stuerner, K., Kolster, M., Wolthausen, J. & Tolosa, E. Phenotypical and functional characterization of T helper 17 cells in multiple sclerosis. *Brain* **132**, 3329-41 (2009).

107. Rivers, T.M., Sprunt, D.H. & Berry, G.P. Observations on Attempts to Produce Acute Disseminated Encephalomyelitis in Monkeys. *J Exp Med* **58**, 39-53 (1933).

108. Freund, J. The mode of action of immunologic adjuvants. *Bibl Tuberc*, 130-48 (1956).

109. Bettelli, E., Baeten, D., Jager, A., Sobel, R.A. & Kuchroo, V.K. Myelin oligodendrocyte glycoprotein-specific T and B cells cooperate to induce a Devic-like disease in mice. *J Clin Invest* **116**, 2393-402 (2006).

110. Krishnamoorthy, G., Lassmann, H., Wekerle, H. & Holz, A. Spontaneous opticospinal encephalomyelitis in a double-transgenic mouse model of autoimmune T cell/B cell cooperation. *J Clin Invest* **116**, 2385-92 (2006).

111. Steinman, L. Assessment of animal models for MS and demyelinating disease in the design of rational therapy. *Neuron* **24**, 511-4 (1999).

112. Gold, R., Linington, C. & Lassmann, H. Understanding pathogenesis and therapy of multiple sclerosis via animal models: 70 years of merits and culprits in experimental autoimmune encephalomyelitis research. *Brain* **129**, 1953-71 (2006).

113. Su, S.B. et al. Essential role of the MyD88 pathway, but nonessential roles of TLRs 2, 4, and 9, in the adjuvant effect promoting Th1-mediated autoimmunity. *J Immunol* **175**, 6303-10 (2005).

114. Friese, M.A. et al. The value of animal models for drug development in multiple sclerosis. *Brain* **129**, 1940-52 (2006).

115. Friese, M.A. et al. Opposing effects of HLA class I molecules in tuning autoreactive CD8+ T cells in multiple sclerosis. *Nat Med* **14**, 1227-35 (2008).

116. Goverman, J. Autoimmune T cell responses in the central nervous system. *Nat Rev Immunol* **9**, 393-407 (2009).

117. Ransohoff, R.M., Kivisakk, P. & Kidd, G. Three or more routes for leukocyte migration into the central nervous system. *Nat Rev Immunol* **3**, 569-81 (2003).

118. Hickey, W.F., Hsu, B.L. & Kimura, H. T-lymphocyte entry into the central nervous system. *J Neurosci Res* **28**, 254-60 (1991).

119. Hickey, W.F. Migration of hematogenous cells through the blood-brain barrier and the initiation of CNS inflammation. *Brain Pathol* **1**, 97-105 (1991).

120. Schluesener, H.J. & Wekerle, H. Autoaggressive T lymphocyte lines recognizing the encephalitogenic region of myelin basic protein: in vitro selection from unprimed rat T lymphocyte populations. *J Immunol* **135**, 3128-33 (1985).

121. Harrington, C.J. et al. Differential tolerance is induced in T cells recognizing distinct epitopes of myelin basic protein. *Immunity* **8**, 571-80 (1998).

122. Seamons, A., Perchellet, A. & Goverman, J. Immune tolerance to myelin proteins. *Immunol Res* **28**, 201-21 (2003).

123. Pribyl, T.M., Campagnoni, C., Kampf, K., Handley, V.W. & Campagnoni, A.T. The major myelin protein genes are expressed in the human thymus. *J Neurosci Res* **45**, 812-9 (1996).

124. Egwuagu, C.E., Charukamnoetkanok, P. & Gery, I. Thymic expression of autoantigens correlates with resistance to autoimmune disease. *J Immunol* **159**, 3109-12 (1997).

125. Klein, L., Klugmann, M., Nave, K.A., Tuohy, V.K. & Kyewski, B. Shaping of the autoreactive T-cell repertoire by a splice variant of self protein expressed in thymic epithelial cells. *Nat Med* **6**, 56-61 (2000).

126. Derbinski, J., Schulte, A., Kyewski, B. & Klein, L. Promiscuous gene expression in medullary thymic epithelial cells mirrors the peripheral self. *Nat Immunol* **2**, 1032-9 (2001).

127. Liu, H., MacKenzie-Graham, A.J., Kim, S. & Voskuhl, R.R. Mice resistant to experimental autoimmune encephalomyelitis have increased thymic expression of myelin basic protein and increased MBP specific T cell tolerance. *J Neuroimmunol* **115**, 118-26 (2001).

128. Campagnoni, A.T. et al. Structure and developmental regulation of Golli-mbp, a 105-kilobase gene that encompasses the myelin basic protein gene and is expressed in cells in the oligodendrocyte lineage in the brain. *J Biol Chem* **268**, 4930-8 (1993).

129. Pribyl, T.M. et al. The human myelin basic protein gene is included within a 179-kilobase transcription unit: expression in the immune and central nervous systems. *Proc Natl Acad Sci U S A* **90**, 10695-9 (1993).

130. Zelenika, D., Grima, B. & Pessac, B. A new family of transcripts of the myelin basic protein gene: expression in brain and in immune system. *J Neurochem* **60**, 1574-7 (1993).

131. Pagany, M. et al. Myelin oligodendrocyte glycoprotein is expressed in the peripheral nervous system of rodents and primates. *Neurosci Lett* **350**, 165-8 (2003).

132. Furtado, G.C. et al. Swift entry of myelin-specific T lymphocytes into the central nervous system in spontaneous autoimmune encephalomyelitis. *J Immunol* **181**, 4648-55 (2008).

133. Zhang, H., Podojil, J.R., Luo, X. & Miller, S.D. Intrinsic and induced regulation of the age-associated onset of spontaneous experimental autoimmune encephalomyelitis. *J Immunol* **181**, 4638-47 (2008).

134. Weller, R.O., Djuanda, E., Yow, H.Y. & Carare, R.O. Lymphatic drainage of the brain and the pathophysiology of neurological disease. *Acta Neuropathol* **117**, 1-14 (2009).

135. Fujinami, R.S. & Oldstone, M.B. Amino acid homology between the encephalitogenic site of myelin basic protein and virus: mechanism for autoimmunity. *Science* **230**, 1043-5 (1985).

136. Wucherpfennig, K.W. & Strominger, J.L. Molecular mimicry in T cell-mediated autoimmunity: viral peptides activate human T cell clones specific for myelin basic protein. *Cell* **80**, 695-705 (1995).

137. Hemmer, B. et al. Identification of high potency microbial and self ligands for a human autoreactive class II-restricted T cell clone. *J Exp Med* **185**, 1651-9 (1997).

138. Hemmer, B. et al. Contribution of individual amino acids within MHC molecule or antigenic peptide to TCR ligand potency. *J Immunol* **164**, 861-71 (2000).

139. Hemmer, B. et al. Predictable TCR antigen recognition based on peptide scans leads to the identification of agonist ligands with no sequence homology. *J Immunol* **160**, 3631-6 (1998).

140. Lang, H.L. et al. A functional and structural basis for TCR cross-reactivity in multiple sclerosis. *Nat Immunol* **3**, 940-3 (2002).

141. Tejada-Simon, M.V., Zang, Y.C., Hong, J., Rivera, V.M. & Zhang, J.Z. Cross-reactivity with myelin basic protein and human herpesvirus-6 in multiple sclerosis. *Ann Neurol* **53**, 189-97 (2003).

142. Munz, C., Lunemann, J.D., Getts, M.T. & Miller, S.D. Antiviral immune responses: triggers of or triggered by autoimmunity? *Nat Rev Immunol* **9**, 246-58 (2009).

143. Reboldi, A. et al. C-C chemokine receptor 6-regulated entry of TH-17 cells into the CNS through the choroid plexus is required for the initiation of EAE. *Nat Immunol* **10**, 514-23 (2009).

144. Brown, D.A. & Sawchenko, P.E. Time course and distribution of inflammatory and neurodegenerative events suggest structural bases for the pathogenesis of experimental autoimmune encephalomyelitis. *J Comp Neurol* **502**, 236-60 (2007).

145. Kivisakk, P. et al. Localizing central nervous system immune surveillance: meningeal antigen-presenting cells activate T cells during experimental autoimmune encephalomyelitis. *Ann Neurol* **65**, 457-69 (2009).

146. Kawakami, N. et al. Live imaging of effector cell trafficking and autoantigen recognition within the unfolding autoimmune encephalomyelitis lesion. *J Exp Med* **201**, 1805-14 (2005).

147. Friese, M.A. & Fugger, L. Autoreactive CD8+ T cells in multiple sclerosis: a new target for therapy? *Brain* **128**, 1747-63 (2005).

148. Matsushita, T., Yanaba, K., Bouaziz, J.D., Fujimoto, M. & Tedder, T.F. Regulatory B cells inhibit EAE initiation in mice while other B cells promote disease progression. *J Clin Invest* **118**, 3420-30 (2008).

149. Goverman, J., Perchellet, A. & Huseby, E.S. The role of CD8(+) T cells in multiple sclerosis and its animal models. *Curr Drug Targets Inflamm Allergy* **4**, 239-45 (2005).

150. Segal, B.M. The role of natural killer cells in curbing neuroinflammation. *J Neuroimmunol* **191**, 2-7 (2007).

151. Wu, L. & Van Kaer, L. Natural killer T cells and autoimmune disease. *Curr Mol Med* **9**, 4-14 (2009).

152. Greter, M. et al. Dendritic cells permit immune invasion of the CNS in an animal model of multiple sclerosis. *Nat Med* **11**, 328-34 (2005).

153. Heppner, F.L. et al. Experimental autoimmune encephalomyelitis repressed by microglial paralysis. *Nat Med* **11**, 146-52 (2005).

154. Miller, S.D., McMahon, E.J., Schreiner, B. & Bailey, S.L. Antigen presentation in the CNS by myeloid dendritic cells drives progression of relapsing experimental autoimmune encephalomyelitis. *Ann N Y Acad Sci* **1103**, 179-91 (2007).

155. Becher, B., Durell, B.G., Miga, A.V., Hickey, W.F. & Noelle, R.J. The clinical course of experimental autoimmune encephalomyelitis and inflammation is controlled by the expression of CD40 within the central nervous system. *J Exp Med* **193**, 967-74 (2001).

156. Tran, E.H., Hoekstra, K., van Rooijen, N., Dijkstra, C.D. & Owens, T. Immune invasion of the central nervous system parenchyma and experimental allergic encephalomyelitis, but not

leukocyte extravasation from blood, are prevented in macrophage-depleted mice. *J Immunol* **161**, 3767-75 (1998).

157. Marta, M., Meier, U.C. & Lobell, A. Regulation of autoimmune encephalomyelitis by toll-like receptors. *Autoimmun Rev* **8**, 506-9 (2009).

158. Iwasaki, A. & Medzhitov, R. Regulation of adaptive immunity by the innate immune system. *Science* **327**, 291-5.

159. Takeda, K. & Akira, S. Toll-like receptors in innate immunity. *Int Immunol* **17**, 1-14 (2005).

160. Buljevac, D. et al. Prospective study on the relationship between infections and multiple sclerosis exacerbations. *Brain* **125**, 952-60 (2002).

161. Correale, J., Fiol, M. & Gilmore, W. The risk of relapses in multiple sclerosis during systemic infections. *Neurology* **67**, 652-9 (2006).

162. Sibley, W.A., Bamford, C.R. & Clark, K. Clinical viral infections and multiple sclerosis. *Lancet* **1**, 1313-5 (1985).

163. Goverman, J. Tolerance and autoimmunity in TCR transgenic mice specific for myelin basic protein. *Immunol Rev* **169**, 147-59 (1999).

164. Nathan, C. Neutrophils and immunity: challenges and opportunities. *Nat Rev Immunol* **6**, 173-82 (2006).

165. Borregaard, N., Sorensen, O.E. & Theilgaard-Monch, K. Neutrophil granules: a library of innate immunity proteins. *Trends Immunol* **28**, 340-5 (2007).

166. Brinkmann, V. & Zychlinsky, A. Beneficial suicide: why neutrophils die to make NETs. *Nat Rev Microbiol* **5**, 577-82 (2007).

167. Soruri, A., Grigat, J., Forssmann, U., Riggert, J. & Zwirner, J. beta-Defensins chemoattract macrophages and mast cells but not lymphocytes and dendritic cells: CCR6 is not involved. *Eur J Immunol* **37**, 2474-86 (2007).

168. Yoshimura, T. & Takahashi, M. IFN-gamma-mediated survival enables human neutrophils to produce MCP-1/CCL2 in response to activation by TLR ligands. *J Immunol* **179**, 1942-9 (2007).

169. Zhu, J. et al. Conversion of proepithelin to epithelins: roles of SLPI and elastase in host defense and wound repair. *Cell* **111**, 867-78 (2002).

170. Molesworth-Kenyon, S.J., Oakes, J.E. & Lausch, R.N. A novel role for neutrophils as a source of T cell-recruiting chemokines IP-10 and Mig during the DTH response to HSV-1 antigen. *J Leukoc Biol* **77**, 552-9 (2005).

171. Bliss, S.K., Butcher, B.A. & Denkers, E.Y. Rapid recruitment of neutrophils containing prestored IL-12 during microbial infection. *J Immunol* **165**, 4515-21 (2000).

172. Denkers, E.Y., Del Rio, L. & Bennouna, S. Neutrophil production of IL-12 and other cytokines during microbial infection. *Chem Immunol Allergy* **83**, 95-114 (2003).

173. Bennouna, S. & Denkers, E.Y. Microbial antigen triggers rapid mobilization of TNF-alpha to the surface of mouse neutrophils transforming them into inducers of high-level dendritic cell TNF-alpha production. *J Immunol* **174**, 4845-51 (2005).

174. Bennouna, S., Bliss, S.K., Curiel, T.J. & Denkers, E.Y. Cross-talk in the innate immune system: neutrophils instruct recruitment and activation of dendritic cells during microbial infection. *J Immunol* **171**, 6052-8 (2003).

175. Zhang, X., Majlessi, L., Deriaud, E., Leclerc, C. & Lo-Man, R. Coactivation of Syk kinase and MyD88 adaptor protein pathways by bacteria promotes regulatory properties of neutrophils. *Immunity* **31**, 761-71 (2009).

176. Muller, I., Munder, M., Kropf, P. & Hansch, G.M. Polymorphonuclear neutrophils and T lymphocytes: strange bedfellows or brothers in arms? *Trends Immunol* **30**, 522-30 (2009).

177. Park, H. et al. A distinct lineage of CD4 T cells regulates tissue inflammation by producing interleukin 17. *Nat Immunol* **6**, 1133-41 (2005).

178. Weaver, C.T., Hatton, R.D., Mangan, P.R. & Harrington, L.E. IL-17 family cytokines and the expanding diversity of effector T cell lineages. *Annu Rev Immunol* **25**, 821-52 (2007).

179. Intlekofer, A.M. et al. Anomalous type 17 response to viral infection by CD8+ T cells lacking T-bet and eomesodermin. *Science* **321**, 408-11 (2008).

180. Haak, S. et al. IL-17A and IL-17F do not contribute vitally to autoimmune neuro-inflammation in mice. *J Clin Invest* **119**, 61-9 (2009).

181. Prat, A. et al. Migration of multiple sclerosis lymphocytes through brain endothelium. *Arch Neurol* **59**, 391-7 (2002).

182. Ehrlich, L.C. et al. Cytokine regulation of human microglial cell IL-8 production. *J Immunol* **160**, 1944-8 (1998).

183. Ishizu, T. et al. Intrathecal activation of the IL-17/IL-8 axis in opticospinal multiple sclerosis. *Brain* **128**, 988-1002 (2005).

184. Lucchinetti, C.F. et al. A role for humoral mechanisms in the pathogenesis of Devic's neuromyelitis optica. *Brain* **125**, 1450-61 (2002).

185. Ziaber, J. et al. The immunoregulatory abilities of polymorphonuclear neutrophils in the course of multiple sclerosis. *Mediators Inflamm* **7**, 335-8 (1998).

186. Guarnieri, B., Lolli, F. & Amaducci, L. Polymorphonuclear neutral protease activity in multiple sclerosis and other diseases. *Ann Neurol* **18**, 620-2 (1985).

187. Carlson, T., Kroenke, M., Rao, P., Lane, T.E. & Segal, B. The Th17-ELR+ CXC chemokine pathway is essential for the development of central nervous system autoimmune disease. *J Exp Med* **205**, 811-23 (2008).

188. Godiska, R., Chantry, D., Dietsch, G.N. & Gray, P.W. Chemokine expression in murine experimental allergic encephalomyelitis. *J Neuroimmunol* **58**, 167-76 (1995).

189. Nygardas, P.T., Maatta, J.A. & Hinkkanen, A.E. Chemokine expression by central nervous system resident cells and infiltrating neutrophils during experimental autoimmune encephalomyelitis in the BALB/c mouse. *Eur J Immunol* **30**, 1911-8 (2000).

190. Maatta, J.A., Sjoholm, U.R., Nygardas, P.T., Salmi, A.A. & Hinkkanen, A.E. Neutrophils secreting tumor necrosis factor alpha infiltrate the central nervous system of BALB/c mice with experimental autoimmune encephalomyelitis. *J Neuroimmunol* **90**, 162-75 (1998).

191. Traugott, U., McFarlin, D.E. & Raine, C.S. Immunopathology of the lesion in chronic relapsing experimental autoimmune encephalomyelitis in the mouse. *Cell Immunol* **99**, 395-410 (1986).

192. McColl, S.R. et al. Treatment with anti-granulocyte antibodies inhibits the effector phase of experimental autoimmune encephalomyelitis. *J Immunol* **161**, 6421-6 (1998).

193. Daley, J.M., Thomay, A.A., Connolly, M.D., Reichner, J.S. & Albina, J.E. Use of Ly6G-specific monoclonal antibody to deplete neutrophils in mice. *J Leukoc Biol* **83**, 64-70 (2008).

194. Bruck, W. The pathology of multiple sclerosis is the result of focal inflammatory demyelination with axonal damage. *J Neurol* **252 Suppl 5**, v3-9 (2005).

195. Antel, J. Oligodendrocyte/myelin injury and repair as a function of the central nervous system environment. *Clin Neurol Neurosurg* **108**, 245-9 (2006).

196. Matute, C. et al. The link between excitotoxic oligodendroglial death and demyelinating diseases. *Trends Neurosci* **24**, 224-30 (2001).

197. Matute, C. Oligodendrocyte NMDA receptors: a novel therapeutic target. *Trends Mol Med* **12**, 289-92 (2006).

198. Touil, T., Deloire-Grassin, M.S., Vital, C., Petry, K.G. & Brochet, B. In vivo damage of CNS myelin and axons induced by peroxynitrite. *Neuroreport* **12**, 3637-44 (2001).

199. Scott, G.S., Virag, L., Szabo, C. & Hooper, D.C. Peroxynitrite-induced oligodendrocyte toxicity is not dependent on poly(ADP-ribose) polymerase activation. *Glia* **41**, 105-16 (2003).

200. Smith, K.J. & Lassmann, H. The role of nitric oxide in multiple sclerosis. *Lancet Neurol* **1**, 232-41 (2002).

201. Schluesener, H.J., Sobel, R.A., Linington, C. & Weiner, H.L. A monoclonal antibody against a myelin oligodendrocyte glycoprotein induces relapses and demyelination in central nervous system autoimmune disease. *J Immunol* **139**, 4016-21 (1987).

202. Linington, C., Bradl, M., Lassmann, H., Brunner, C. & Vass, K. Augmentation of demyelination in rat acute allergic encephalomyelitis by circulating mouse monoclonal antibodies directed against a myelin/oligodendrocyte glycoprotein. *Am J Pathol* **130**, 443-54 (1988).

203. Genain, C.P. et al. Antibody facilitation of multiple sclerosis-like lesions in a nonhuman primate. *J Clin Invest* **96**, 2966-74 (1995).

204. Jack, C., Ruffini, F., Bar-Or, A. & Antel, J.P. Microglia and multiple sclerosis. *J Neurosci Res* **81**, 363-73 (2005).

205. Carroll, W.M. & Jennings, A.R. Early recruitment of oligodendrocyte precursors in CNS demyelination. *Brain* **117 (Pt 3)**, 563-78 (1994).

206. Barkhof, F. et al. Remyelinated lesions in multiple sclerosis: magnetic resonance image appearance. *Arch Neurol* **60**, 1073-81 (2003).

207. Stadelmann, C. & Bruck, W. Interplay between mechanisms of damage and repair in multiple sclerosis. *J Neurol* **255 Suppl 1**, 12-8 (2008).

208. Patrikios, P. et al. Remyelination is extensive in a subset of multiple sclerosis patients. *Brain* **129**, 3165-72 (2006).

209. Goldschmidt, T., Antel, J., Konig, F.B., Bruck, W. & Kuhlmann, T. Remyelination capacity of the MS brain decreases with disease chronicity. *Neurology* **72**, 1914-21 (2009).

210. Trapp, B.D. & Nave, K.A. Multiple sclerosis: an immune or neurodegenerative disorder? *Annu Rev Neurosci* **31**, 247-69 (2008).

211. Kornek, B. & Lassmann, H. Axonal pathology in multiple sclerosis. A historical note. *Brain Pathol* **9**, 651-6 (1999).

212. Frischer, J.M. et al. The relation between inflammation and neurodegeneration in multiple sclerosis brains. *Brain* **132**, 1175-89 (2009).

213. Dutta, R. et al. Mitochondrial dysfunction as a cause of axonal degeneration in multiple sclerosis patients. *Ann Neurol* **59**, 478-89 (2006).

214. Ganter, P., Prince, C. & Esiri, M.M. Spinal cord axonal loss in multiple sclerosis: a post-mortem study. *Neuropathol Appl Neurobiol* **25**, 459-67 (1999).

215. Bjartmar, C., Kidd, G., Mork, S., Rudick, R. & Trapp, B.D. Neurological disability correlates with spinal cord axonal loss and reduced N-acetyl aspartate in chronic multiple sclerosis patients. *Ann Neurol* **48**, 893-901 (2000).

216. Lovas, G., Palkovits, M. & Komoly, S. Increased c-Jun expression in neurons affected by lysolecithin-induced demyelination in rats. *Neurosci Lett* **292**, 71-4 (2000).

217. Kutzelnigg, A. et al. Cortical demyelination and diffuse white matter injury in multiple sclerosis. *Brain* **128**, 2705-12 (2005).

218. Schwab, M.E. & Bartholdi, D. Degeneration and regeneration of axons in the lesioned spinal cord. *Physiol Rev* **76**, 319-70 (1996).

219. Chen, Z.L., Yu, W.M. & Strickland, S. Peripheral regeneration. *Annu Rev Neurosci* **30**, 209-33 (2007).

220. David, S. & Aguayo, A.J. Axonal elongation into peripheral nervous system "bridges" after central nervous system injury in adult rats. *Science* **214**, 931-3 (1981).

221. Richardson, P.M. & Issa, V.M. Peripheral injury enhances central regeneration of primary sensory neurones. *Nature* **309**, 791-3 (1984).

222. Neumann, S. & Woolf, C.J. Regeneration of dorsal column fibers into and beyond the lesion site following adult spinal cord injury. *Neuron* **23**, 83-91 (1999).

223. Berry, M. Post-injury myelin-breakdown products inhibit axonal growth: an hypothesis to explain the failure of axonal regeneration in the mammalian central nervous system. *Bibl Anat*, 1-11 (1982).

224. Niclou, S.P., Ehlert, E.M. & Verhaagen, J. Chemorepellent axon guidance molecules in spinal cord injury. *J Neurotrauma* **23**, 409-21 (2006).

225. Ridet, J.L., Malhotra, S.K., Privat, A. & Gage, F.H. Reactive astrocytes: cellular and molecular cues to biological function. *Trends Neurosci* **20**, 570-7 (1997).

226. Domeniconi, M. & Filbin, M.T. Overcoming inhibitors in myelin to promote axonal regeneration. *J Neurol Sci* **233**, 43-7 (2005).

227. Wang, D. et al. Astrocyte-associated axonal damage in pre-onset stages of experimental autoimmune encephalomyelitis. *Glia* **51**, 235-40 (2005).

228. Luo, J. et al. Glia-dependent TGF-beta signaling, acting independently of the TH17 pathway, is critical for initiation of murine autoimmune encephalomyelitis. *J Clin Invest* **117**, 3306-15 (2007).

229. Voskuhl, R.R. et al. Reactive astrocytes form scar-like perivascular barriers to leukocytes during adaptive immune inflammation of the CNS. *J Neurosci* **29**, 11511-22 (2009).

230. Schwab, M.E. & Thoenen, H. Dissociated neurons regenerate into sciatic but not optic nerve explants in culture irrespective of neurotrophic factors. *J Neurosci* **5**, 2415-23 (1985).

231. Schwab, M.E. & Caroni, P. Oligodendrocytes and CNS myelin are nonpermissive substrates for neurite growth and fibroblast spreading in vitro. *J Neurosci* **8**, 2381-93 (1988).

232. Savio, T. & Schwab, M.E. Rat CNS white matter, but not gray matter, is nonpermissive for neuronal cell adhesion and fiber outgrowth. *J Neurosci* **9**, 1126-33 (1989).

233. Bandtlow, C., Zachleder, T. & Schwab, M.E. Oligodendrocytes arrest neurite growth by contact inhibition. *J Neurosci* **10**, 3837-48 (1990).

234. McKerracher, L. et al. Identification of myelin-associated glycoprotein as a major myelin-derived inhibitor of neurite growth. *Neuron* **13**, 805-11 (1994).

235. Mukhopadhyay, G., Doherty, P., Walsh, F.S., Crocker, P.R. & Filbin, M.T. A novel role for myelin-associated glycoprotein as an inhibitor of axonal regeneration. *Neuron* **13**, 757-67 (1994).

236. Chen, M.S. et al. Nogo-A is a myelin-associated neurite outgrowth inhibitor and an antigen for monoclonal antibody IN-1. *Nature* **403**, 434-9 (2000).

237. GrandPre, T., Nakamura, F., Vartanian, T. & Strittmatter, S.M. Identification of the Nogo inhibitor of axon regeneration as a Reticulon protein. *Nature* **403**, 439-44 (2000).

238. Prinjha, R. et al. Inhibitor of neurite outgrowth in humans. *Nature* **403**, 383-4 (2000).

239. Wang, K.C. et al. Oligodendrocyte-myelin glycoprotein is a Nogo receptor ligand that inhibits neurite outgrowth. *Nature* **417**, 941-4 (2002).

240. Li, C. et al. Myelination in the absence of myelin-associated glycoprotein. *Nature* **369**, 747-50 (1994).

241. Trapp, B.D. Myelin-associated glycoprotein. Location and potential functions. *Ann N Y Acad Sci* **605**, 29-43 (1990).

242. DeBellard, M.E., Tang, S., Mukhopadhyay, G., Shen, Y.J. & Filbin, M.T. Myelin-associated glycoprotein inhibits axonal regeneration from a variety of neurons via interaction with a sialoglycoprotein. *Mol Cell Neurosci* **7**, 89-101 (1996).

243. Schafer, M., Fruttiger, M., Montag, D., Schachner, M. & Martini, R. Disruption of the gene for the myelin-associated glycoprotein improves axonal regrowth along myelin in C57BL/Wlds mice. *Neuron* **16**, 1107-13 (1996).

244. Domeniconi, M. et al. MAG induces regulated intramembrane proteolysis of the p75 neurotrophin receptor to inhibit neurite outgrowth. *Neuron* **46**, 849-55 (2005).

245. Caroni, P. & Schwab, M.E. Antibody against myelin-associated inhibitor of neurite growth neutralizes nonpermissive substrate properties of CNS white matter. *Neuron* **1**, 85-96 (1988).

246. Schnell, L. & Schwab, M.E. Axonal regeneration in the rat spinal cord produced by an antibody against myelin-associated neurite growth inhibitors. *Nature* **343**, 269-72 (1990).

247. Bregman, B.S. et al. Recovery from spinal cord injury mediated by antibodies to neurite growth inhibitors. *Nature* **378**, 498-501 (1995).

248. Oertle, T., Huber, C., van der Putten, H. & Schwab, M.E. Genomic structure and functional characterisation of the promoters of human and mouse nogo/rtn4. *J Mol Biol* **325**, 299-323 (2003).

249. Oertle, T. et al. Nogo-A inhibits neurite outgrowth and cell spreading with three discrete regions. *J Neurosci* **23**, 5393-406 (2003).

250. Fournier, A.E., GrandPre, T. & Strittmatter, S.M. Identification of a receptor mediating Nogo-66 inhibition of axonal regeneration. *Nature* **409**, 341-6 (2001).

251. Fiedler, M., Horn, C., Bandtlow, C., Schwab, M.E. & Skerra, A. An engineered IN-1 F(ab) fragment with improved affinity for the Nogo-A axonal growth inhibitor permits immunochemical detection and shows enhanced neutralizing activity. *Protein Eng* **15**, 931-41 (2002).

252. Dodd, D.A. et al. Nogo-A, -B, and -C are found on the cell surface and interact together in many different cell types. *J Biol Chem* **280**, 12494-502 (2005).

253. Vourc'h, P. et al. Oligodendrocyte myelin glycoprotein growth inhibition function requires its conserved leucine-rich repeat domain, not its glycosylphosphatidyl-inositol anchor. *J Neurochem* **85**, 889-97 (2003).

254. Habib, A.A., Gulcher, J.R., Hognason, T., Zheng, L. & Stefansson, K. The OMgp gene, a second growth suppressor within the NF1 gene. *Oncogene* **16**, 1525-31 (1998).

255. Vourc'h, P. & Andres, C. Oligodendrocyte myelin glycoprotein (OMgp): evolution, structure and function. *Brain Res Brain Res Rev* **45**, 115-24 (2004).

256. Huang, J.K. et al. Glial membranes at the node of Ranvier prevent neurite outgrowth. *Science* **310**, 1813-7 (2005).

257. Domeniconi, M. et al. Myelin-associated glycoprotein interacts with the Nogo66 receptor to inhibit neurite outgrowth. *Neuron* **35**, 283-90 (2002).

258. Liu, B.P., Fournier, A., GrandPre, T. & Strittmatter, S.M. Myelin-associated glycoprotein as a functional ligand for the Nogo-66 receptor. *Science* **297**, 1190-3 (2002).

259. Wang, K.C., Kim, J.A., Sivasankaran, R., Segal, R. & He, Z. P75 interacts with the Nogo receptor as a co-receptor for Nogo, MAG and OMgp. *Nature* **420**, 74-8 (2002).

260. Wong, S.T. et al. A p75(NTR) and Nogo receptor complex mediates repulsive signaling by myelin-associated glycoprotein. *Nat Neurosci* **5**, 1302-8 (2002).

261. Mi, S. et al. LINGO-1 is a component of the Nogo-66 receptor/p75 signaling complex. *Nat Neurosci* **7**, 221-8 (2004).

262. Shao, Z. et al. TAJ/TROY, an orphan TNF receptor family member, binds Nogo-66 receptor 1 and regulates axonal regeneration. *Neuron* **45**, 353-9 (2005).

263. Niederost, B., Oertle, T., Fritsche, J., McKinney, R.A. & Bandtlow, C.E. Nogo-A and myelin-associated glycoprotein mediate neurite growth inhibition by antagonistic regulation of RhoA and Rac1. *J Neurosci* **22**, 10368-76 (2002).

264. Linseman, D.A. & Loucks, F.A. Diverse roles of Rho family GTPases in neuronal development, survival, and death. *Front Biosci* **13**, 657-76 (2008).

265. Pignot, V. et al. Characterization of two novel proteins, NgRH1 and NgRH2, structurally and biochemically homologous to the Nogo-66 receptor. *J Neurochem* **85**, 717-28 (2003).

266. Barton, W.A. et al. Structure and axon outgrowth inhibitor binding of the Nogo-66 receptor and related proteins. *Embo J* **22**, 3291-302 (2003).

267. Lauren, J., Airaksinen, M.S., Saarma, M. & Timmusk, T. Two novel mammalian Nogo receptor homologs differentially expressed in the central and peripheral nervous systems. *Mol Cell Neurosci* **24**, 581-94 (2003).

268. Venkatesh, K. et al. The Nogo-66 receptor homolog NgR2 is a sialic acid-dependent receptor selective for myelin-associated glycoprotein. *J Neurosci* **25**, 808-22 (2005).

269. Barrette, B., Vallieres, N., Dube, M. & Lacroix, S. Expression profile of receptors for myelin-associated inhibitors of axonal regeneration in the intact and injured mouse central nervous system. *Mol Cell Neurosci* **34**, 519-38 (2007).

270. Atwal, J.K. et al. PirB is a functional receptor for myelin inhibitors of axonal regeneration. *Science* **322**, 967-70 (2008).

271. Borges, L., Hsu, M.L., Fanger, N., Kubin, M. & Cosman, D. A family of human lymphoid and myeloid Ig-like receptors, some of which bind to MHC class I molecules. *J Immunol* **159**, 5192-6 (1997).

272. Arm, J.P., Nwankwo, C. & Austen, K.F. Molecular identification of a novel family of human Ig superfamily members that possess immunoreceptor tyrosine-based inhibition motifs and homology to the mouse gp49B1 inhibitory receptor. *J Immunol* **159**, 2342-9 (1997).

273. Syken, J., Grandpre, T., Kanold, P.O. & Shatz, C.J. PirB restricts ocular-dominance plasticity in visual cortex. *Science* **313**, 1795-800 (2006).

274. Hu, F. & Strittmatter, S.M. The N-terminal domain of Nogo-A inhibits cell adhesion and axonal outgrowth by an integrin-specific mechanism. *J Neurosci* **28**, 1262-9 (2008).

275. Fontoura, P. et al. Immunity to the extracellular domain of Nogo-A modulates experimental autoimmune encephalomyelitis. *J Immunol* **173**, 6981-92 (2004).

276. Karnezis, T. et al. The neurite outgrowth inhibitor Nogo A is involved in autoimmune-mediated demyelination. *Nat Neurosci* **7**, 736-44 (2004).

277. Fry, E.J., Ho, C. & David, S. A role for Nogo receptor in macrophage clearance from injured peripheral nerve. *Neuron* **53**, 649-62 (2007).

278. Pool, M. et al. Myelin regulates immune cell adhesion and motility. *Exp Neurol* **217**, 371-7 (2009).

279. David, S., Fry, E.J. & Lopez-Vales, R. Novel roles for Nogo receptor in inflammation and disease. *Trends Neurosci* **31**, 221-6 (2008).

280. Satoh, J., Onoue, H., Arima, K. & Yamamura, T. Nogo-A and nogo receptor expression in demyelinating lesions of multiple sclerosis. *J Neuropathol Exp Neurol* **64**, 129-38 (2005).

281. Dimou, L. et al. Nogo-A-deficient mice reveal strain-dependent differences in axonal regeneration. *J Neurosci* **26**, 5591-603 (2006).

282. Zhang, L. et al. Identification of BLyS (B lymphocyte stimulator), a non-myelin-associated protein, as a functional ligand for Nogo-66 receptor. *J Neurosci* **29**, 6348-52 (2009).

283. Zheng, B. et al. Genetic deletion of the Nogo receptor does not reduce neurite inhibition in vitro or promote corticospinal tract regeneration in vivo. *Proc Natl Acad Sci U S A* **102**, 1205-10 (2005).

284. Worter, V. et al. Inhibitory activity of myelin-associated glycoprotein on sensory neurons is largely independent of NgR1 and NgR2 and resides within Ig-Like domains 4 and 5. *PLoS One* **4**, e5218 (2009).

285. Tepper, R.I., Coffman, R.L. & Leder, P. An eosinophil-dependent mechanism for the antitumor effect of interleukin-4. *Science* **257**, 548-51 (1992).

286. King, I.L., Dickendesher, T.L. & Segal, B.M. Circulating Ly-6C+ myeloid precursors migrate to the CNS and play a pathogenic role during autoimmune demyelinating disease. *Blood* **113**, 3190-7 (2009).

287. Mildner, A. et al. CCR2+Ly-6Chi monocytes are crucial for the effector phase of autoimmunity in the central nervous system. *Brain* **132**, 2487-500 (2009).

288. Choi, E.Y., Santoso, S. & Chavakis, T. Mechanisms of neutrophil transendothelial migration. *Front Biosci* **14**, 1596-605 (2009).

289. Gelderblom, M. et al. Temporal and spatial dynamics of cerebral immune cell accumulation in stroke. *Stroke* **40**, 1849-57 (2009).

290. Raghavendra, V., Tanga, F.Y. & DeLeo, J.A. Complete Freunds adjuvant-induced peripheral inflammation evokes glial activation and proinflammatory cytokine expression in the CNS. *Eur J Neurosci* **20**, 467-73 (2004).

291. Mombaerts, P. et al. Mutations in T-cell antigen receptor genes alpha and beta block thymocyte development at different stages. *Nature* **360**, 225-31 (1992).

292. Soulika, A.M. et al. Initiation and progression of axonopathy in experimental autoimmune encephalomyelitis. *J Neurosci* **29**, 14965-79 (2009).

293. Ignatowski, T.A. et al. Neuronal-associated tumor necrosis factor (TNF alpha): its role in noradrenergic functioning and modification of its expression following antidepressant drug administration. *J Neuroimmunol* **79**, 84-90 (1997).

294. Rothwell, N.J. & Luheshi, G.N. Interleukin 1 in the brain: biology, pathology and therapeutic target. *Trends Neurosci* **23**, 618-25 (2000).

295. Watkins, L.R. & Maier, S.F. Immune regulation of central nervous system functions: from sickness responses to pathological pain. *J Intern Med* **257**, 139-55 (2005).

296. Liu, L. et al. CXCR2-positive neutrophils are essential for cuprizone-induced demyelination: relevance to multiple sclerosis. *Nat Neurosci* **13**, 319-26.

297. van der Valk, P. & Amor, S. Preactive lesions in multiple sclerosis. *Curr Opin Neurol* **22**, 207-13 (2009).

298. t Hart, B.A., Hintzen, R.Q. & Laman, J.D. Multiple sclerosis - a response-to-damage model. *Trends Mol Med* **15**, 235-44 (2009).

299. Chertov, O. et al. Identification of human neutrophil-derived cathepsin G and azurocidin/CAP37 as chemoattractants for mononuclear cells and neutrophils. *J Exp Med* **186**, 739-47 (1997).

300. Soehnlein, O. et al. Neutrophil secretion products pave the way for inflammatory monocytes. *Blood* **112**, 1461-71 (2008).

301. Shi, G. et al. Unlike Th1, Th17 cells mediate sustained autoimmune inflammation and are highly resistant to restimulation-induced cell death. *J Immunol* **183**, 7547-56 (2009).

302. O'Connor, R.A., Malpass, K.H. & Anderton, S.M. The inflamed central nervous system drives the activation and rapid proliferation of Foxp3+ regulatory T cells. *J Immunol* **179**, 958-66 (2007).

303. Zhou, X. et al. Instability of the transcription factor Foxp3 leads to the generation of pathogenic memory T cells in vivo. *Nat Immunol* **10**, 1000-7 (2009).

304. Zhou, X., Bailey-Bucktrout, S., Jeker, L.T. & Bluestone, J.A. Plasticity of CD4(+) FoxP3(+) T cells. *Curr Opin Immunol* **21**, 281-5 (2009).

305. Korn, T. et al. Myelin-specific regulatory T cells accumulate in the CNS but fail to control autoimmune inflammation. *Nat Med* **13**, 423-31 (2007).

306. McMahon, E.J., Bailey, S.L., Castenada, C.V., Waldner, H. & Miller, S.D. Epitope spreading initiates in the CNS in two mouse models of multiple sclerosis. *Nat Med* **11**, 335-9 (2005).

307. Scheffold, A., Assenmacher, M., Reiners-Schramm, L., Lauster, R. & Radbruch, A. High-sensitivity immunofluorescence for detection of the pro- and anti-inflammatory cytokines gamma interferon and interleukin-10 on the surface of cytokine-secreting cells. *Nat Med* **6**, 107-10 (2000).

308. Assenmacher, M. et al. Specific expression of surface interferon-gamma on interferon-gamma producing T cells from mouse and man. *Eur J Immunol* **26**, 263-7 (1996).

309. Brucklacher-Waldert, V. et al. Phenotypical characterization of human Th17 cells unambiguously identified by surface IL-17A expression. *J Immunol* **183**, 5494-501 (2009).

310. Moseley, T.A., Haudenschild, D.R., Rose, L. & Reddi, A.H. Interleukin-17 family and IL-17 receptors. *Cytokine Growth Factor Rev* **14**, 155-74 (2003).

311. Kim, J.E., Liu, B.P., Park, J.H. & Strittmatter, S.M. Nogo-66 receptor prevents raphespinal and rubrospinal axon regeneration and limits functional recovery from spinal cord injury. *Neuron* **44**, 439-51 (2004).

312. Li, S. et al. Blockade of Nogo-66, myelin-associated glycoprotein, and oligodendrocyte myelin glycoprotein by soluble Nogo-66 receptor promotes axonal sprouting and recovery after spinal injury. *J Neurosci* **24**, 10511-20 (2004).

313. Kerschensteiner, M., Meinl, E. & Hohlfeld, R. Neuro-immune crosstalk in CNS diseases. *Neuroscience* **158**, 1122-32 (2009).

314. Besser, M. & Wank, R. Cutting edge: clonally restricted production of the neurotrophins brain-derived neurotrophic factor and neurotrophin-3 mRNA by human immune cells and Th1/Th2-polarized expression of their receptors. *J Immunol* **162**, 6303-6 (1999).

315. Moalem, G. et al. Production of neurotrophins by activated T cells: implications for neuroprotective autoimmunity. *J Autoimmun* **15**, 331-45 (2000).

316. Kerschensteiner, M. et al. Activated human T cells, B cells, and monocytes produce brain-derived neurotrophic factor in vitro and in inflammatory brain lesions: a neuroprotective role of inflammation? *J Exp Med* **189**, 865-70 (1999).

317. Kerschensteiner, M., Stadelmann, C., Dechant, G., Wekerle, H. & Hohlfeld, R. Neurotrophic cross-talk between the nervous and immune systems: implications for neurological diseases. *Ann Neurol* **53**, 292-304 (2003).

318. Zhong, J., Dietzel, I.D., Wahle, P., Kopf, M. & Heumann, R. Sensory impairments and delayed regeneration of sensory axons in interleukin-6-deficient mice. *J Neurosci* **19**, 4305-13 (1999).

319. Lyons, J.A., San, M., Happ, M.P. & Cross, A.H. B cells are critical to induction of experimental allergic encephalomyelitis by protein but not by a short encephalitogenic peptide. *Eur J Immunol* **29**, 3432-9 (1999).

320. Oh, S., Cudrici, C., Ito, T. & Rus, H. B-cells and humoral immunity in multiple sclerosis. Implications for therapy. *Immunol Res* **40**, 224-34 (2008).

321. Krumbholz, M. et al. BAFF is produced by astrocytes and up-regulated in multiple sclerosis lesions and primary central nervous system lymphoma. *J Exp Med* **201**, 195-200 (2005).

APPENDIX

Abbreviations

ANOVA	Analysis of variance
APC	Allophycocyanin Antigen presenting cell
APC-Cy7	Allophycocyanin – cyanine 7
APL	Altered peptide ligands
APS	Ammoniumperoxodisulfate
Arham	Armenian hamster
BALB/c	Bagg-albino/ c
BBB	Blood brain barrier
BDNF	Brain derived neutrophic factor
BLyS	B lymphocyte stimulator
BS	Bielschowsky silver
BSA	Bovine serum albumin
C57BL/6	C57 black 6
CCL	CC chemokine ligand
CD	Cluster of differentiation
CFA	Complete Freunds adjuvant
ch	Chicken
CIS	Clinically isolated syndrome
CNS	Central nervous system
cpm	Counts per minute
CSF	Cerebrospinal fluid
CST	Corticospinal tract
CTL	Cytotoxic T lymphocyte
CXCR2	CXC chemokine receptor type 2
CXCL8	Chemokine, CXC motif, ligand 8
DAB	Diaminobenzidine
DC	Dendritic cell Dorsal column
DEPC	Diethylpyrocarbonate
DMSO	Dimethylsulfoxid
DTT	1,4-Dithiothreitol

EAE	Experimental autoimmune encephalomyelitis
EBV	Ebstein-Barr-virus
EDTA	Ethylenediaminetetraacetic acid
EGTA	Ethyleneglycoltetraacetic acid
FITC	Fluorescein isothiocyanate
FOXP	Forkhead box protein
GA	Glatiramer acetate
G-CSF	Granulocyte-colony stimulating factor
GM-CSF	Granulocyte macrophage-colony stimulating factor
GPI	Glycosylphosohatidylinositol
H 33258	Hoechst 33258
HBP	Heparin binding protein
HCl	Hydrochloride acid
HC	Healthy control
HE	Hematoxylin/ eosin
HEPES	4-(2-hydroxyethyl)-1-piperazineethanesulfonic acid
HHV6	Human herpes virus 6
HRP	Horseradish peroxidase
ICS	Intracellular cytokine staining
IFN	Interferon
Ig	Immunolglobulin
IL	Interleukin
IL-17RA	Interleukin-17 receptor A
i.p.	Intraperitoneally
iTreg	Inducible regulatory T cells
i.v.	Intravenously
KAc	Potassium acetate
kDa	Kilodalton
LINGO-1	LRR- and immunoglobulin domain-containing protein
LIR	Leukocyte immunoglobulin-like immunoreceptors
LRR	Leucin-rich repeat
M-MLV	Moloney Murine Leukemia Virus
MAG	Myelin-associated protein
MBP	Myelin-basic protein
MesLN	Mesenteric lymph node

mDC	Myeloid dendritic cell
MHC	Major histocompartibility complex
MOG	Myelin oligodendrocyte glycoprotein
MRI	Magnet resonance imaging
ms	Mouse
mRNA	Messenger RNA
MS	Multiple sclerosis
MΦ	Macrophage
NaCl	Sodium chloride
NaOH	Sodium hydroxide
NeuN	Neuronal nuclei
NF	Neurofilament
NgR	Nogo-66 receptor
NK	Natural killer (cell)
NKT	Natural killer T (cell)
NP-40	Nonidet-p40
nTreg	Naturally occurring regulatory T cells
OMG	Oligodendrocyte myelin glycoprotein
PacBlue	Pacific blue
PAMP	Pathogen-associated molecular pattern
PBS	Phosphate buffered saline
PE	Phycoerythrin
PE-Cy5.5	Phycoerythrin cyanine 5.5
PE-Cy7	Phycoerythrin cyanine 7
PerCP-Cy5.5	Peridinin chlorophyll protein complex cyanine 5.5
PFA	Para-formaldehyd
PirB	Paired immunoglobulin-like receptor B
PLP	Proteolipid protein
PMA	Phorbol myristate acetate
PMSF	Phenylmethylsulfonyl fluoride
PNS	Peripheral nervous system
PP-MS	Primary progressive multiple sclerosis
PRR	Pattern-recognition receptors
PVDF	Polyvinylidenefluoride
rab	Rabbit

rm	Recombinant mouse
RPMI	Roswell park memorial institute
ROCK	Rho-associated coiled-coil-containing protein kinase
RR-MS	Relapsing-remitting multiple sclerosis
RT	Room temperature
RTN	Reticulon
SAS	Subarachnoid space
SDS	Sodium dodecylsufate
SI	Stimulation index
SP-MS	Secondary progressive multiple sclerosis
TBS	Tris buffered saline
TCR	T cell receptor
TEMED	Tetramethylethylenediamine
TLR	Toll-like receptor
TGF-β	Tumour growth factor-β
Th	T helper
TNF	Tumour necrosis factor
Treg	Regulatory T cells
Tris	Tris(hydroxymethyl)aminomethane
WT	Wildtype

List of figures

List of tables